High Intensity Lasers Application to Advanced Materials Processing: Laser Peening and Related Processes

José L. Ocaña

Centro Láser UPM (Universidad Politécnica de Madrid)
Ctra. de Valencia, km. 7,3. 28031 Madrid. SPAIN.
e-mail: jlocana@etsii.upm.es

Prague, (Czech Republic)
23-28 June 2013

High Intensity Lasers Application to Advanced Materials Processing

1. Introduction
2. Phenomenology of Laser-Matter Interaction at Moderately High Intensities (10^9-10^{12} W/cm^2)
3. Metallic Surfaces Treatment by High Intensity Short Pulse Lasers. Laser Shock Processing
   - 3.1. Concept and Physical Basis
   - 3.2. Process Modelling
   - 3.3. Experimental Implementation
   - 3.4. Experimental Results
   - 3.5. Discussion and Outlook
4. Final Discussion. Application of High Intensity Short Pulse Lasers to other Materials Processing Applications
   - 4.1. Laser shock microforming (LSmF®)

Phenomenology of Laser-Matter Interaction at Moderately High Intensities (10^9-10^{12} W/cm^2) Macroscopic Approach

$$\mathbf{F}_e = m_e \frac{d\mathbf{v}}{dt} = -e\,\mathbf{E} = -\mathbf{E}_0 \exp(i\omega t) \qquad [A.24]$$

$$\mathbf{v}(t) = -\frac{e}{m_e}\int \mathbf{E}(t)dt = -i\frac{e}{\omega\, m_e}\mathbf{E}(t) \qquad [A.25]$$

$$\mathbf{J}(t) = -N\,e\,\mathbf{v}(t) = -i\frac{N\,e^2}{\omega\, m_e}\mathbf{E}(t) = \sigma\,\mathbf{E}(t) \quad \Rightarrow \quad \sigma(\omega) = -i\frac{N\,e^2}{\omega\, m_e} \qquad [A.26]$$

$$P = \langle \mathbf{J}\cdot\mathbf{E}\rangle = \langle \sigma\mathbf{E}\cdot\mathbf{E}\rangle = \frac{1}{2}\Re\left(\sigma \mathbf{E}\mathbf{E}'\right) = 0 \qquad [A.27]$$

$$\mathbf{J}_t = \sigma\mathbf{E} + \frac{\partial \mathbf{D}}{\partial t} = (\sigma + i\omega\varepsilon)\mathbf{E} \cong (\sigma + i\omega\varepsilon_0)\mathbf{E} \qquad [A.28]$$

$$\mathbf{J}_t = \left(i\omega\varepsilon_0 - i\frac{N e^2}{\omega\, m_e}\right)\mathbf{E} = i\omega\varepsilon_0\left(1 - \frac{N e^2}{\omega^2 m_e \varepsilon_0}\right)\mathbf{E} \qquad [A.29]$$

$$\mathbf{J}_t = i\omega\varepsilon_0\left(1 - \left(\frac{\omega_p}{\omega}\right)^2\right)\mathbf{E} \qquad [A.30]$$

$$\omega_p = \left(\frac{N e^2}{m_e \varepsilon_0}\right)^{1/2} \qquad [A.31]$$

Figure A.3: Energy transport mechanisms in laser-plasma interaction. The appearance of a critical density inhibiting further beam penetration is shown.

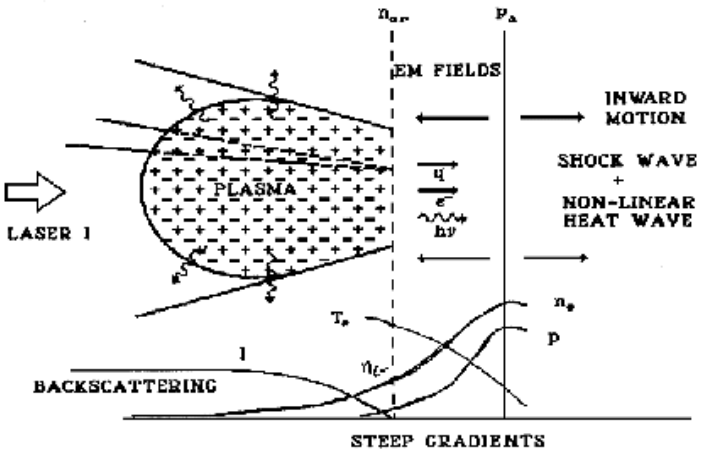

$$k^2(\omega) = \omega^2\varepsilon_0\mu\left(1 - i\frac{\sigma}{\omega\varepsilon_0}\right) = \omega^2\varepsilon_0\mu\left(1 - \left(\frac{\omega_p}{\omega}\right)^2\right) = \frac{\omega^2}{c^2}\left(1 - \left(\frac{\omega_p}{\omega}\right)^2\right) \qquad [A.32]$$

$$N_{cr}(\omega) = \frac{m_e \varepsilon_0 \omega^2}{e^2} \qquad [A.33]$$

OCAÑA, J.L.: "Laser Matter Interaction in High Intensity Processing Applications. EUROLASER ACADEMY (2001)

Phenomenology of Laser-Matter Interaction at Moderately High Intensities (10^9-10^{12} W/cm^2) Macroscopic approach

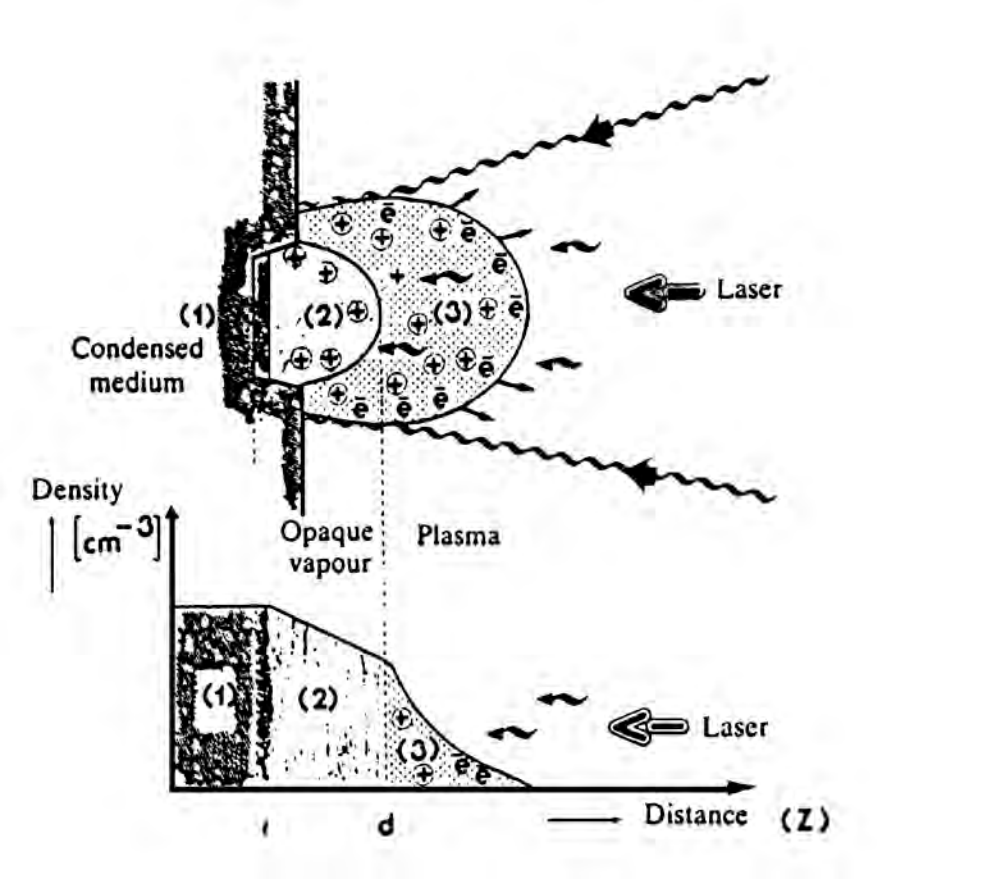

ELOY, J.F.: "Power Lasers". Ellis Horwood (1987)

Phenomenology of Laser-Matter Interaction at Moderately High Intensities (10^9-10^{12} W/cm^2) Macroscopic Approach

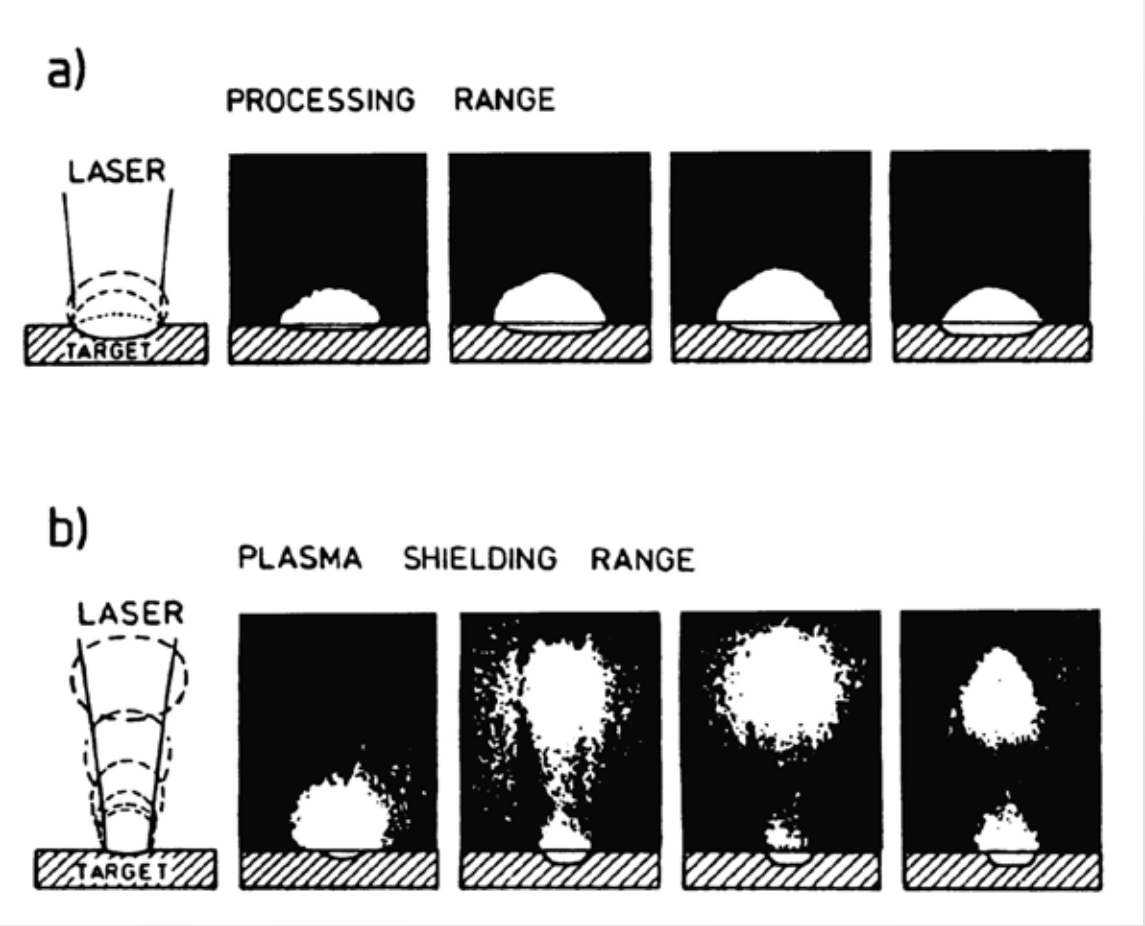

Phenomenology of Laser-Matter Interaction at Moderately High Intensities (10^9-10^{12} W/cm^2) Macroscopic Approach

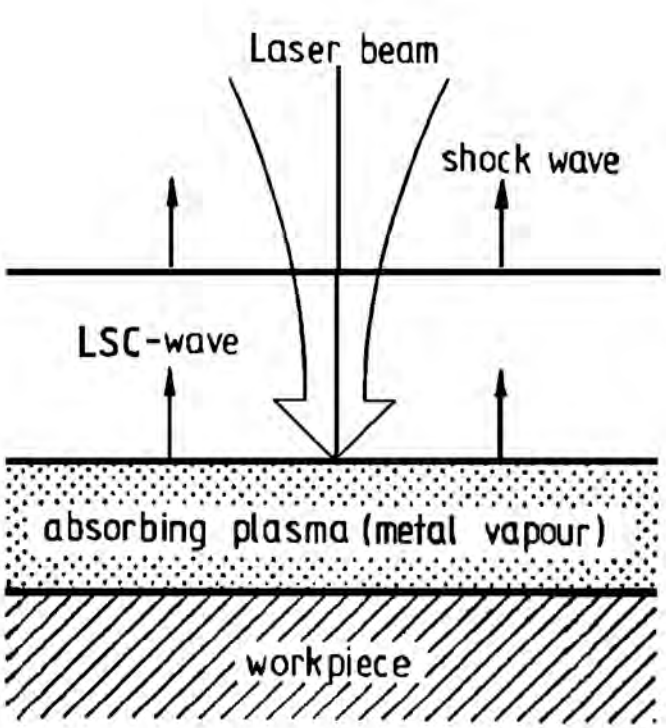

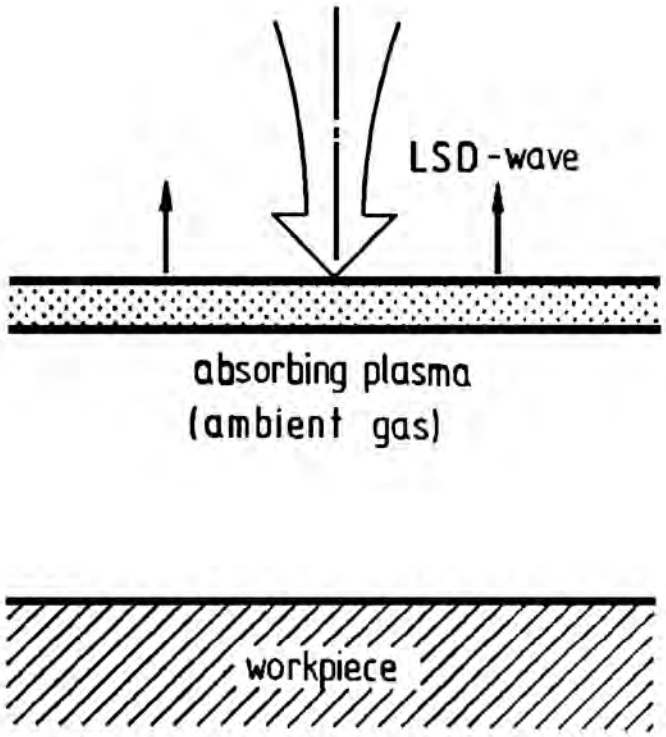

Phenomenology of Laser-Matter Interaction at Moderately High Intensities (10^9-10^{12} W/cm^2) Macroscopic Approach

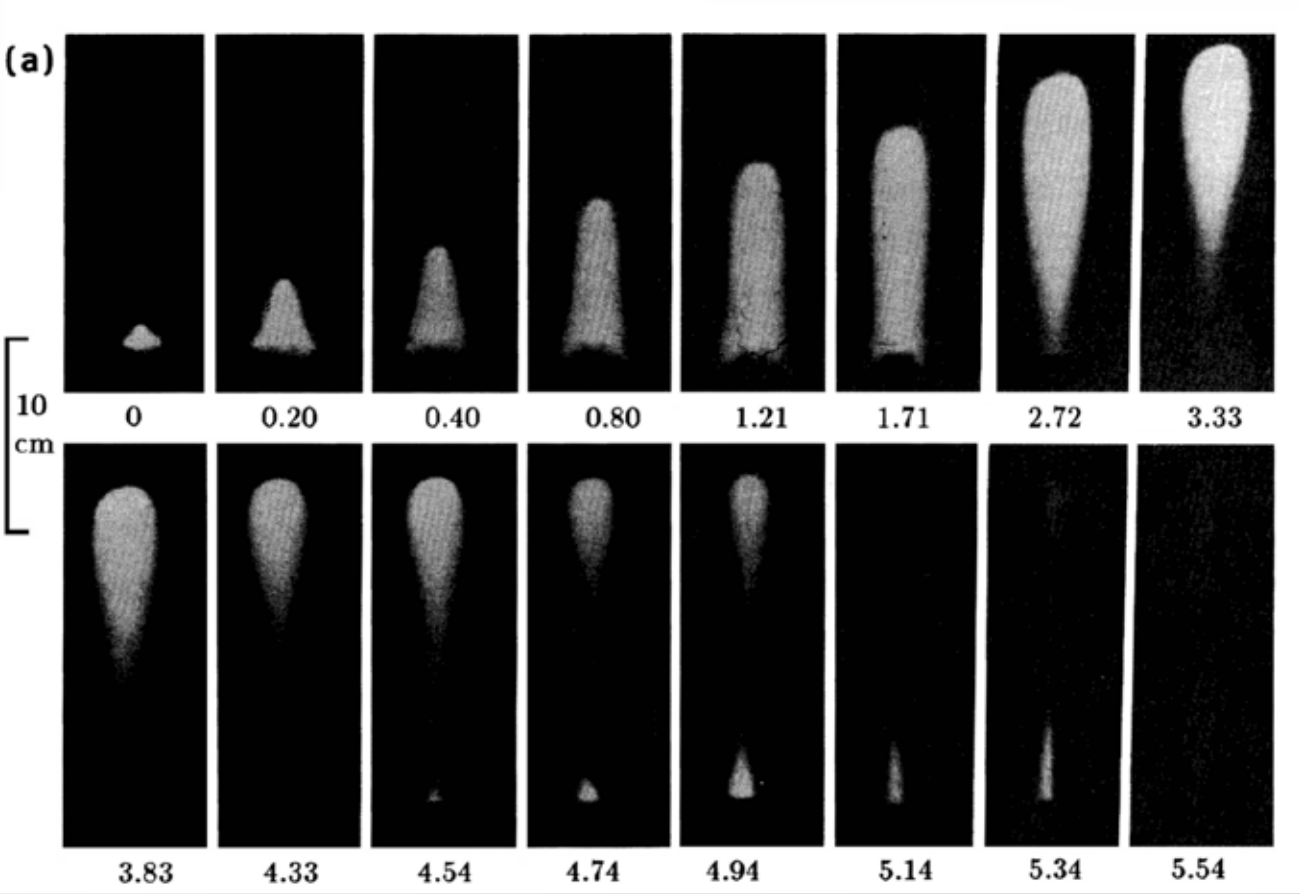

VON ALLMEN, M., BLATTER, A.: "Laser Beam Interaction with Materials". Springer-Verlag (1995)

Phenomenology of Laser-Matter Interaction at Moderately High Intensities (10^9-10^{12} W/cm^2) Macroscopic Approach

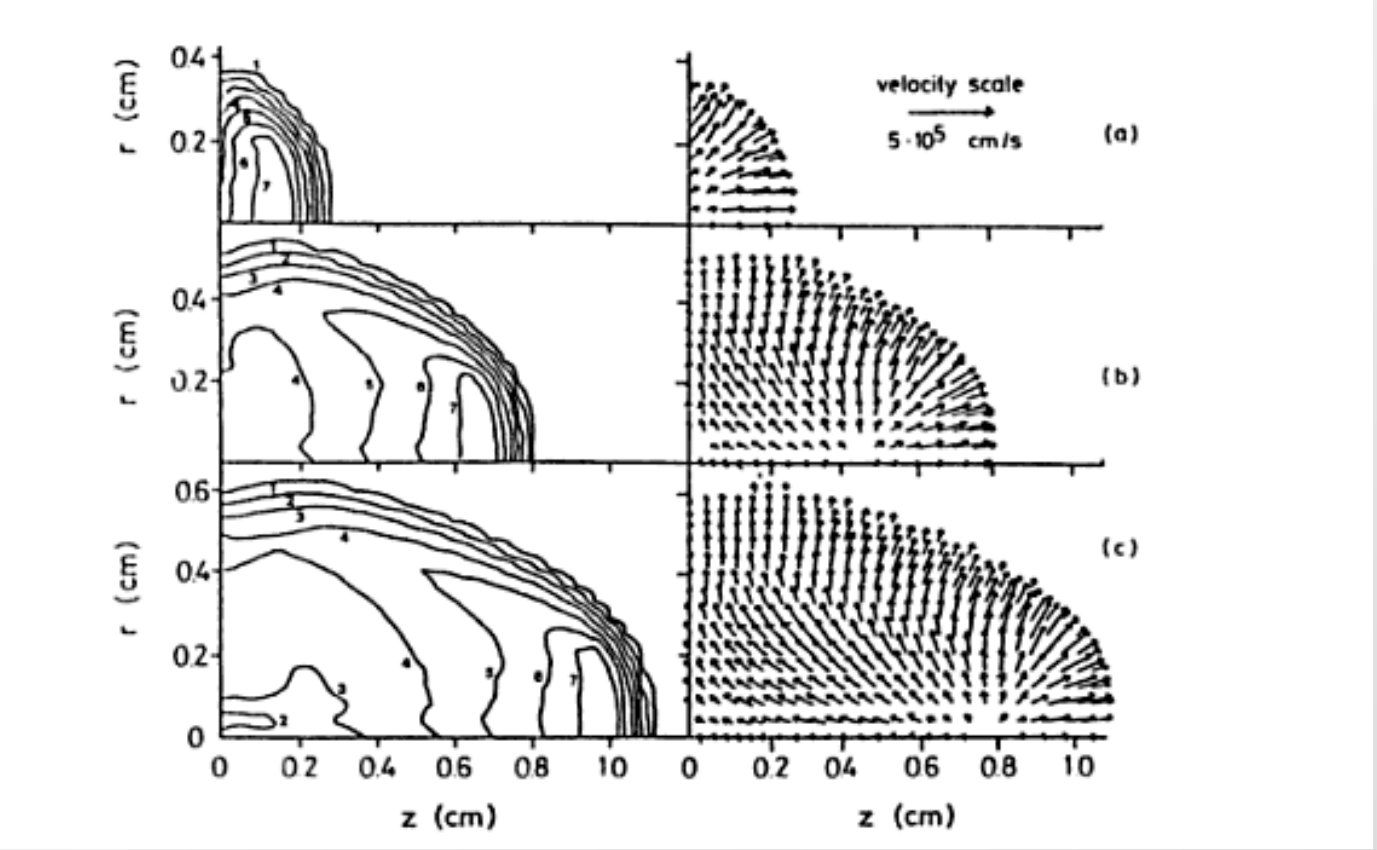

NIELSEN, P.E.: J. Appl. Phys. , 46 (1975), 4501-4505

Phenomenology of Laser-Matter Interaction at Moderately High Intensities (10^9-10^{12} W/cm^2) Detailed Physical Approach

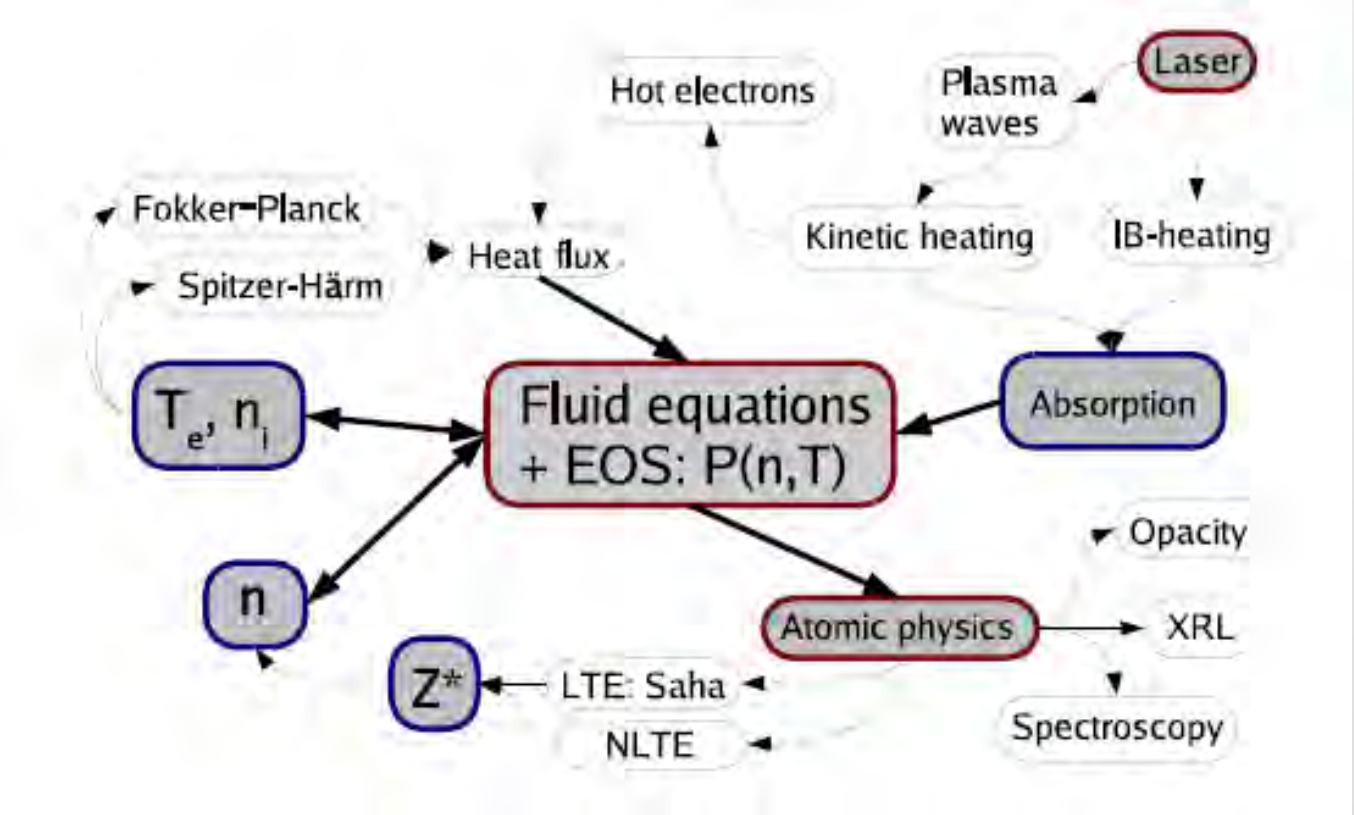

GIBBON, P.: Short Pulse Laser Interactions with Matter. Imperial College Press (2005)

LSP Concept

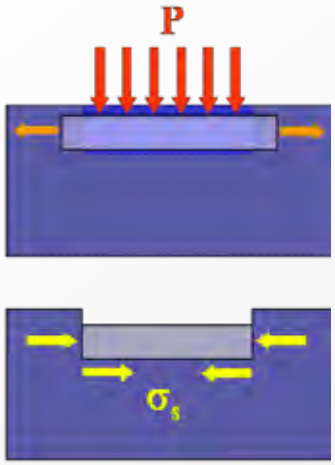
P
σ_s

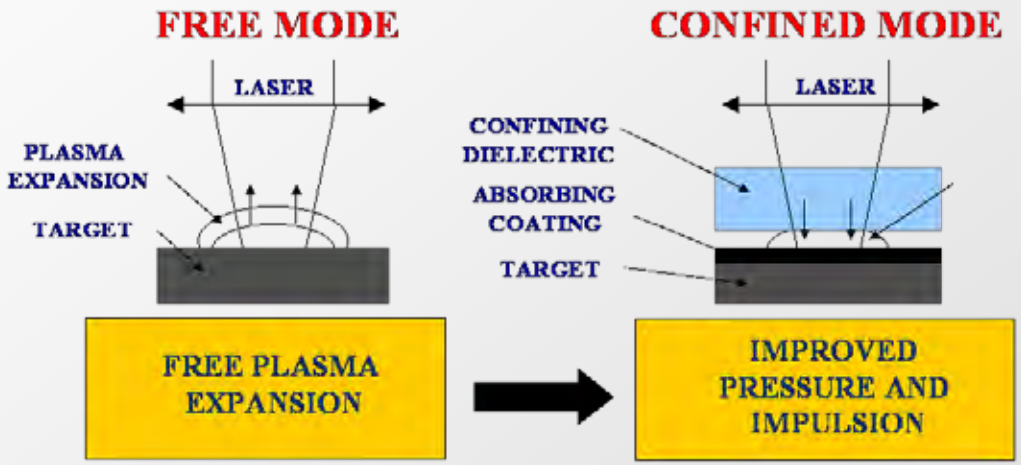
FREE MODE
LASER
PLASMA EXPANSION
TARGET
CONFINED MODE
LASER
CONFINING DIELECTRIC
ABSORBING COATING
TARGET
FREE PLASMA EXPANSION
IMPROVED PRESSURE AND IMPULSION

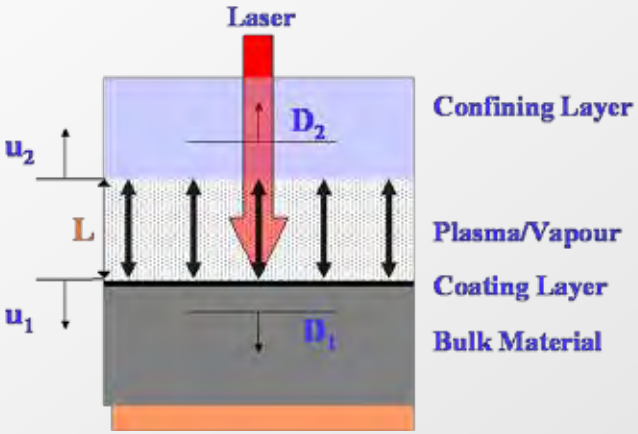
Laser
D_2
u_2
L
u_1
D_1
Confining Layer
Plasma/Vapour
Coating Layer
Bulk Material

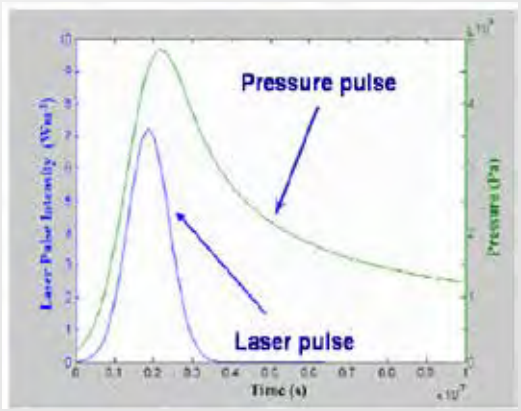
Pressure pulse
Laser pulse
Time (s)

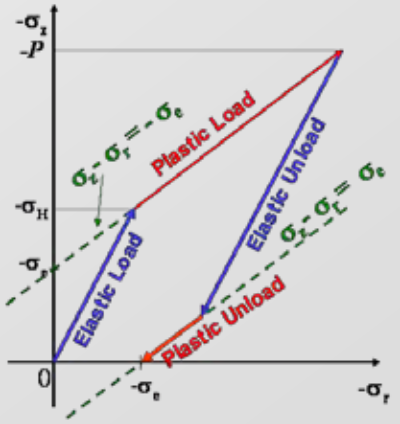
$-\sigma_z$
$-P$
$-\sigma_H$
$-\sigma_r$
0
$-\sigma_\theta$
$-\sigma_z$
Plastic Load
Elastic Unload
Elastic Load
Plastic Unload

LSP Concept

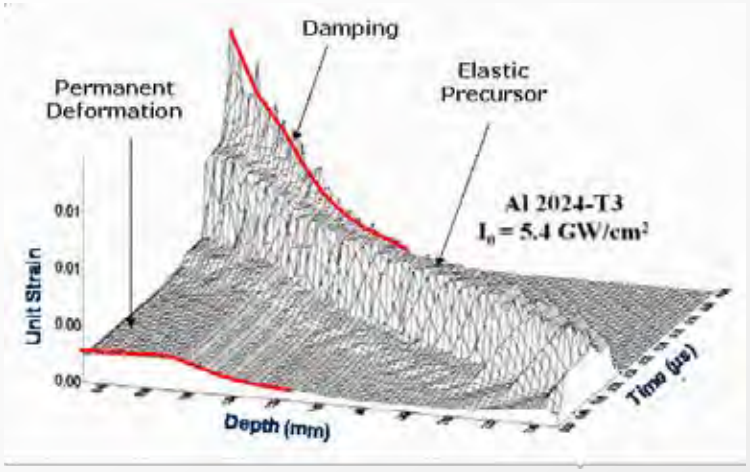
Damping
Permanent Deformation
Elastic Precursor
Al 2024-T3
I_0 = 5.4 GW/cm²
Unit Strain
0.01
0.01
0.00
0.00
Depth (mm)
Time (ps)

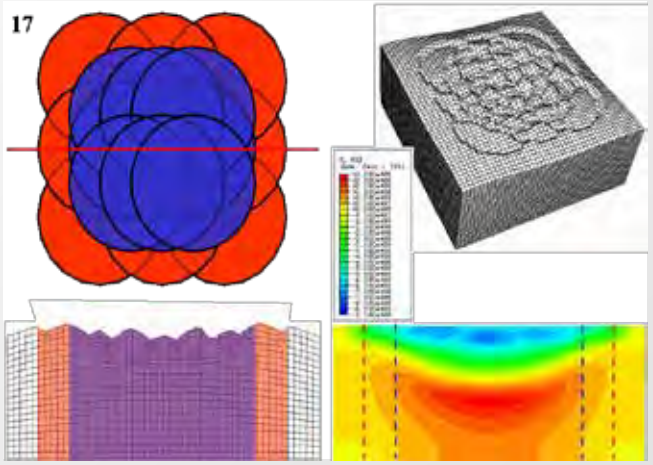
17

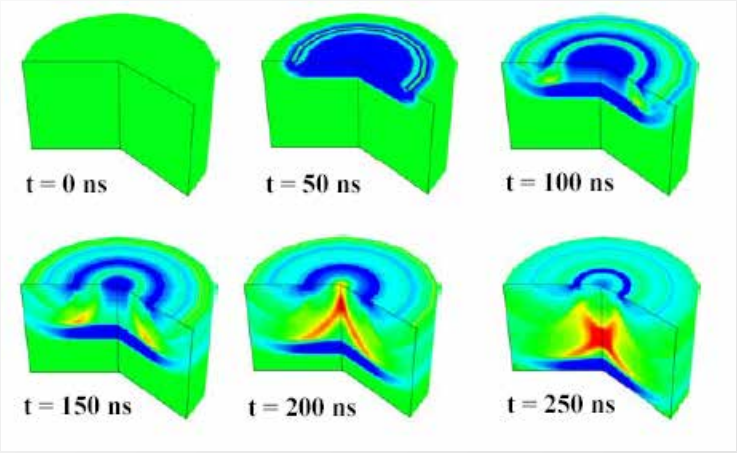
t = 0 ns
t = 50 ns
t = 100 ns
t = 150 ns
t = 200 ns
t = 250 ns

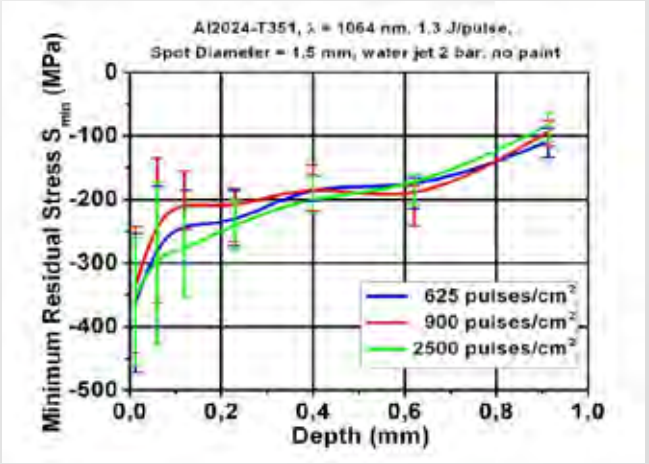
Al2024-T351, λ = 1064 nm, 1.3 J/pulse,
Spot Diameter = 1.5 mm, water jet 2 bar, no paint
Minimum Residual Stress S_{min} (MPa)
0
-100
-200
-300
-400
-500
0,0
0,2
0,4
0,6
0,8
1,0
Depth (mm)
625 pulses/cm²
900 pulses/cm²
2500 pulses/cm²

LSP Physical Basis

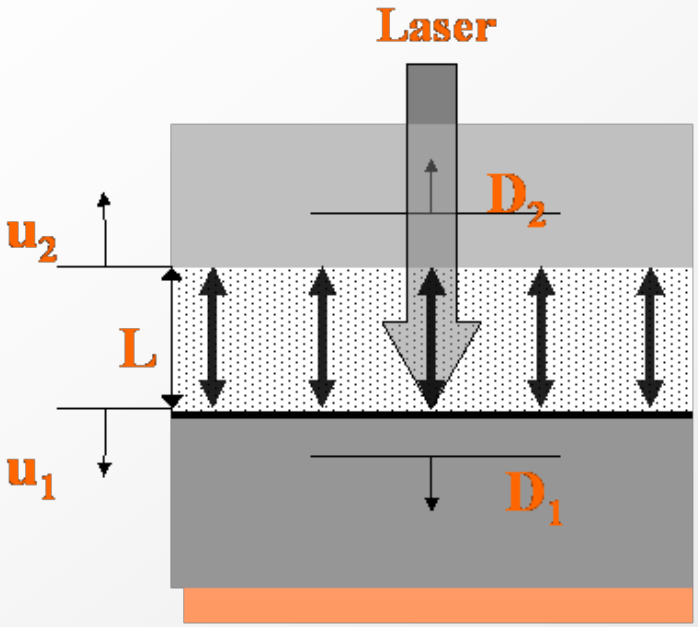

LSPSIM

Interface thickness

$$L(t) = \int_0^t [u_1(t) + u_2(t)]\, dt$$

Shock wave relation

$$P = \rho_i D_i u_i$$

Heating phase

$$I(t) = P(t)\frac{dL(t)}{dt} + \frac{d[E_i(t)L(t)]}{dt}$$

$$P(t) = \frac{2}{3}E_t(t) = \frac{2}{3}\alpha E_i(t)$$

Solid/Liquid $D = C + Su$

Gas $D = u = \left(\frac{(\gamma+1)}{2}\frac{P}{\rho}\right)^{1/2}$

LSP Physical Basis

Pressure pulse applied to Al target with water as confining medium

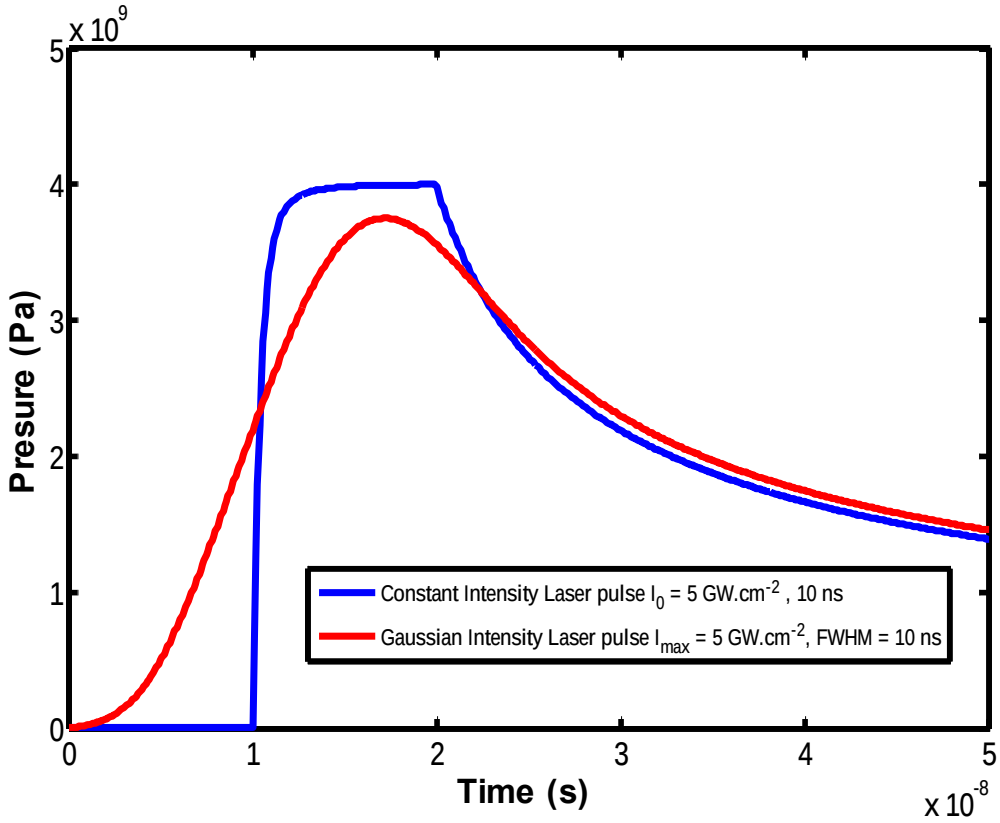

LSP Physical Basis

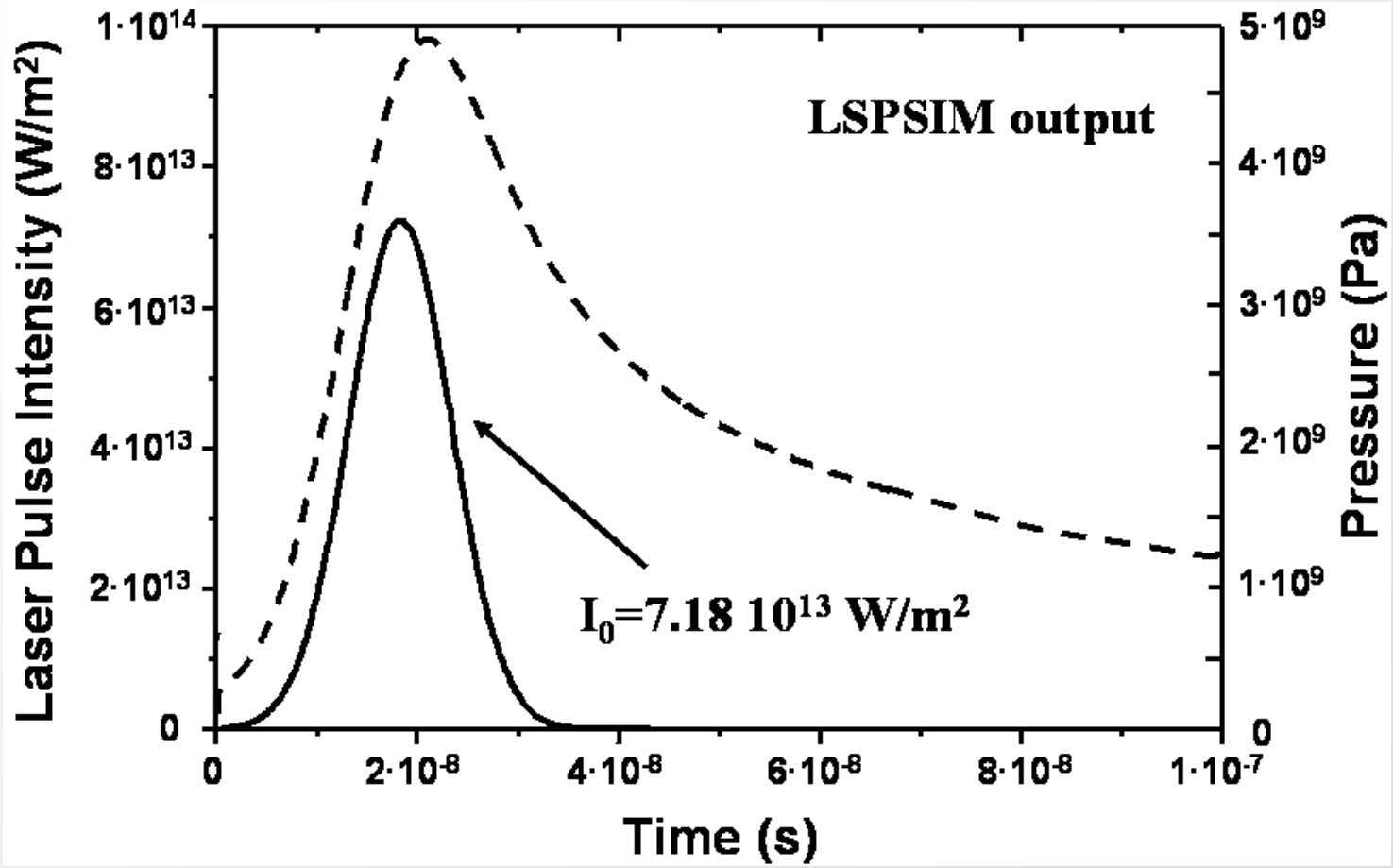

LSP Physical Basis

Maximum transmitted pressure and pressure pulse duration vs. laser intensity; l =532 nm, 1064 nm

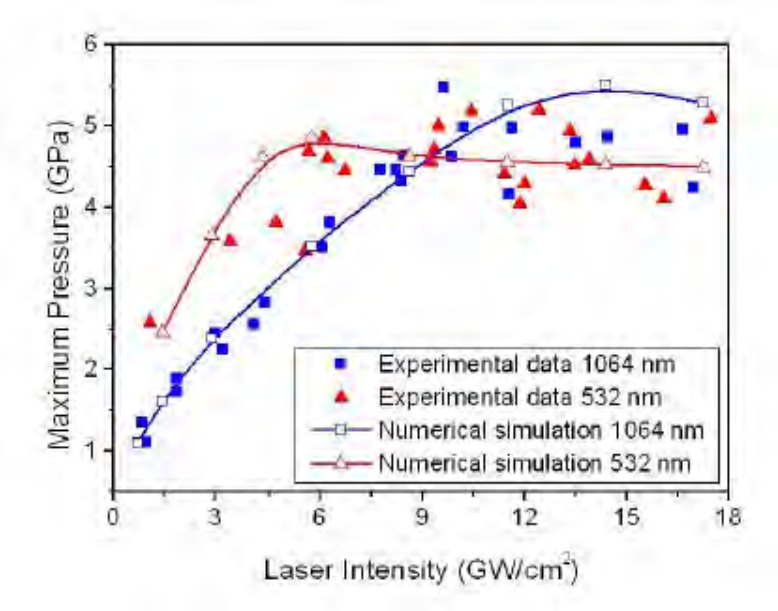

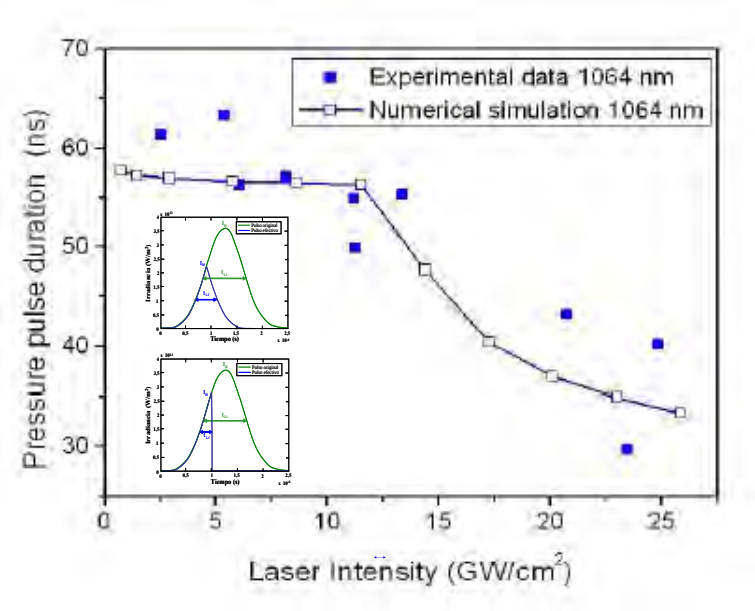

Experimental data from: BERTHE, L. et al. in J. Appl. Phys., 85 (1999), 7552-7555

LSP Physical Basis

Water dielectric breakdown thresholds; l =1064 nm

Purified water

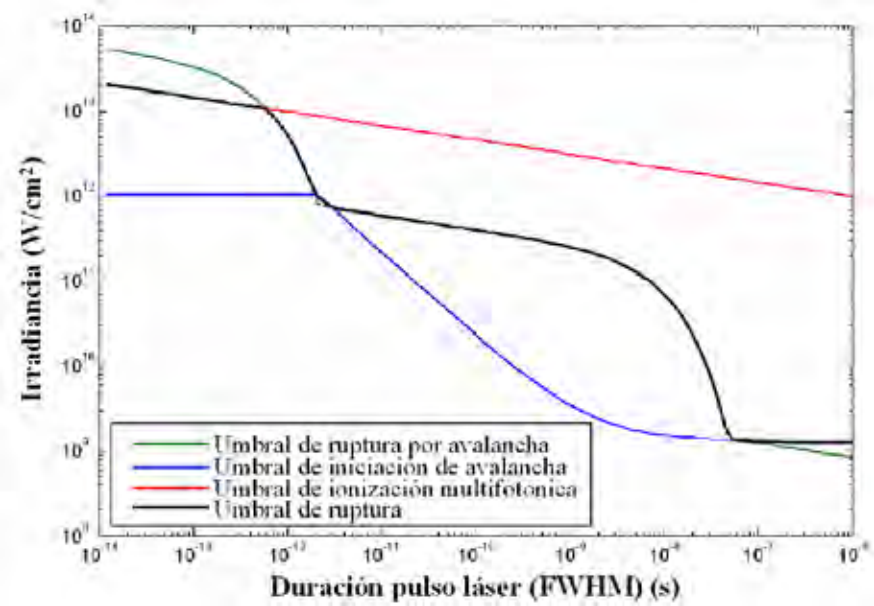

Water with impurities

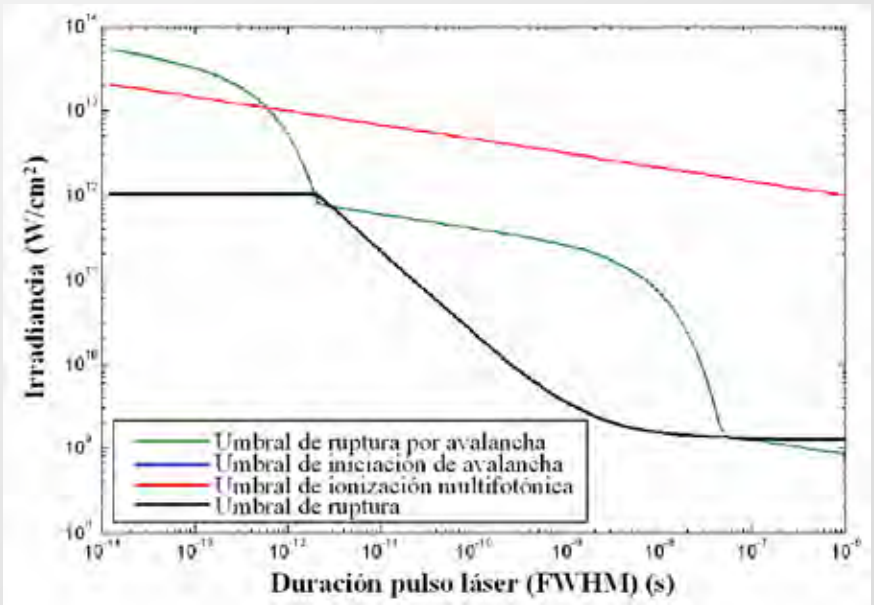

LSP Physical Basis

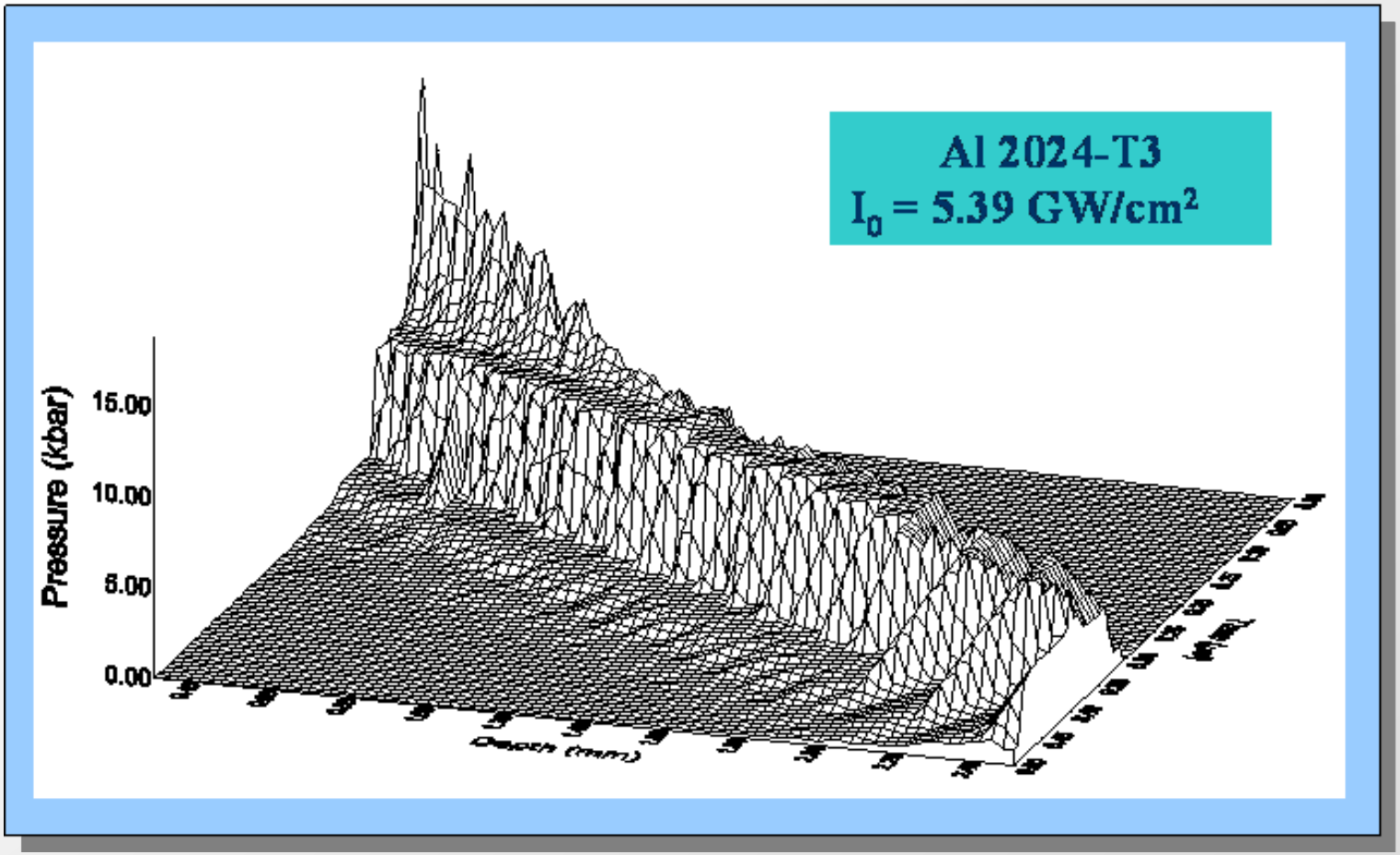

LSP Physical Basis

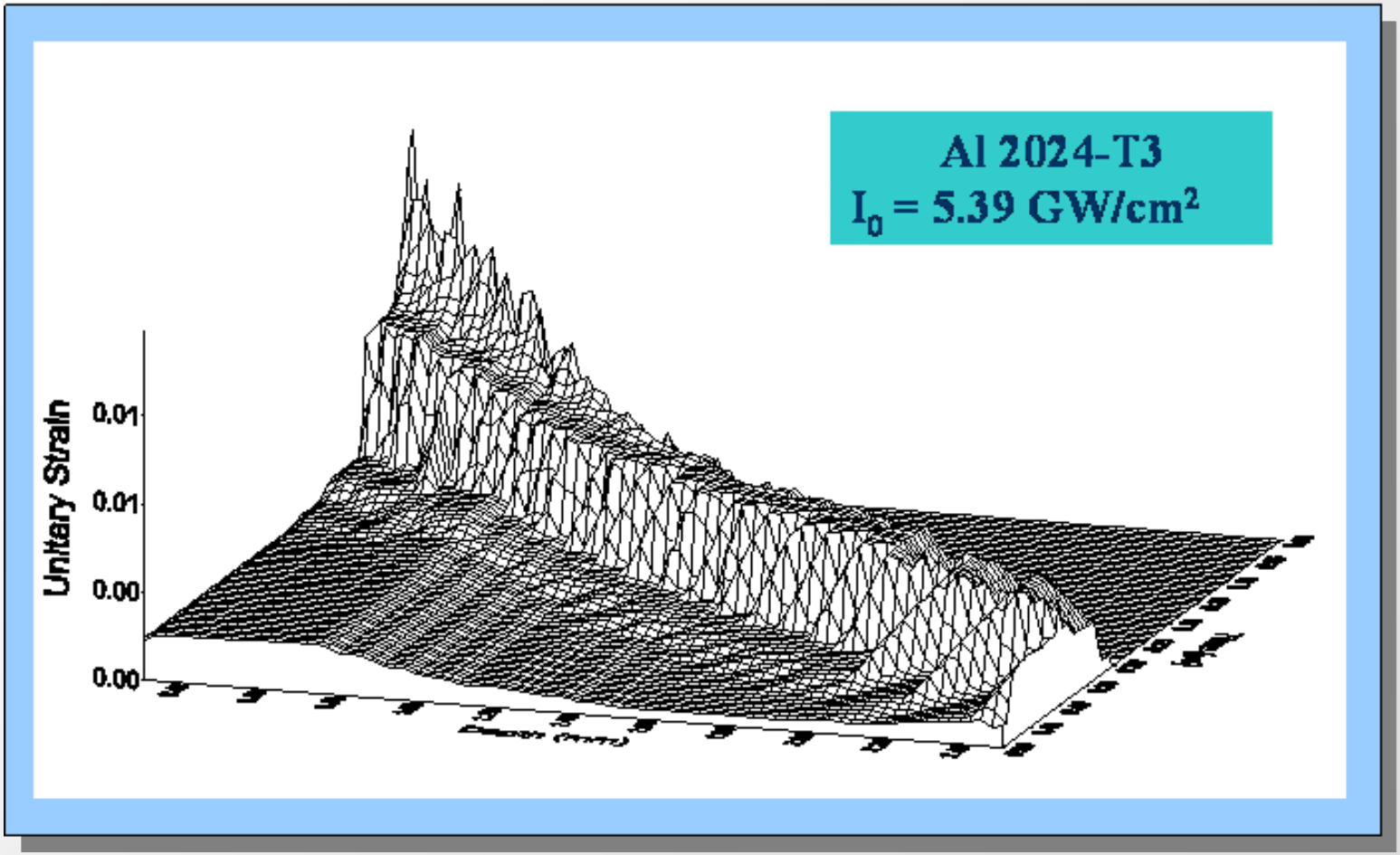

Ti6Al4V

Radial stress dynamic analysis

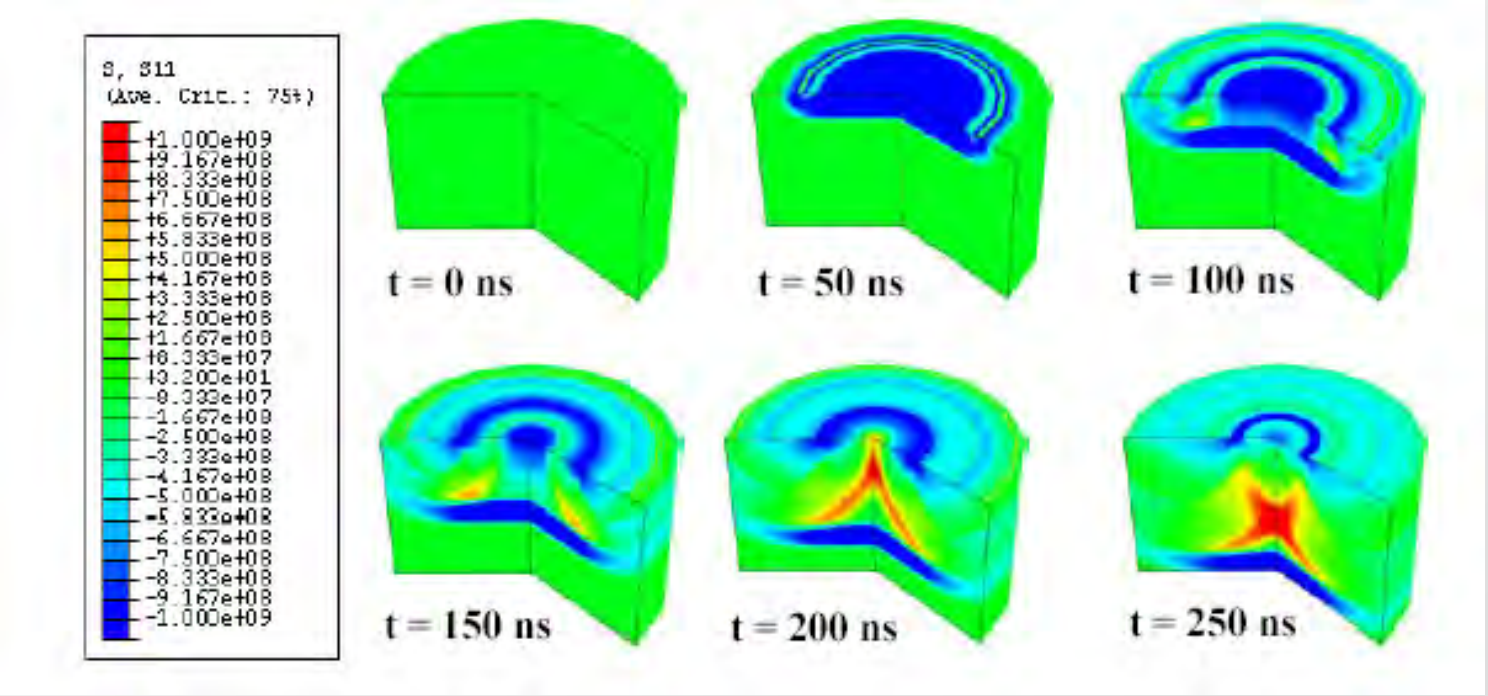

LSP Physical Basis

Ti6Al4V

Nd:YAG (1064 nm)
P_{av}= 5,7 W/cm^2
Spot radius = 0.75 mm
FWHM = 0 ns
a = 0.15

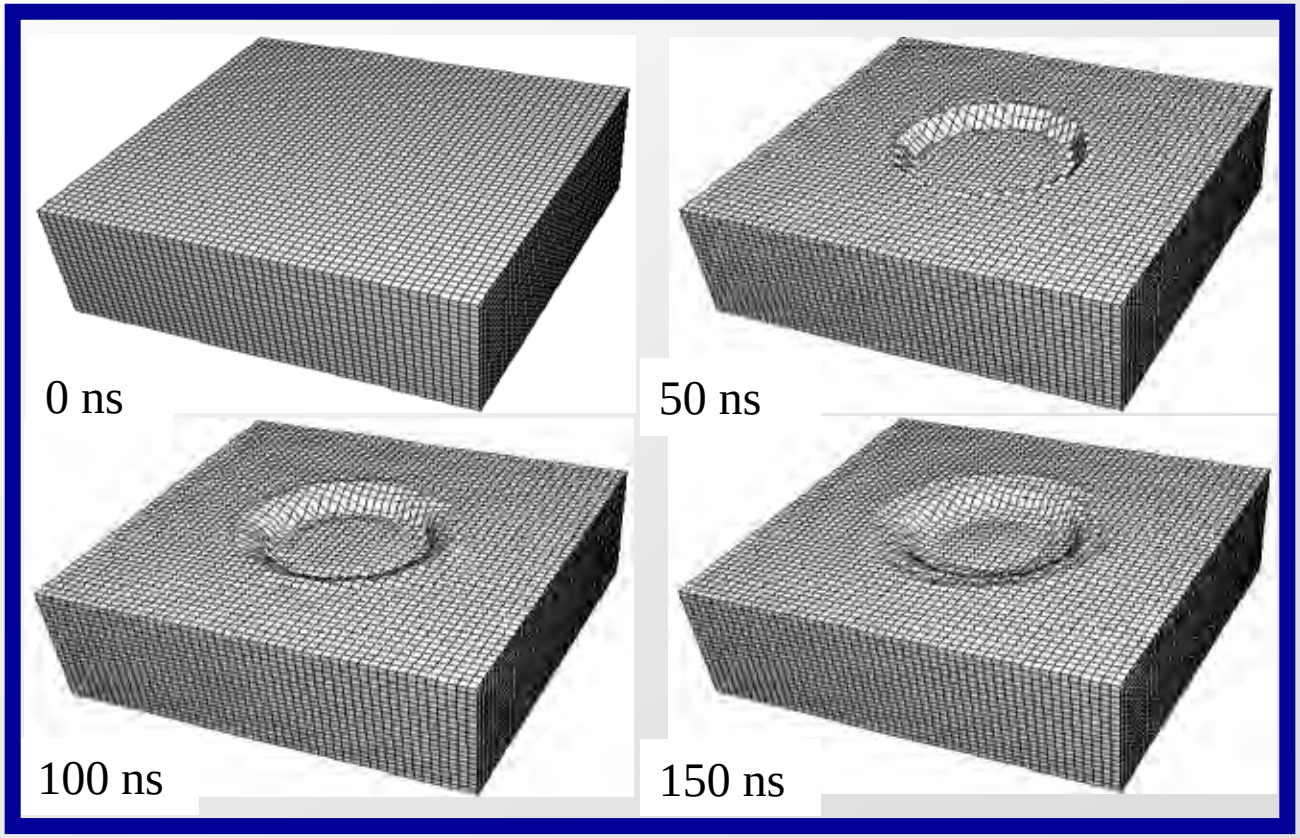

Multiple shocks dynamic analysis

The SHOCKLAS Calculational System

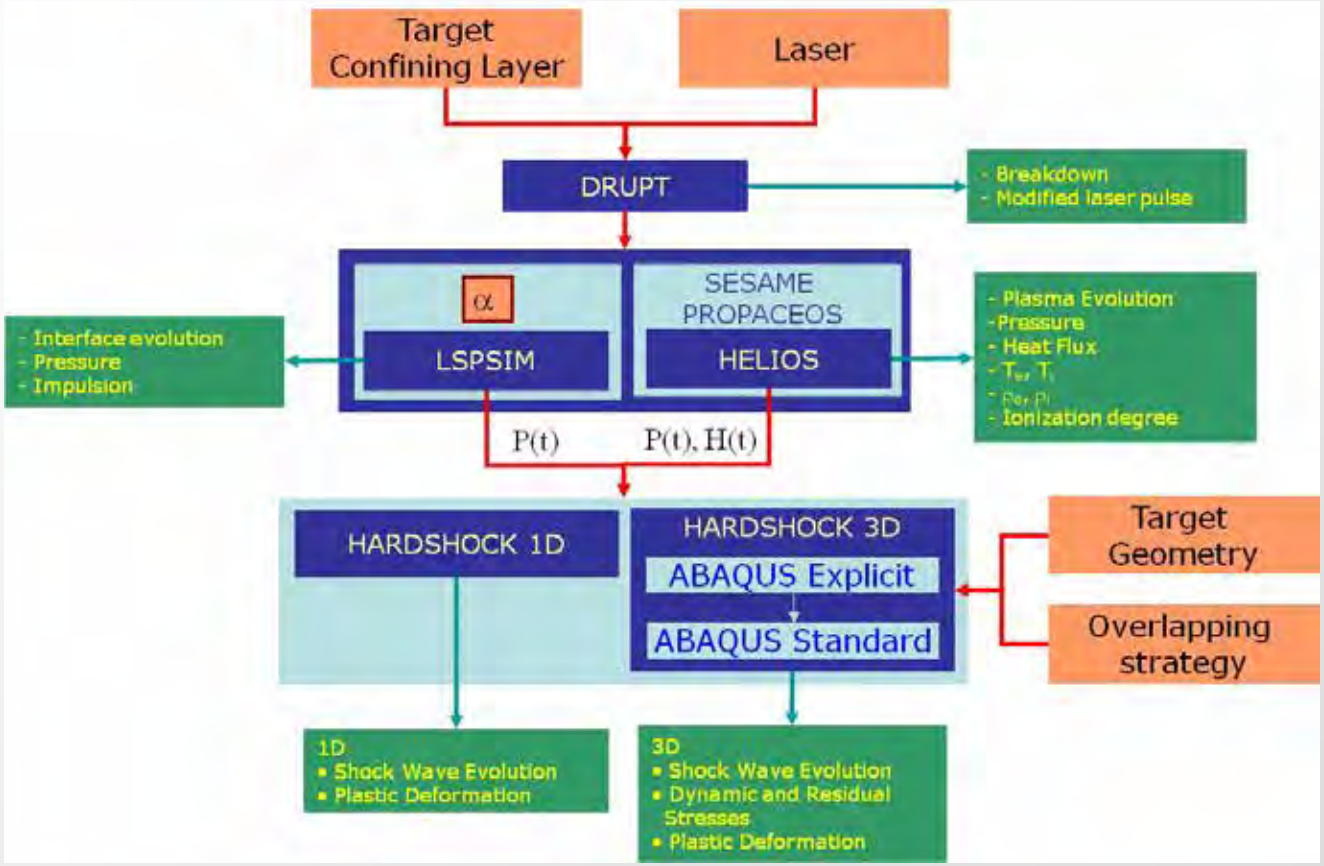

Process Modelling

HELIOS

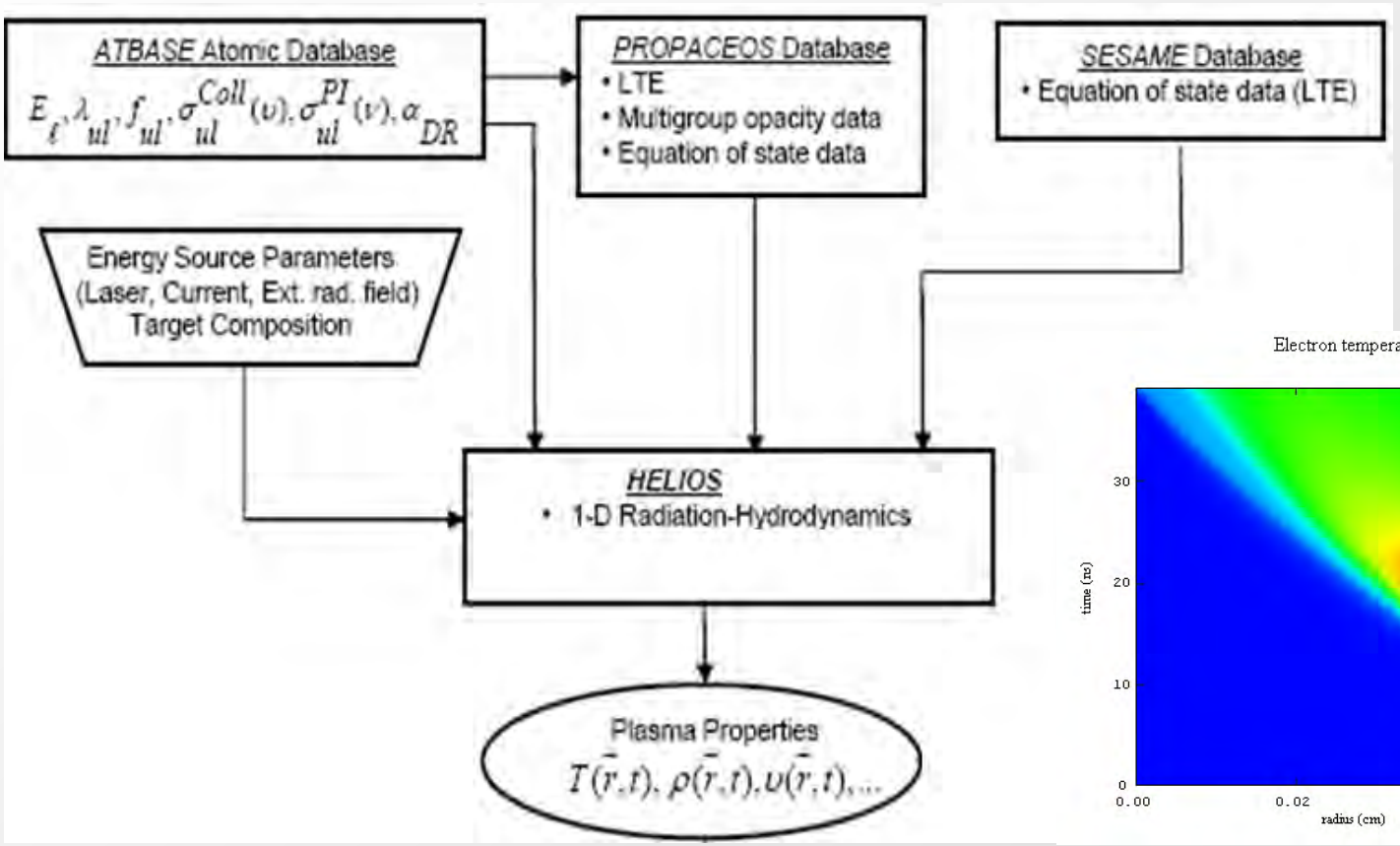

HELIOS Analysis of relative influence of confining material

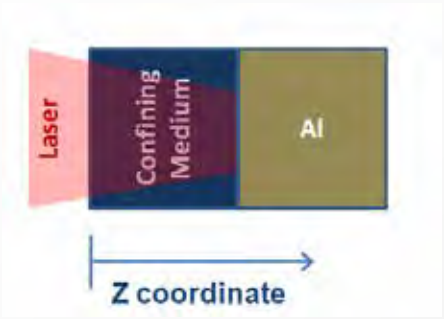

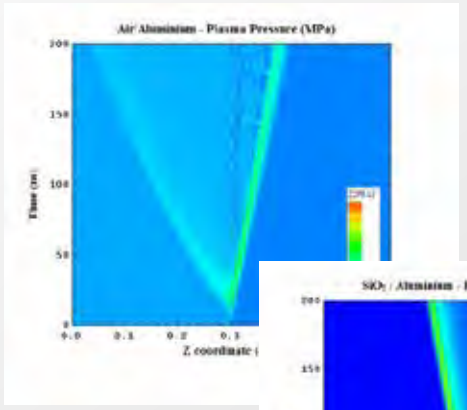

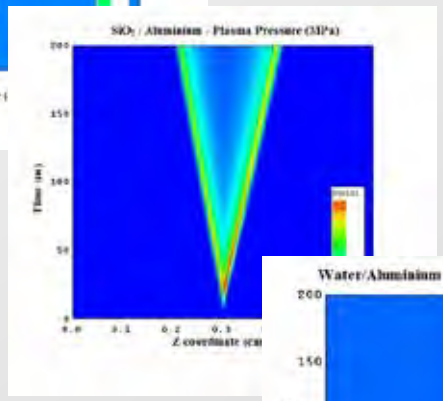

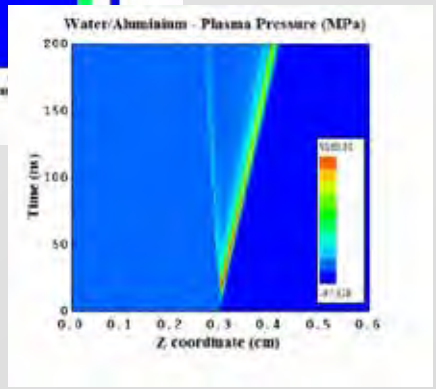

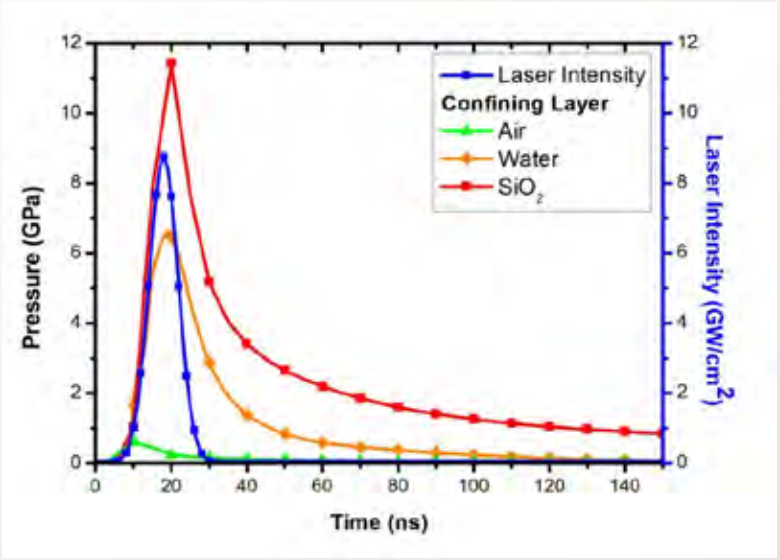

HELIOS

Analysis of influence of water layer thickness

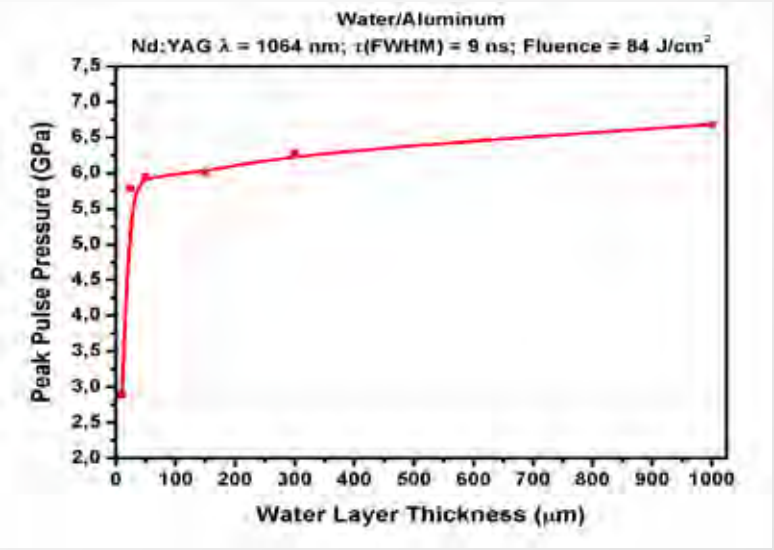

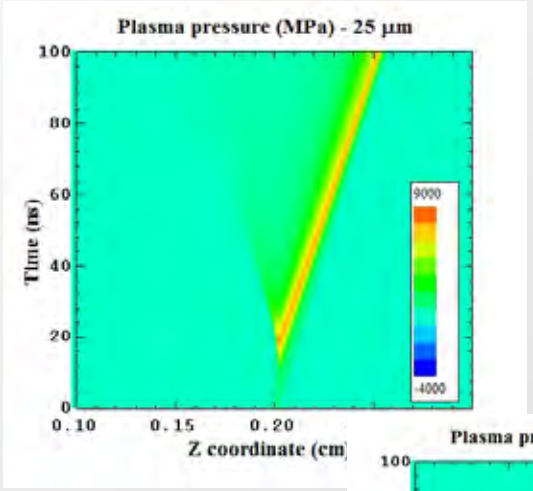

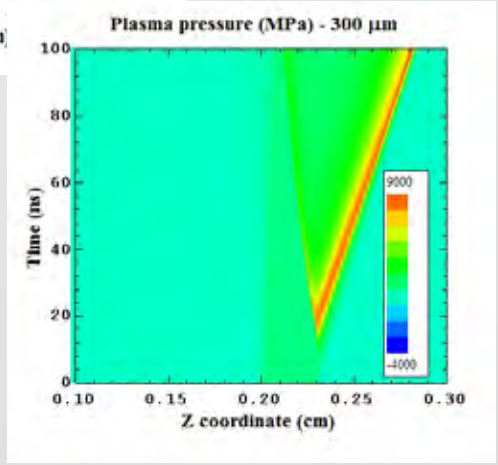

HELIOS

Analysis of plasma for LSP conditions

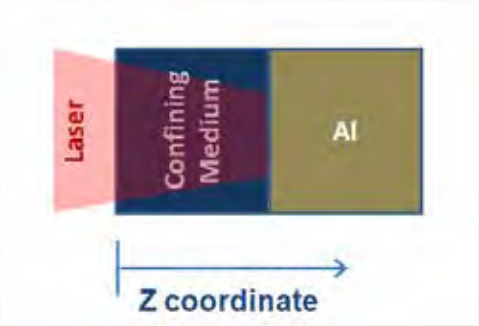

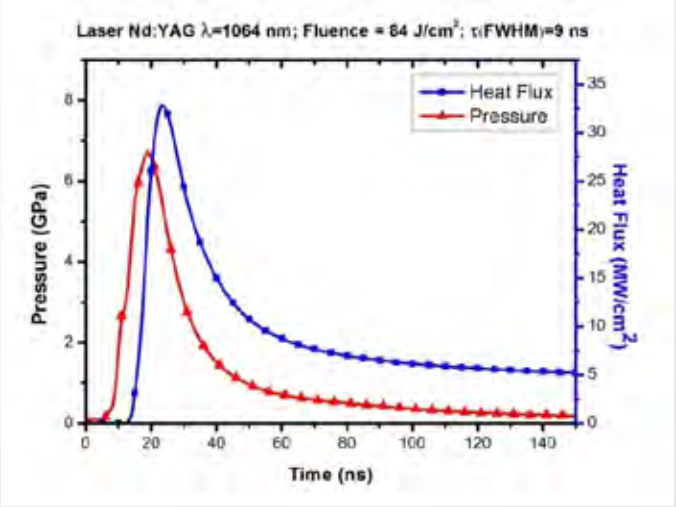

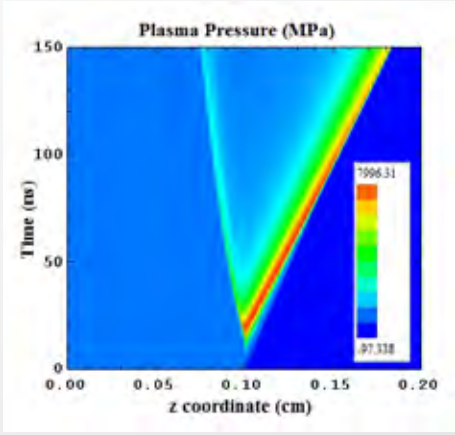

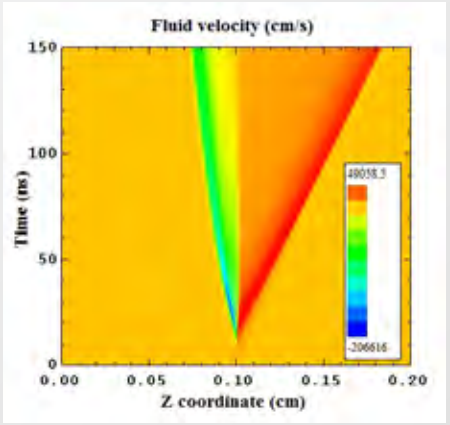

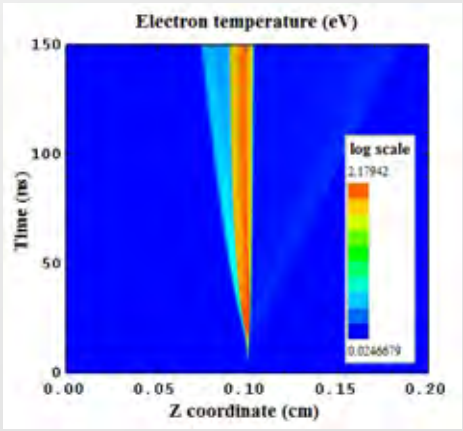

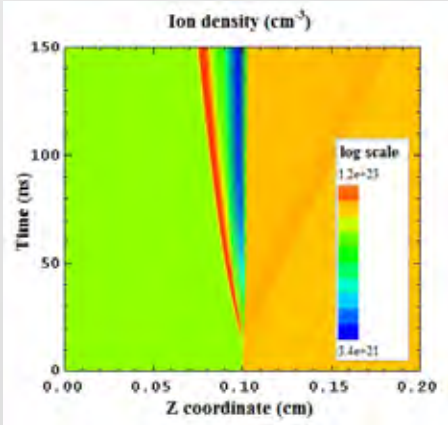

HARDSHOCK-1D*

- 1D Motion: Mass
  Momentum
  Energy

  (Method of characteristics)

- Hydrodynamic/elastic-plastic
  (Von Mises yield criterion)

- Ideal gas/Grüneisen E.O.S.

$$r_1 u_1 = r_0 u_0$$
$$P_1 + r_1 u_1^2 = P_0 + r_0 u_0^2$$
$$e_1 + \frac{P_1}{r_1} + \frac{u_1^2}{2} = e_0 + \frac{P_0}{r_0} + \frac{u_0^2}{2}$$

$$|s_x - s_r| < -YS$$

$$P = P_h + \Gamma\rho\,(W - W_h)$$
$$W_h = \frac{P_h e}{2\rho_0} \qquad P_h = \frac{\rho_0 C_0^2 e}{(1 - Se)^2}$$
$$U_s = C_0 + S \cdot U_p$$

* L.M. BARKER, L.M., YOUNG, E.G.:
"SWAP-9: An Improved Stress Wave Analyzing Program", Sandia Laboratories, Report SLA-74-0009 (1974).

Johnson-Cook deformation model

$$\sigma = \left[A + B \cdot \varepsilon_{eq}^{pl\ n}\right] \cdot \left[1 + C \ln\left(\frac{\dot{\varepsilon}_{eq}^{pl}}{\dot{\varepsilon}_0}\right)\right] \cdot (1 - \theta^m)$$

$$\varepsilon_{eq}^{pl} = \int_0^t \dot{\varepsilon}_{eq}^{pl}\, dt$$

$$\dot{\varepsilon}_{eq}^{pl} = \sqrt{\frac{2}{3}\left(\dot{\varepsilon}^{pl} : \dot{\varepsilon}^{pl}\right)}$$

$$\theta = \begin{cases} 0 & T < T_r \\ (T - T_r)/(T_m - T_r) & T_r \leq T \leq T_m \\ 1 & T > T_m \end{cases}$$

$T_r \equiv$ room temperature

$T_m \equiv$ melting temperature

Material Properties effects

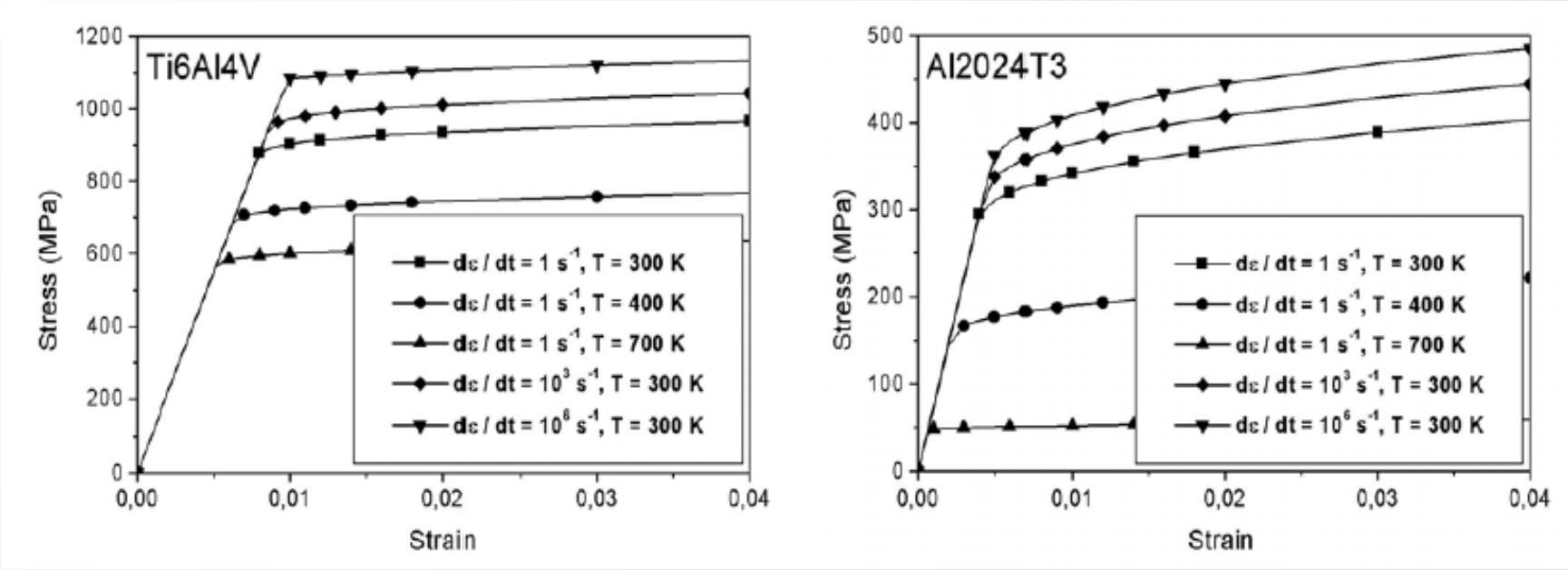

Process Modelling

Ti6Al4V

Nd:YAG (1064 nm)
P_{av}= 5,7 W/cm^2
Spot radius = 0.75 mm
FWHM = 0 ns
a = 0.15

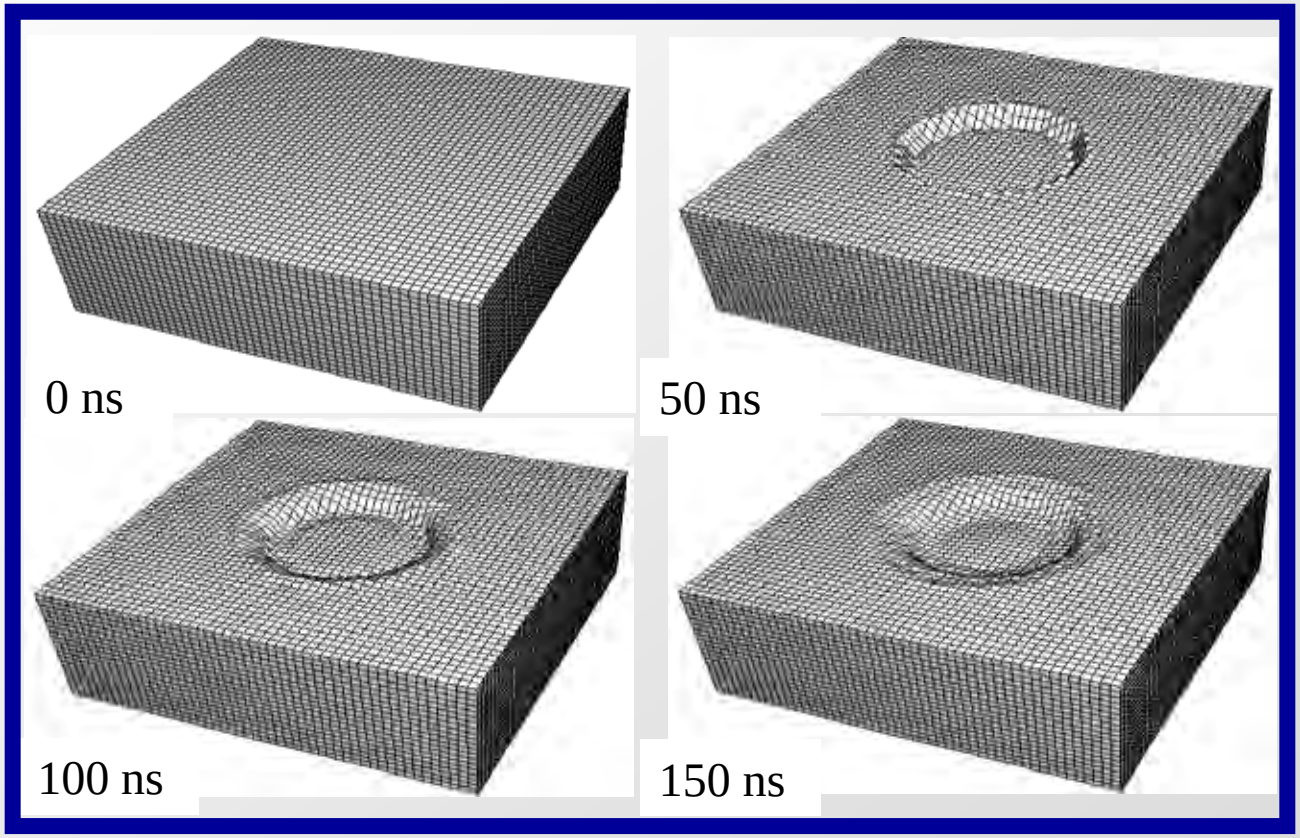

Multiple shocks dynamic analysis

HARDSHOCK-2D Semi-infinite

Ti6Al4V

Nd:YAG (1064 nm)
P_{av}= 5,7 W/cm^2
Spot radius = 0.75 mm
FWHM = 0 ns
a = 0.15

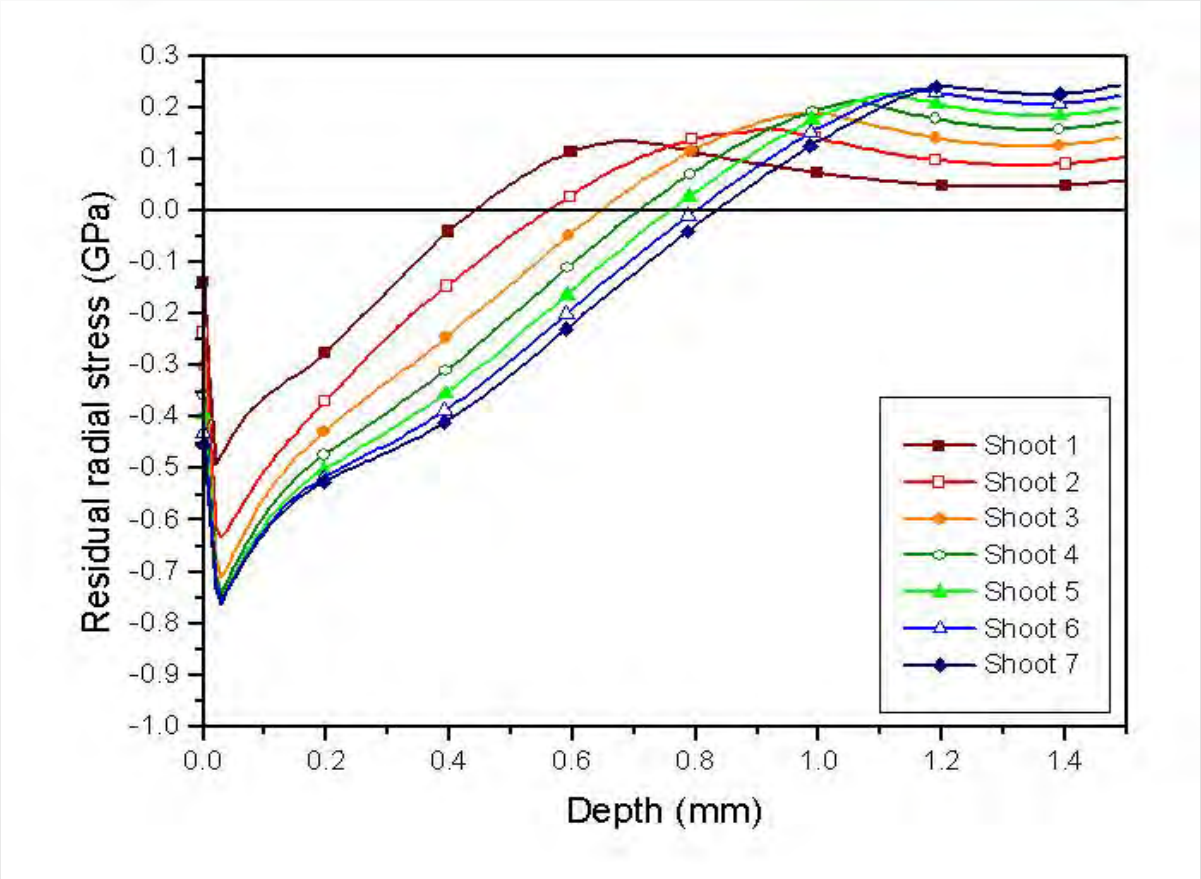

Multiple shocks dynamic analysis

HARDSHOCK-2D Semi-infinite

Ti6Al4V

Nd:YAG (1064 nm)
P_{av}= 5,7 W/cm^2
Spot radius = 0.75 mm
FWHM = 0 ns
a = 0.15

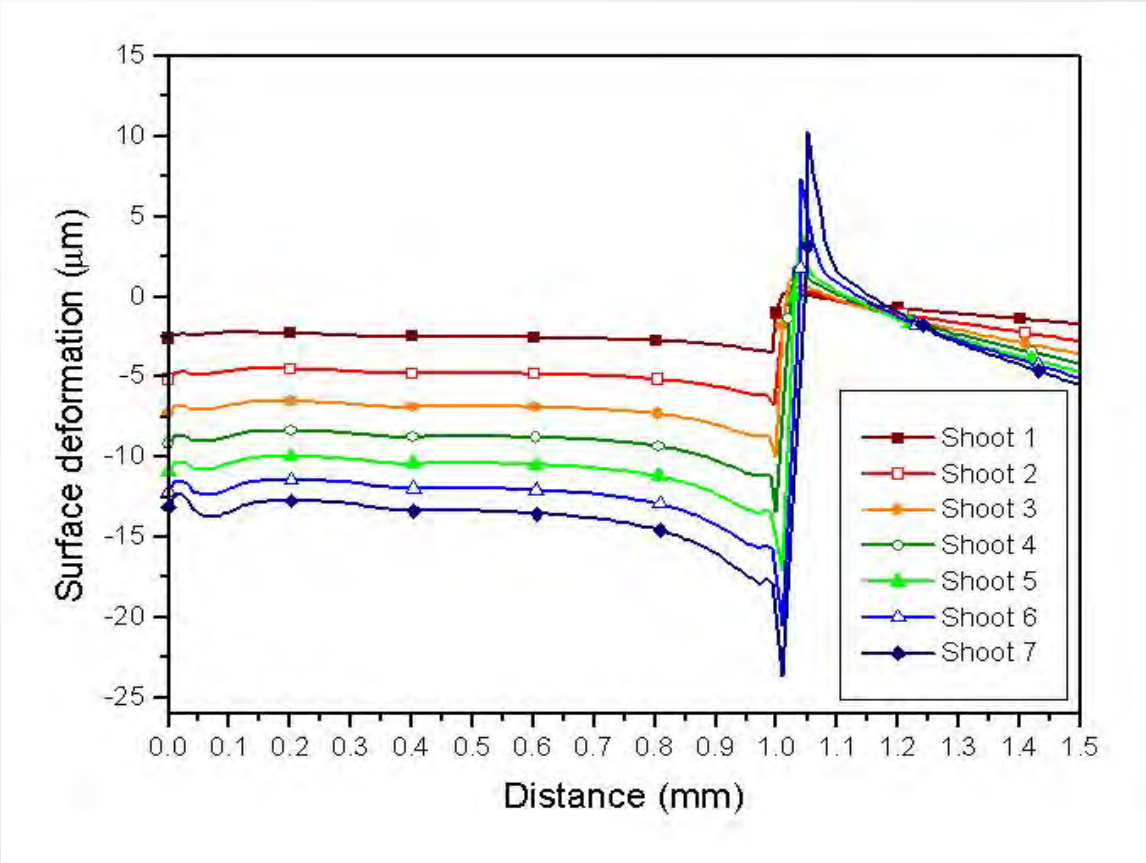

Multiple shocks dynamic analysis

HARDSHOCK-3D (full scope)

Ti6Al4V

Nd:YAG (1064 nm)
P_{av}= 5,7 W/cm^2
Spot radius = 0.75 mm
FWHM = 0 ns
a= 0.15
Overlapping = 900/cm^2

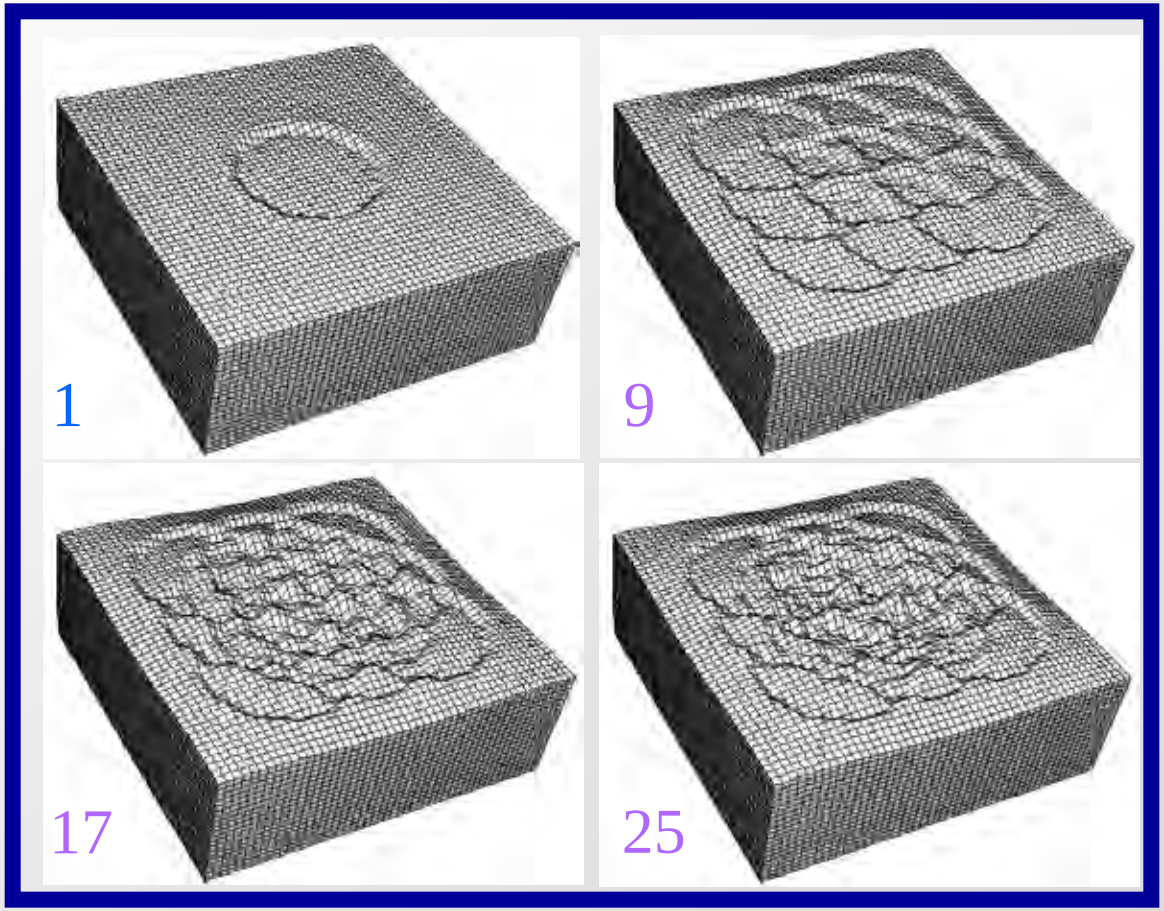

HARDSHOCK-3D (full scope)

Ti6Al4V

Nd:YAG (1064 nm)
P_{av}= 5,7 W/cm^2
Spot radius = 0.75 mm
FWHM = 0 ns
a= 0.15
Overlapping = 900/cm^2

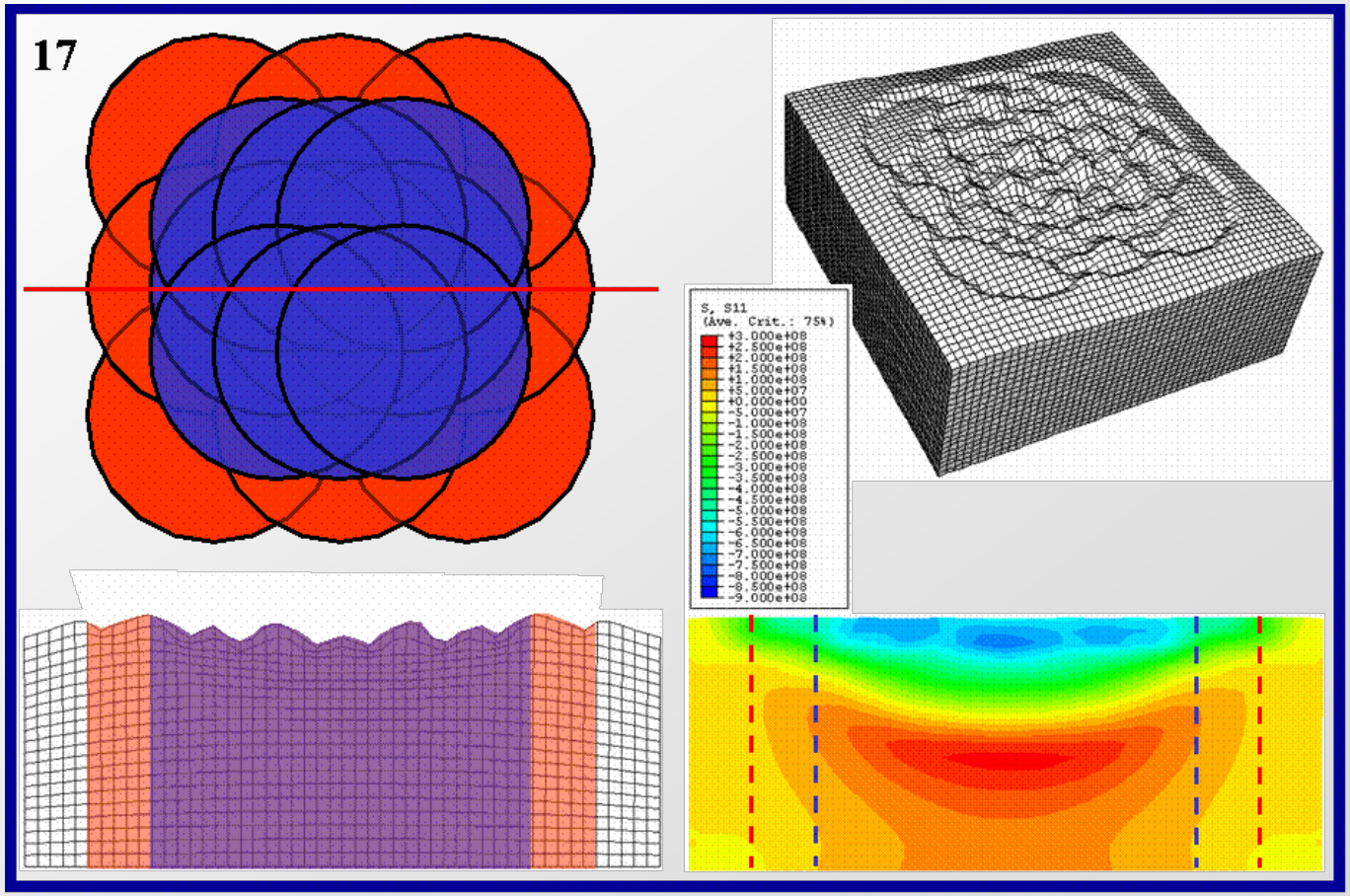

HARDSHOCK-3D (full scope)

Ti6Al4V

Nd:YAG (1064 nm)
P_{av}= 5,7 W/cm^2
Spot radius = 0.75 mm
FWHM = 0 ns
a= 0.15
Overlapping = 900/cm^2

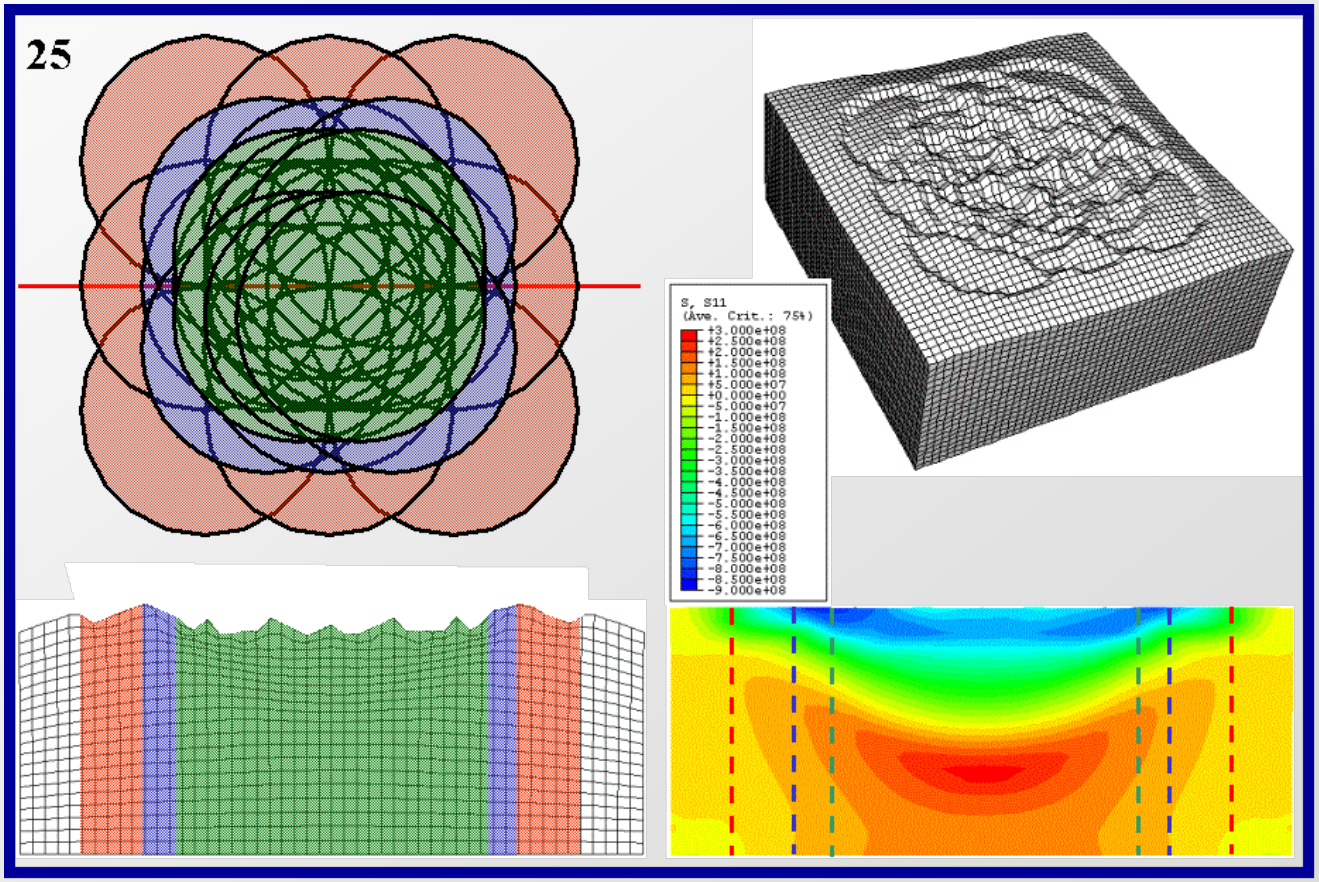

Process Modelling

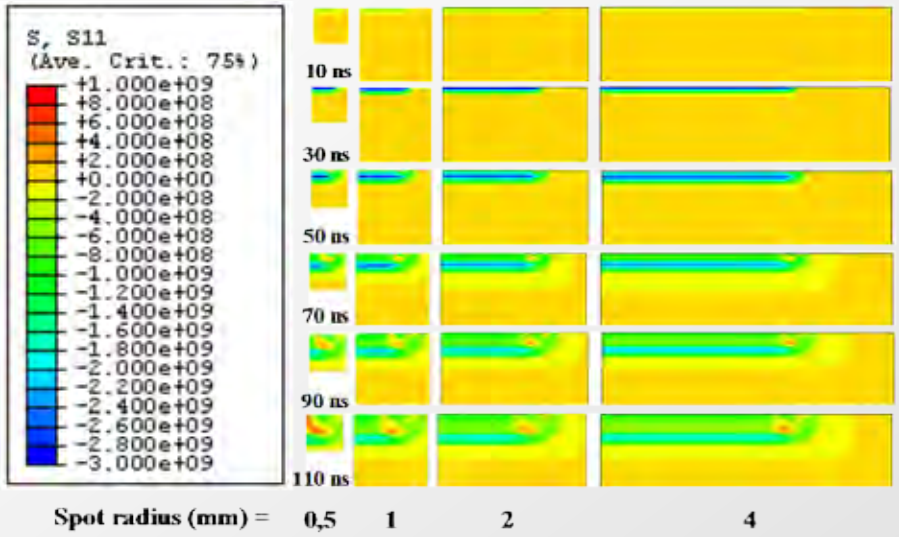

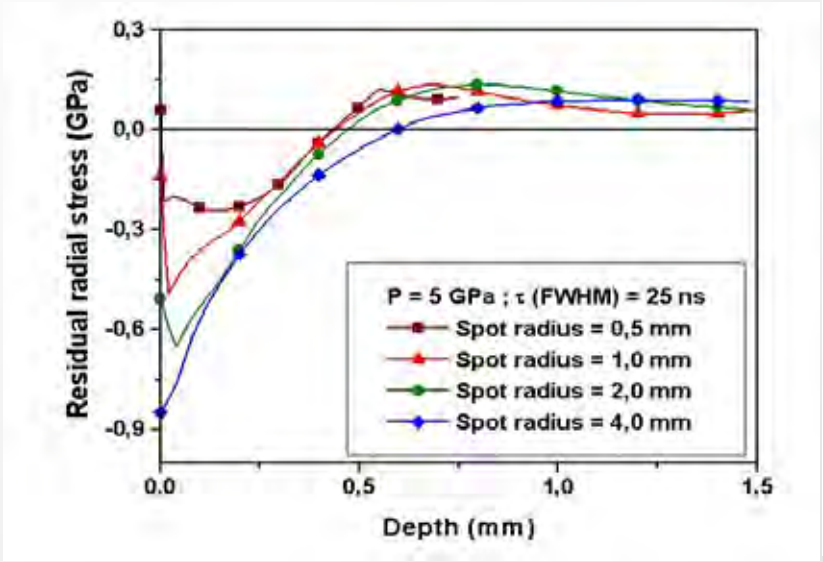

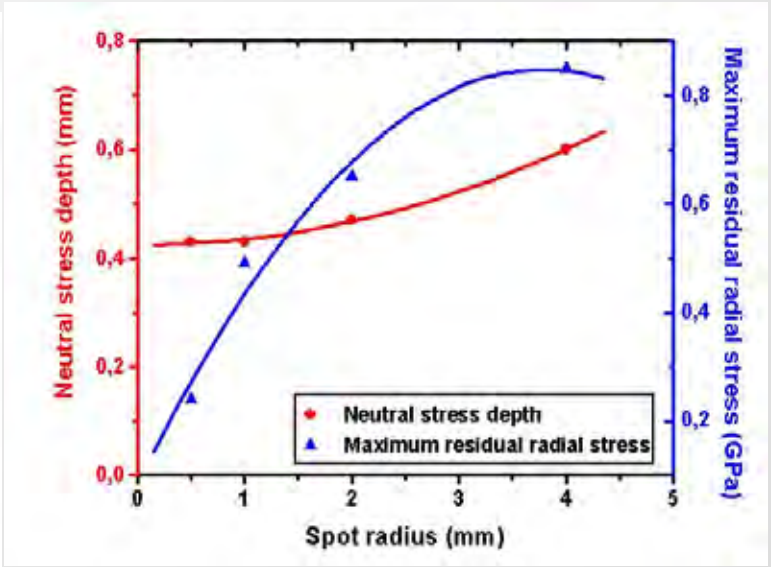

OCAÑA, J.L. et al.: "Predictive assessment and experimental characterization of the influence of irradiation parameters on surface deformation and residual stresses in laser-shock-processed metallic alloys". Proc. SPIE 5448, 642-653 (2004)

Material Properties effects

PROPERTY	TI6AI4V	AI2024T3
ρ Density (kg.m^{-3})	4 500	2 785
ν Poisson's ratio	0,342	0.330
E Elastic Modulus (MPa)	110	73.45
Y Yield strength (GPa)	1.345	0.330
HEL Hugoniot Elastic Limit (GPa)	2.8	0.65
T_m Melting temperature (K)	1878	775
Deformation model A (MPa)	862	265
Deformation model B (MPa)	331	426
Deformation model C	0.012	0.015
Deformation model m	0.8	1.0
Deformation model n	0.34	0.34

HARDSHOCK-3D (full scope)

Al2024T3

Residual Stress s_x (Pa)
(at middle xz plane)

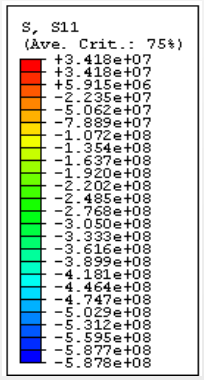

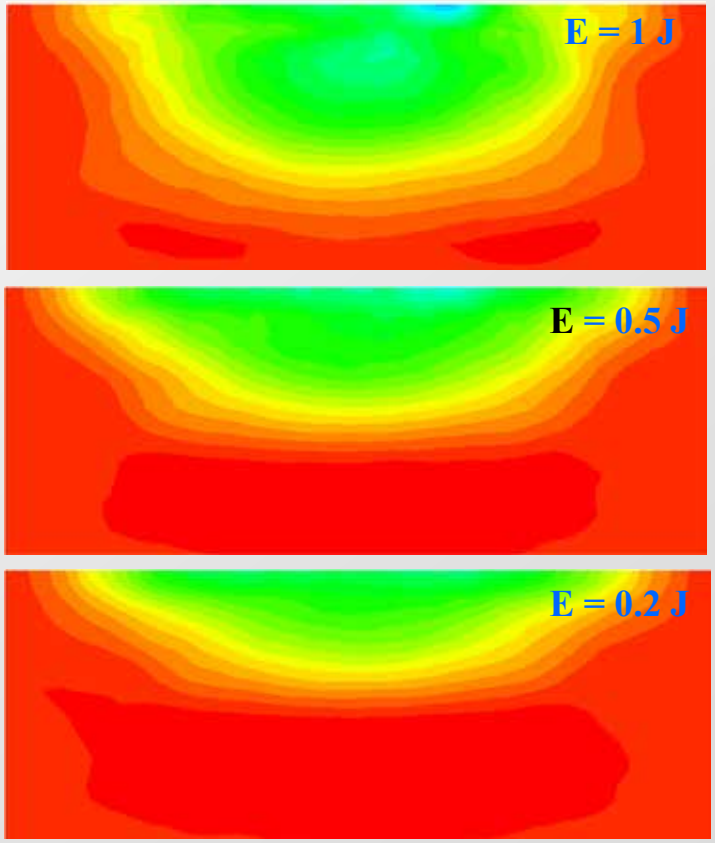

Laser Nd:YAG (l =1064 nm)
Effective Energy 1 J , 0.5 J and 0.2 J
FWHM 10 ns
Spot radius = 0.75 mm
Spot overlapping 900 pulses/cm^2
a= 0.15

HARDSHOCK-3D (full scope)

Al2024T3

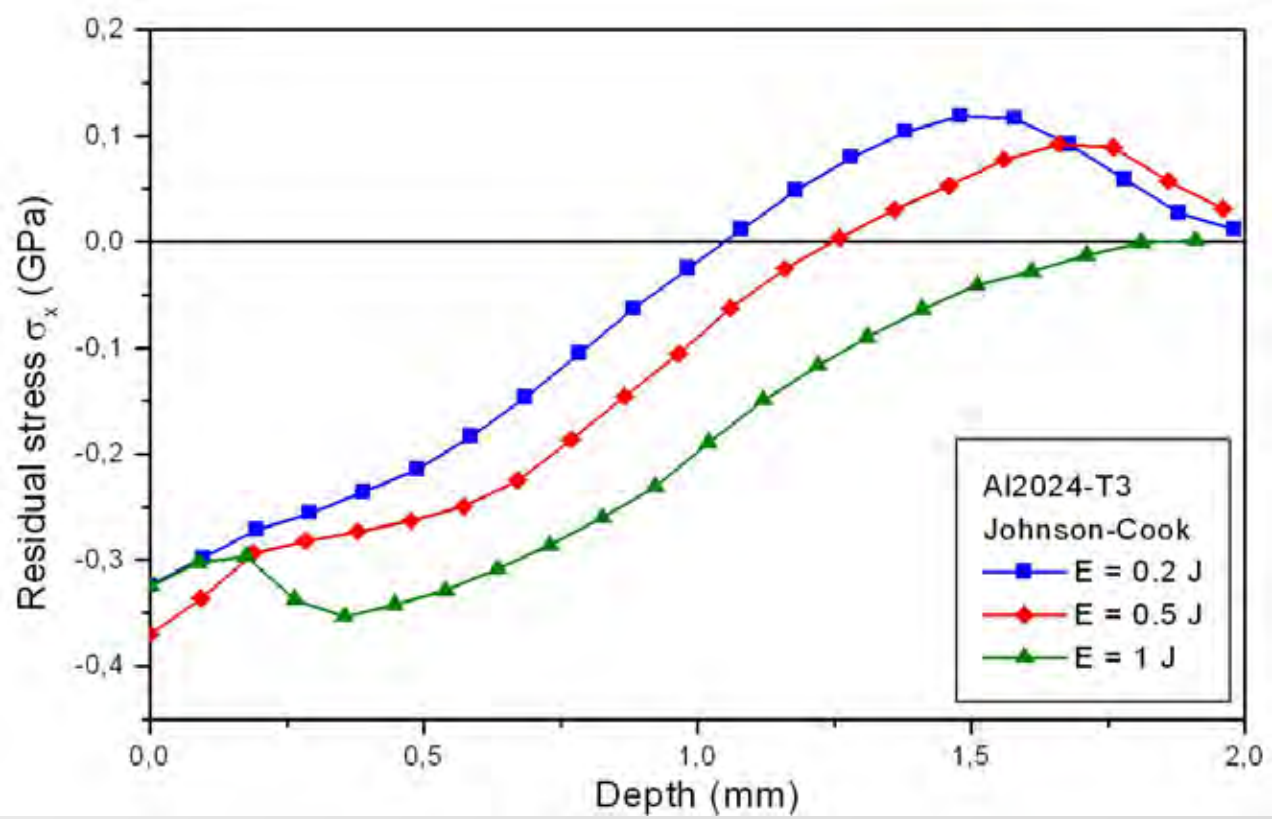

HARDSHOCK-3D (full scope)

Ti6Al4V

Residual Stress s_x (Pa)
(at middle xz plane)

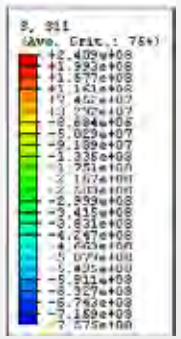

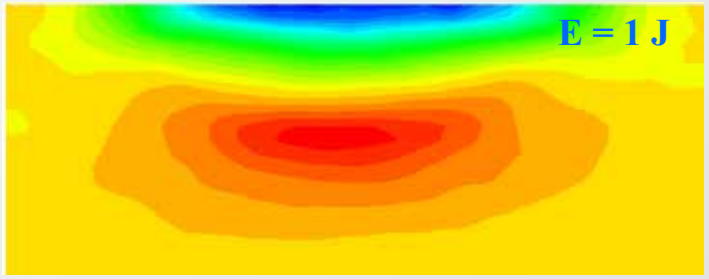

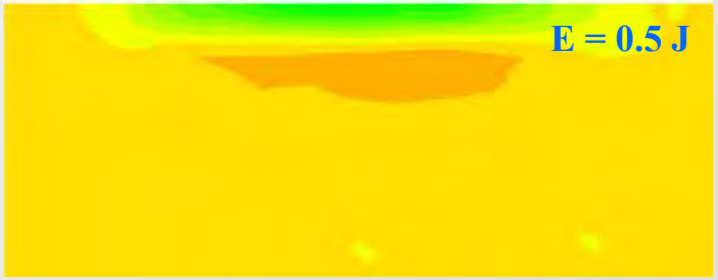

Laser Nd:YAG (l =1064 nm)
- Effective Energy 1 J , 0.5 J and 0.2 J
- FWHM 10 ns
- Spot radius = 0.75 mm

Spot overlapping 900 pulses/cm²
a= 0.15

HARDSHOCK-3D (full scope)

Ti6Al4V

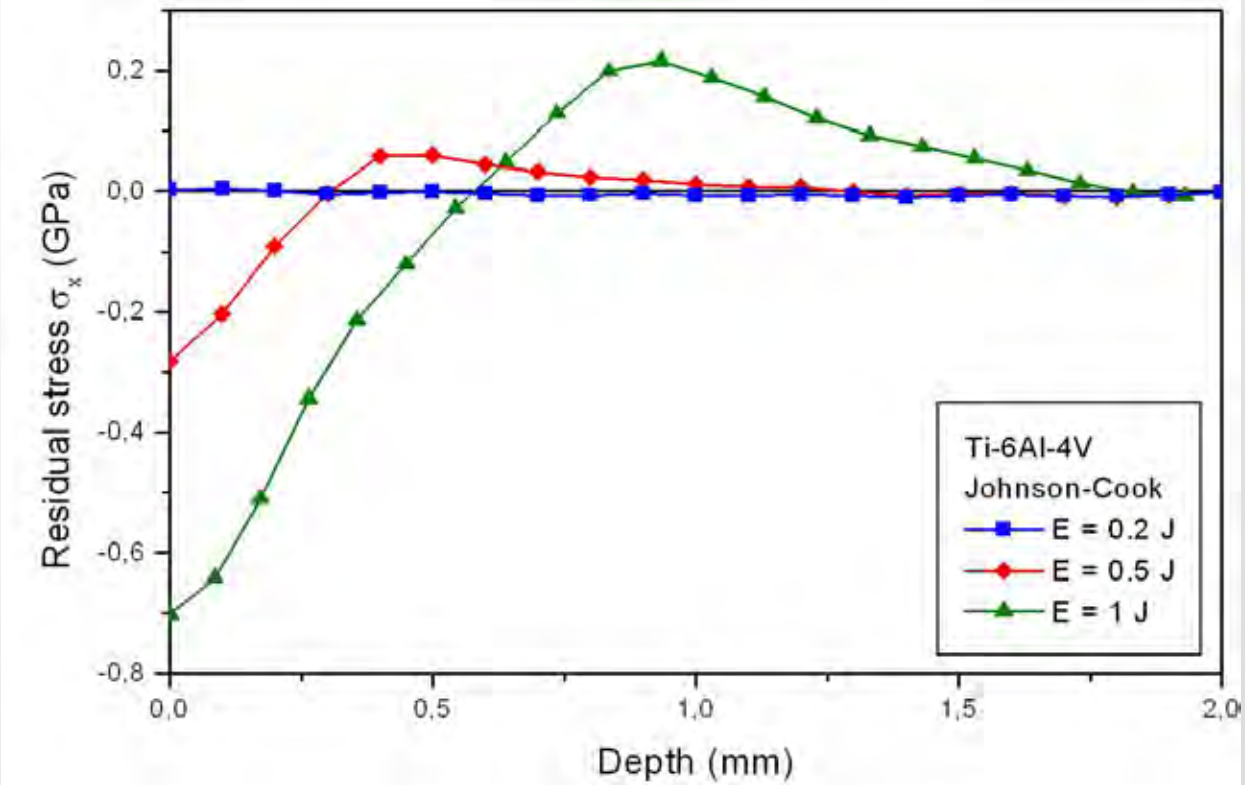

HARDSHOCK-3D (Materials comparison)

Ti6Al4V

Al2024T3

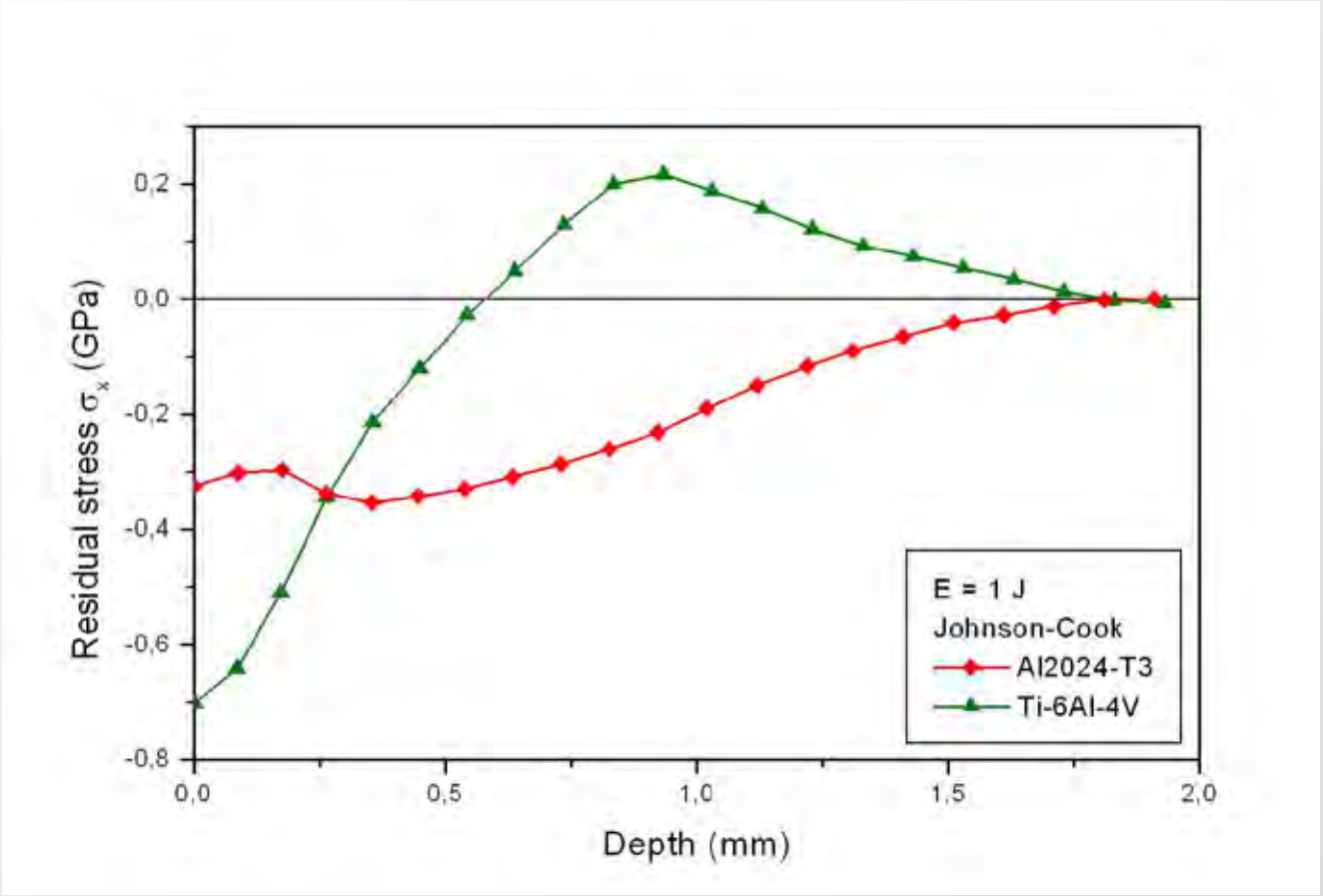

Process Modelling

Evaluation of relative effects of thermal and mechanical waves on shocked material

Water / Aluminium
Nd:YAG (1064 nm),
t = 9 ns
F = 84 J/cm²
R = 1.5 mm

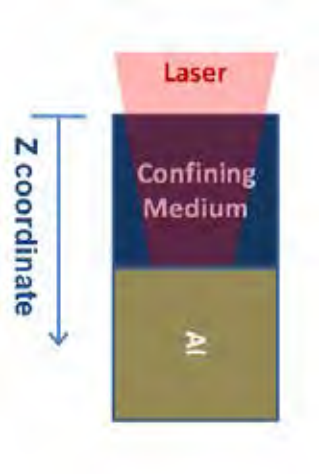

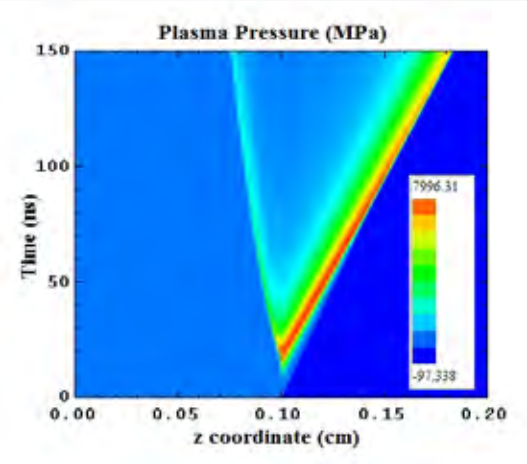

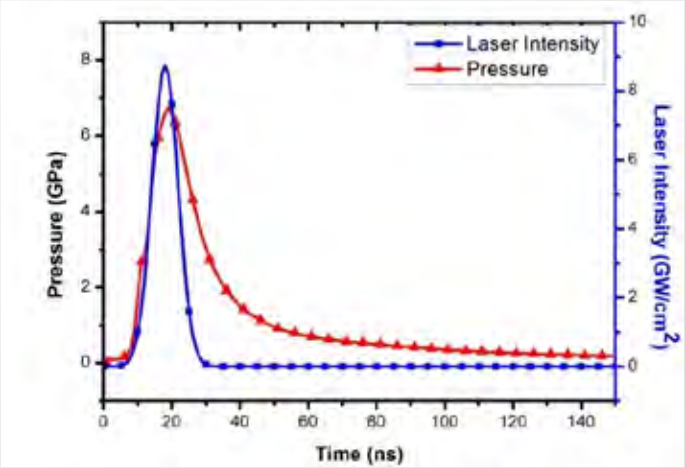

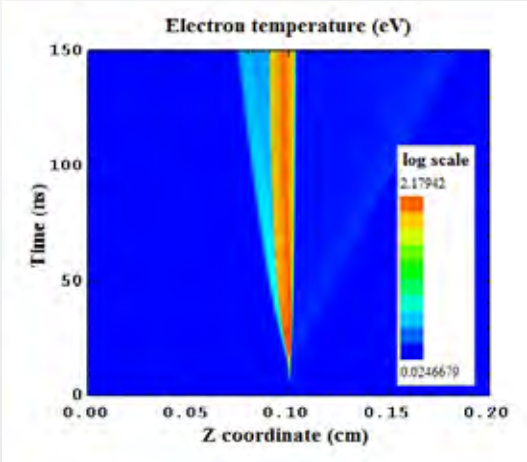

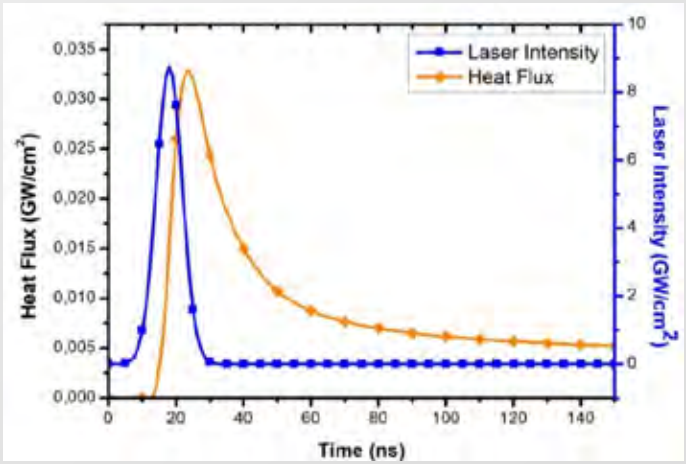

Evaluation of relative effects of thermal and mechanical waves on shocked material

Water / Aluminium; Nd:YAG (1064 nm),

t= 9 ns, F= 84 J/cm^2, radius = 1.5 mm

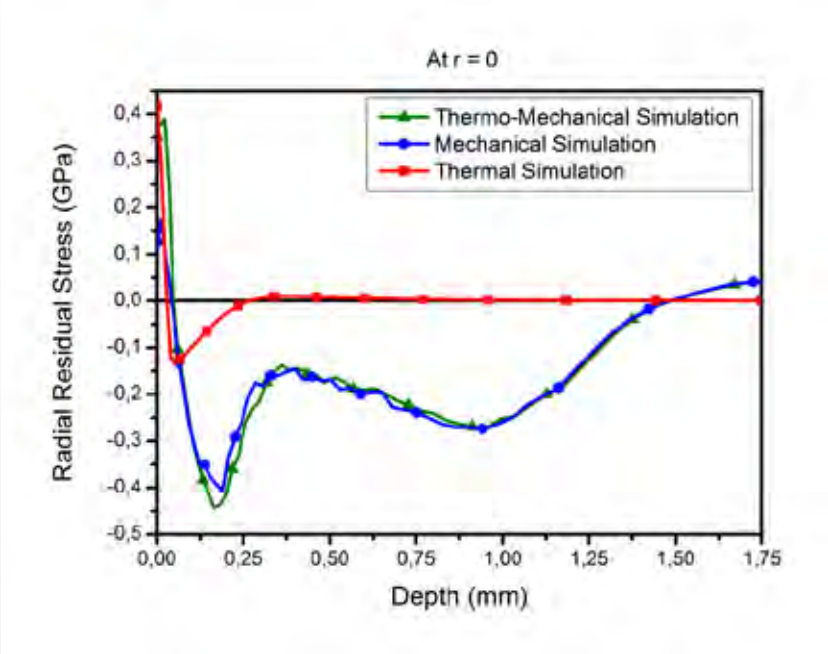

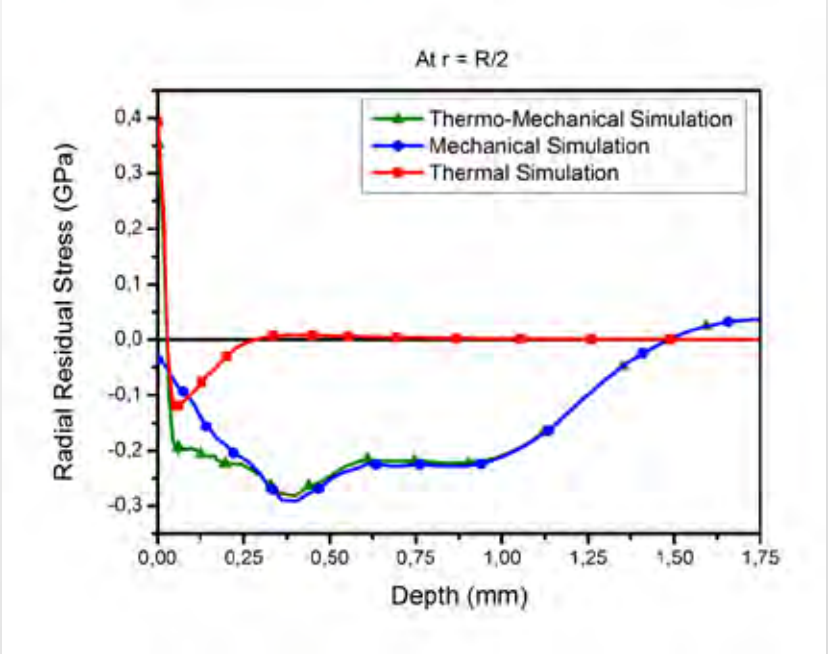

Process Modelling

Evaluation of the residual stress and deformation obtained by application of adjacent pulses covering an extended surface

Laser Nd:YAG (| =532 nm)
- Energy 200 mJ
- FWHM 8 ns
- Spot radius = 0.4 mm

Material: Ac304 20%CW

Spot overlapping:
3500 pulses/cm^2

SIMULATION
LSPSIM
a=0,2 (experimental)
+
HARDSHOCK 3D /ABAQUS

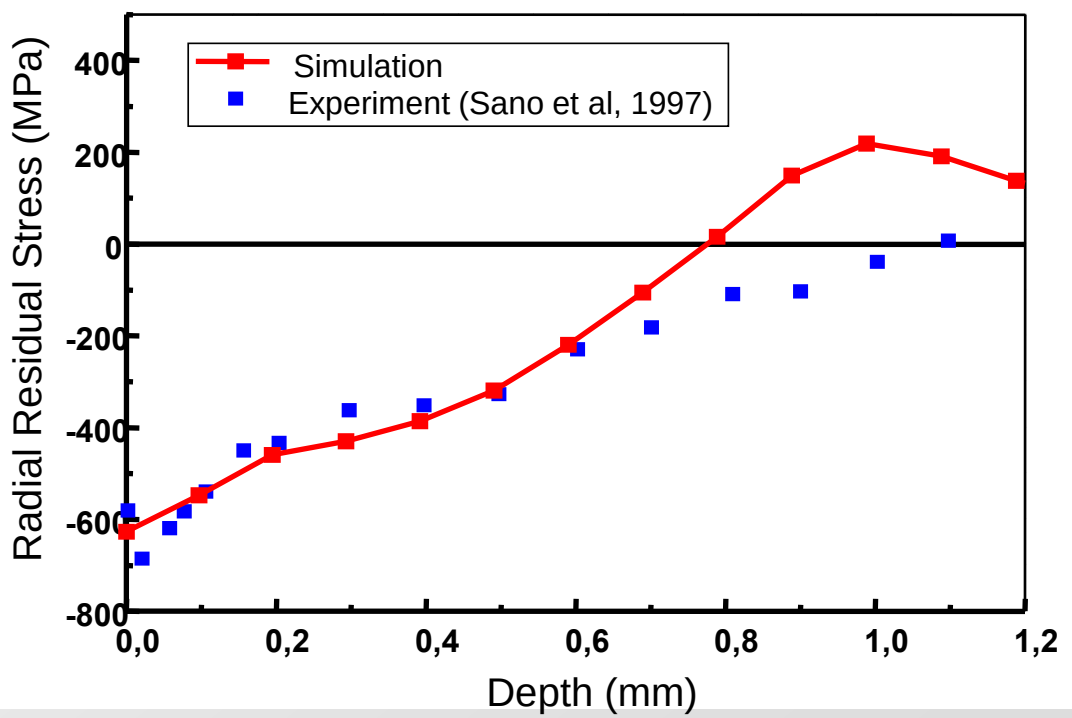

Experimental Implementation

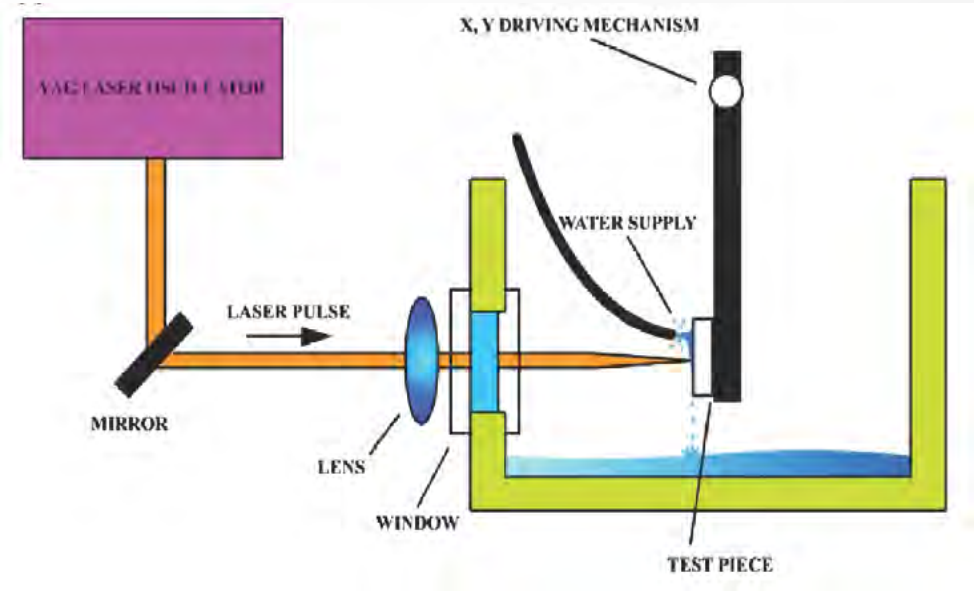

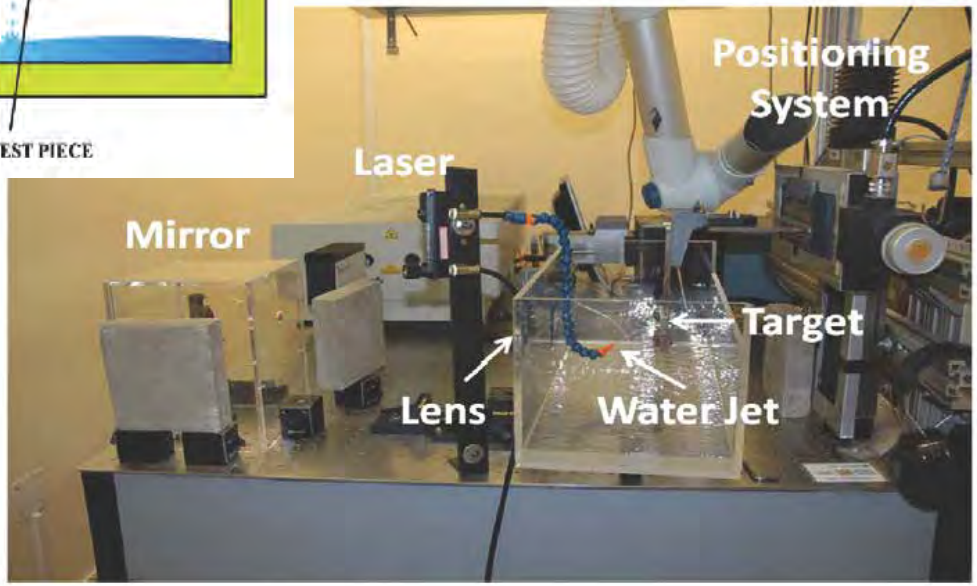

Experimental Implementation

Q-SWITCHED Nd:YAG LASER

$\lambda = 1064\,nm;\ E = 2{,}5\,J/pulse$

$\lambda = 532\,nm;\ E = 1{,}4\,J/pulse$

t = 10 ns; f = 10 Hz

Experimental Implementation

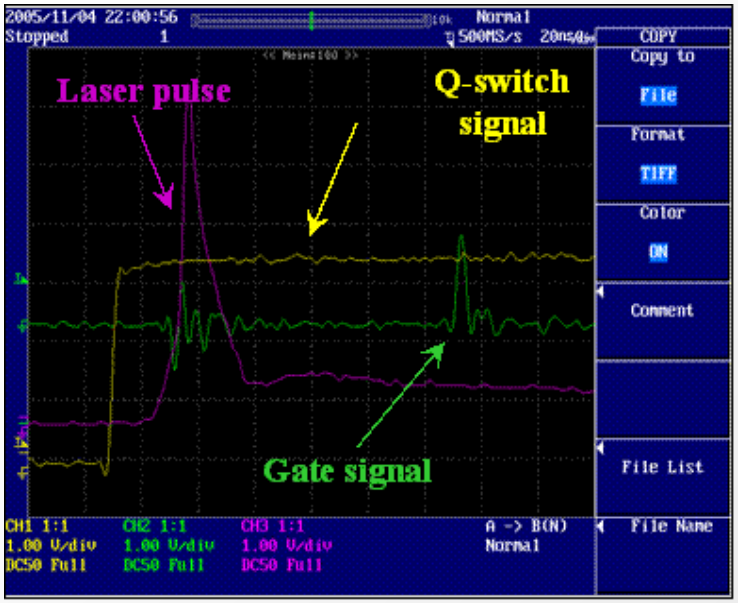

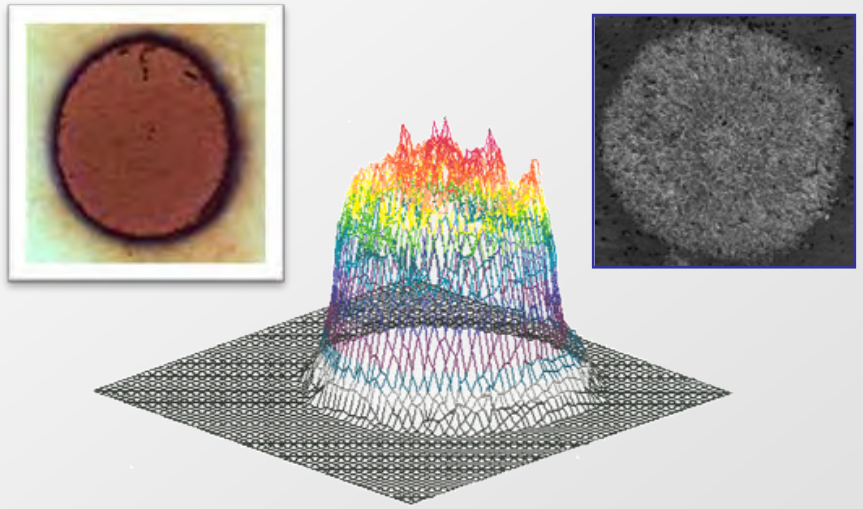

LSP TREATMENT PARAMETERS	
Laser wavelength (nm) ; Q-switched Nd:YAG	1064
Energy per pulse (J/pulse)	2,0
Pulse temporal width (ns)	≈ 9
Laser spot diameter (mm)	1.5
Ratio x-y pitch	1
Confining medium	Water jet ≈ 2 bar
Absorbing coating overlay	No

Ocaña, J.L. et al.: Applied Surface Science 238 501–505 (2004)

Experimental Implementation

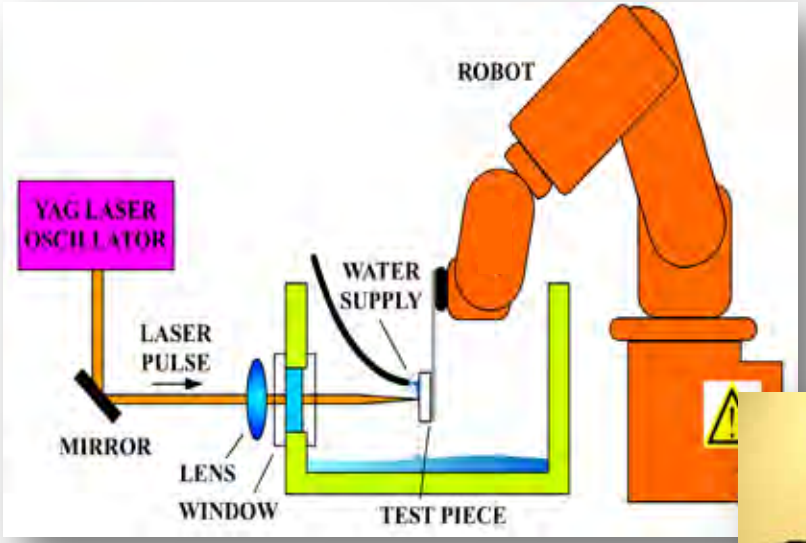

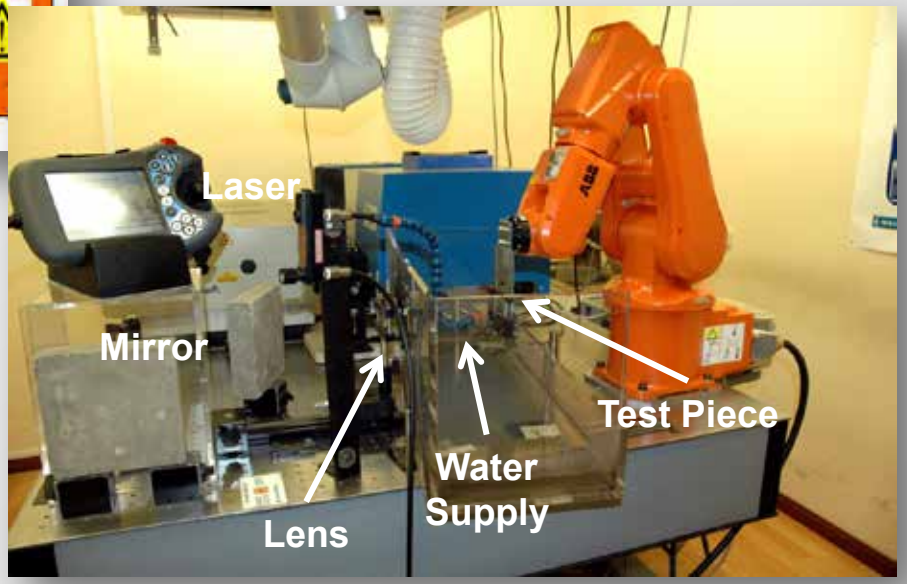

Experimental Implementation

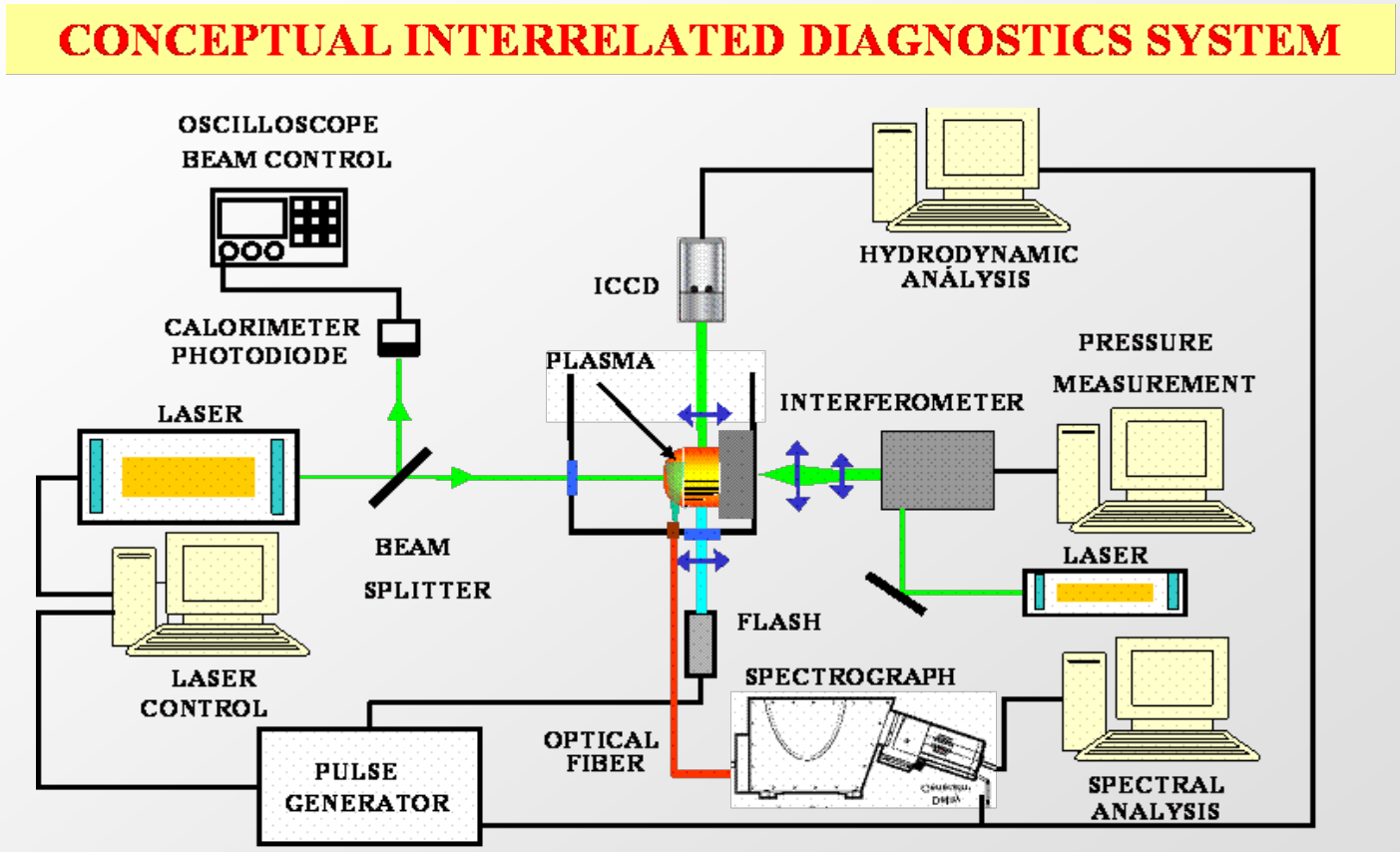

Ocaña, J.L. et al.: ".: "A review of the physics and technological issues of high intensity laser shock processing of materials as a method for mechanical properties modification". In XVI International Symposium on Gas Flow, Chemical Lasers and High-Power Lasers, Schuöcker, D., Ed. SPIE Vol. 6346, 63461P, (2006)

Experimental Implementation

Summary of correlated experimental observations and simulation results defined for plasma monitoring and process design

PLASMA EXPLORED CHARACTERISTICS	EXPERIMENTAL OBSERVATION NEEDED	MATCHING SIMULATION RESULTS
Average plasma ionization energy in interaction region	Line Spectroscopy (Integrated spectrum energy)	HYDRA ionization model results
Average plasma density and temperature in interaction region	Line Spectroscopy (collisional line broadening)	HYDRA hydrodynamic simulation
Space resolved plasma density	Shadowgraphy + Schlieren photography	HYDRA hydrodynamic simulation
Shock wave generation and plasma expansion speed	Shadowgraphy + Schlieren photography	HYDRA (short times) + LSPSIM free surface evolution simulation
Breakdown in confining medium	Line spectroscopy	Dielectric breakdown evaluation module in LSPSIM

Experimental Implementation

DIRECT IMAGING - HYDRODYNAMIC ANALYSIS

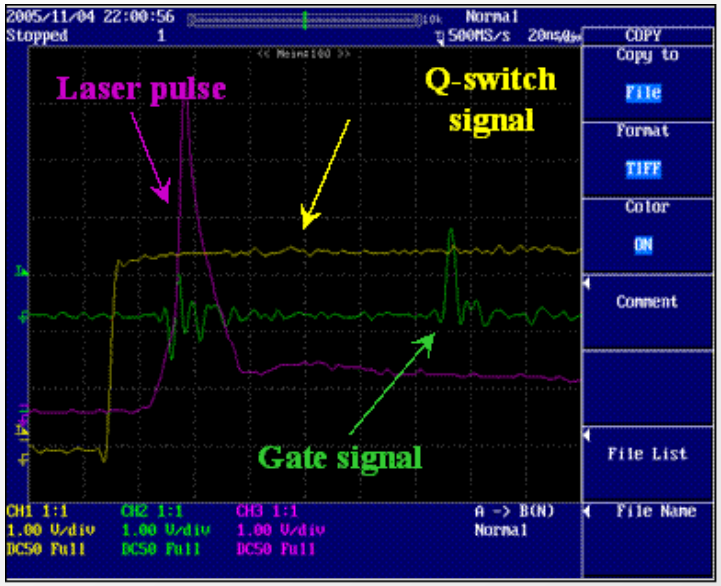

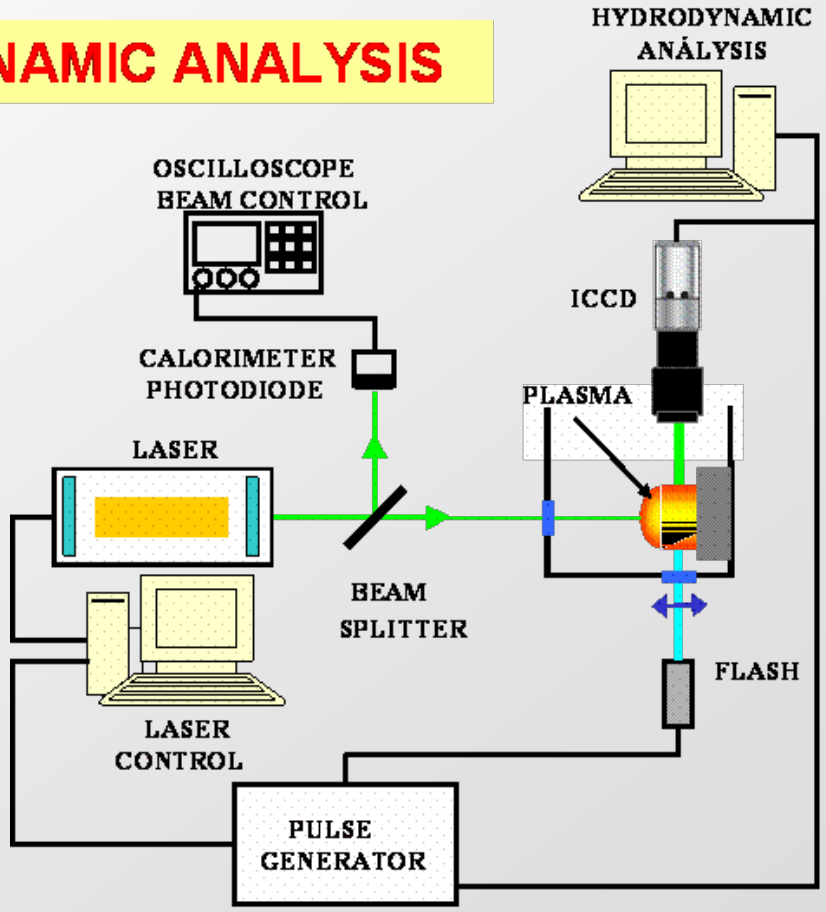

Experimental Implementation

DIRECT IMAGING - HYDRODYNAMIC ANALYSIS

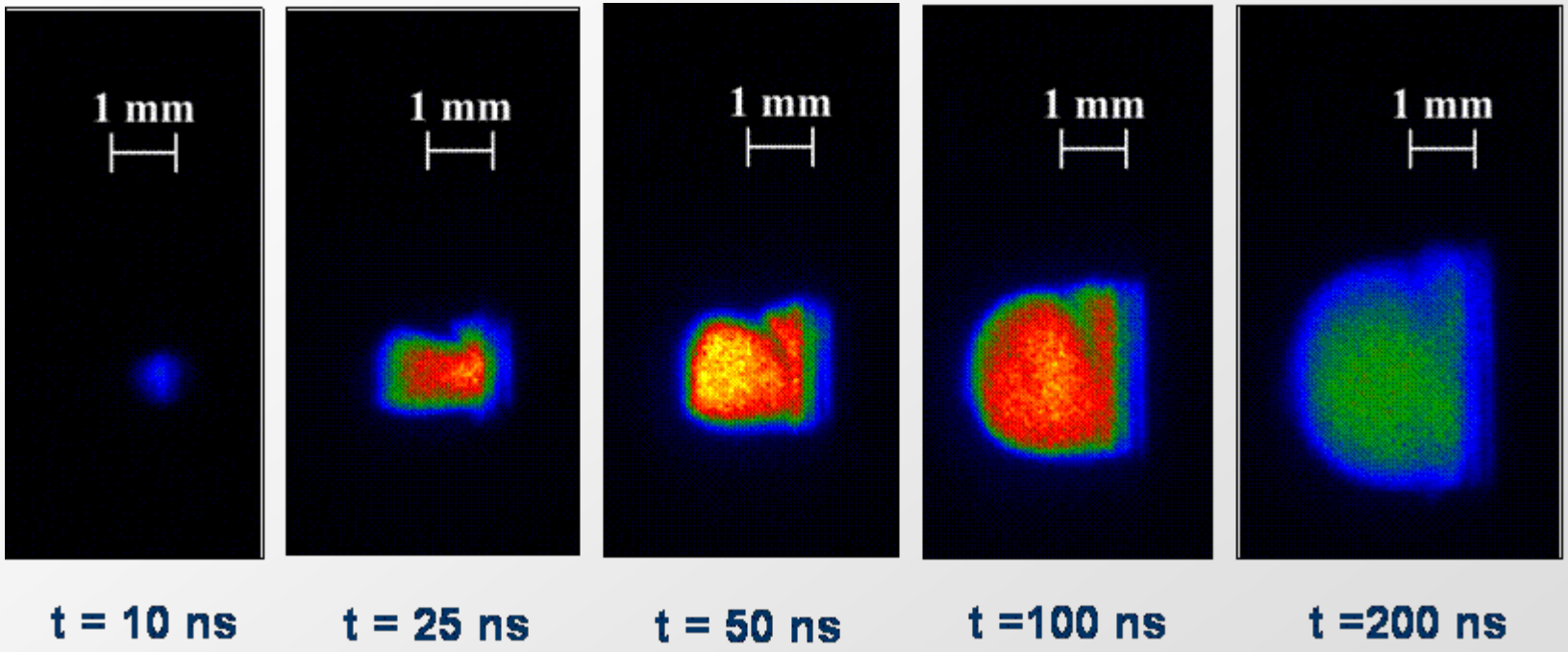

Ocaña, J.L. et al.: ".: "A review of the physics and technological issues of high intensity laser shock processing of materials as a method for mechanical properties modification". In XVI International Symposium on Gas Flow, Chemical Lasers and High-Power Lasers, Schuöcker, D., Ed. SPIE Vol. 6346, 63461P, (2006)

Experimental Implementation

IMAGING TECHNIQUES – SHADOWGRAPHY

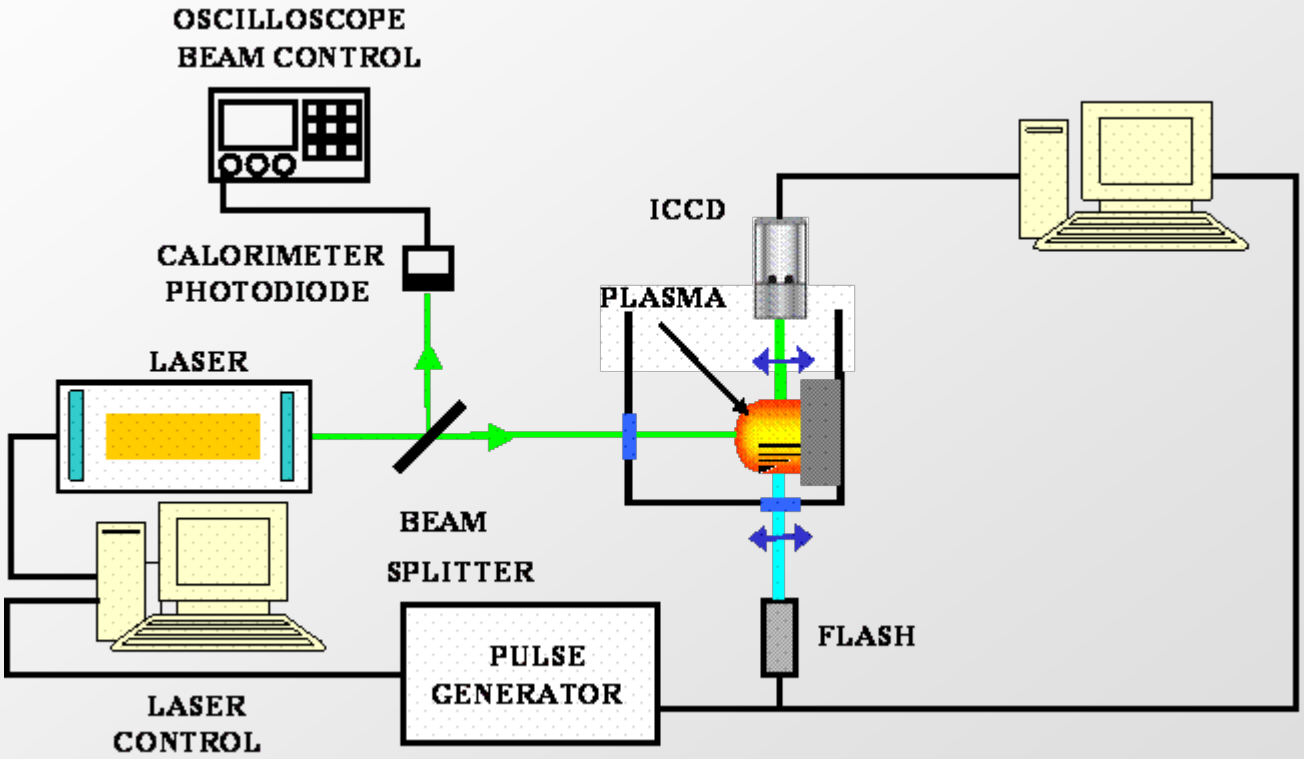

Experimental Implementation

IMAGING TECHNIQUES – SHADOWGRAPHY

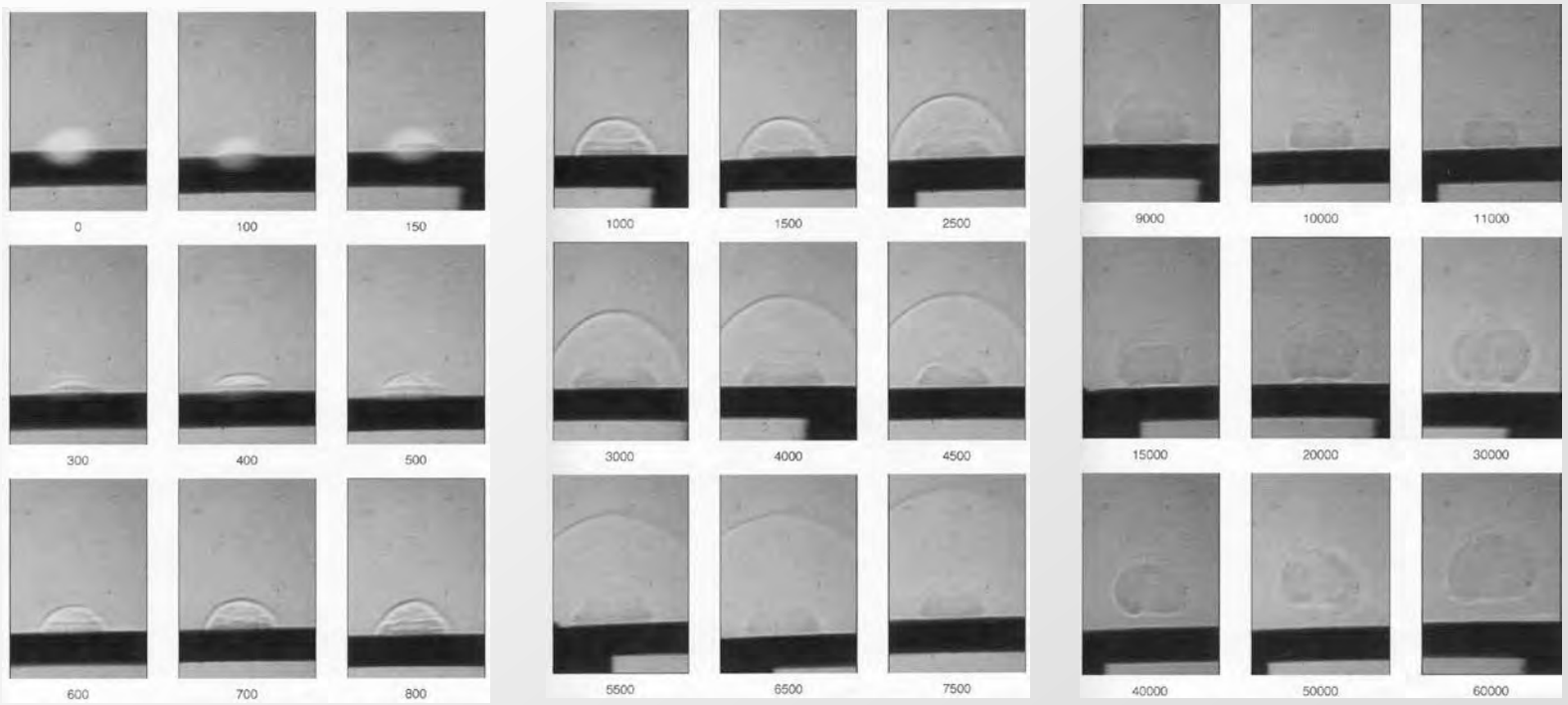

OCAÑA, J.L., et al.: HPLA II (1999)

Experimental Implementation

IMAGING TECHNIQUES – SHADOWGRAPHY

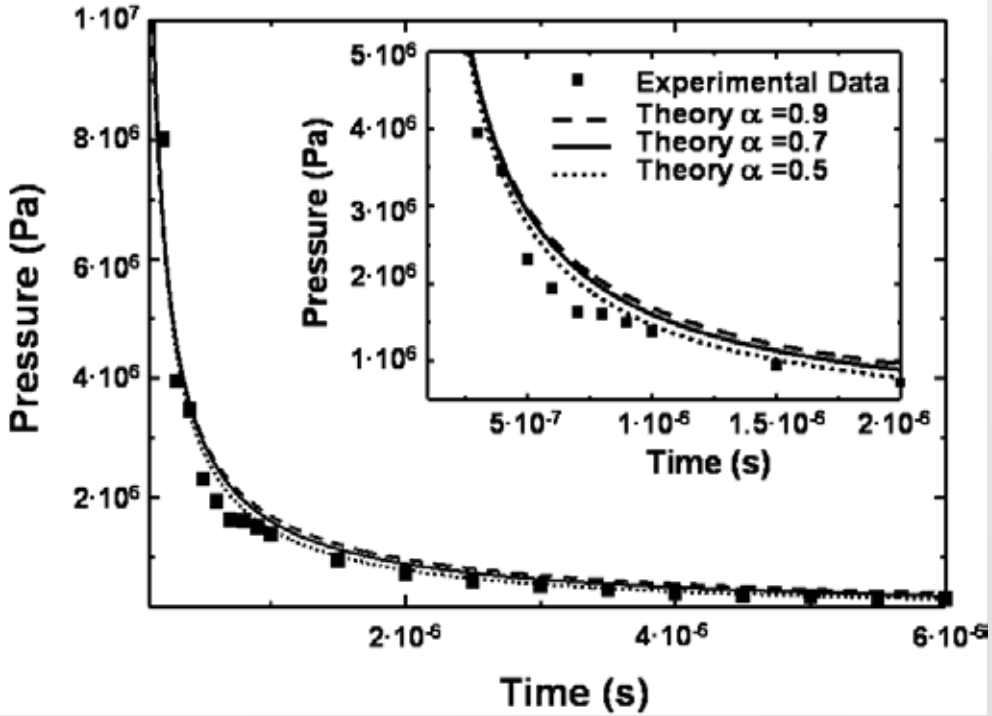

OCAÑA, J.L., et al.: HPLA II (1999)

Experimental Implementation

IMAGING TECHNIQUES – SCHLIEREN / INTERFEROMETRY

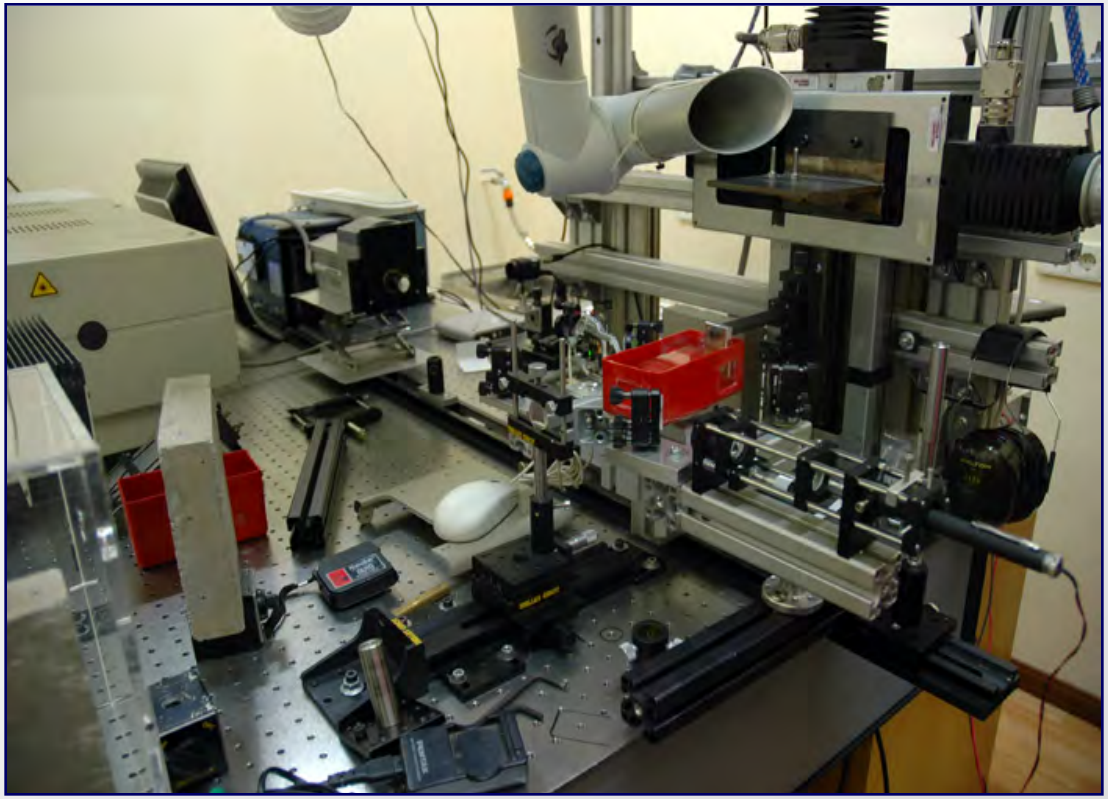

Experimental Implementation

IMAGING TECHNIQUES – SCHLIEREN / INTERFEROMETRY

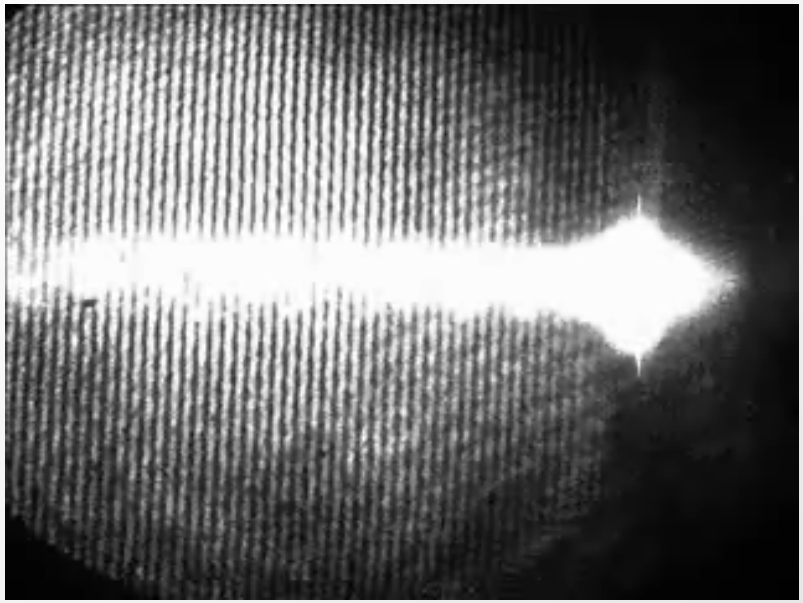

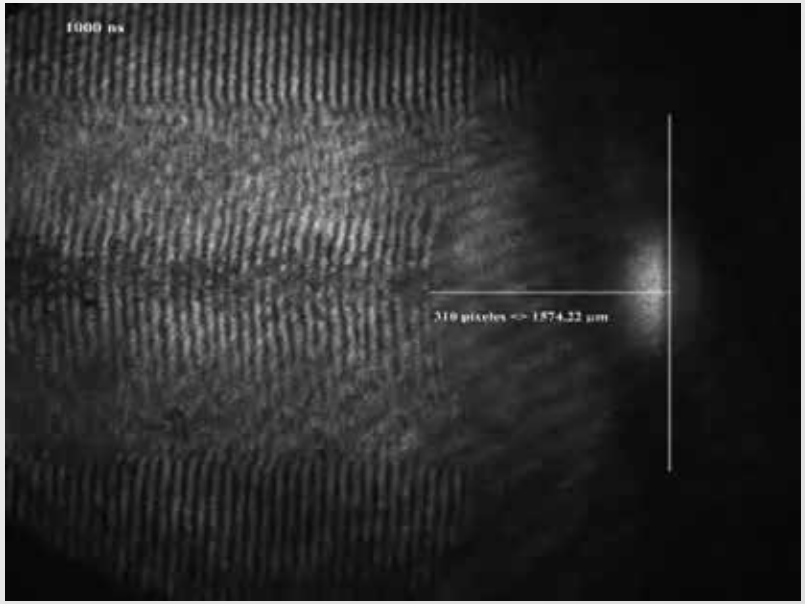

Martí-López, L. et al.: Appl. Optics, 48, 3671-3680 (2009)

Experimental Implementation

IMAGING TECHNIQUES – SCHLIEREN / INTERFEROMETRY

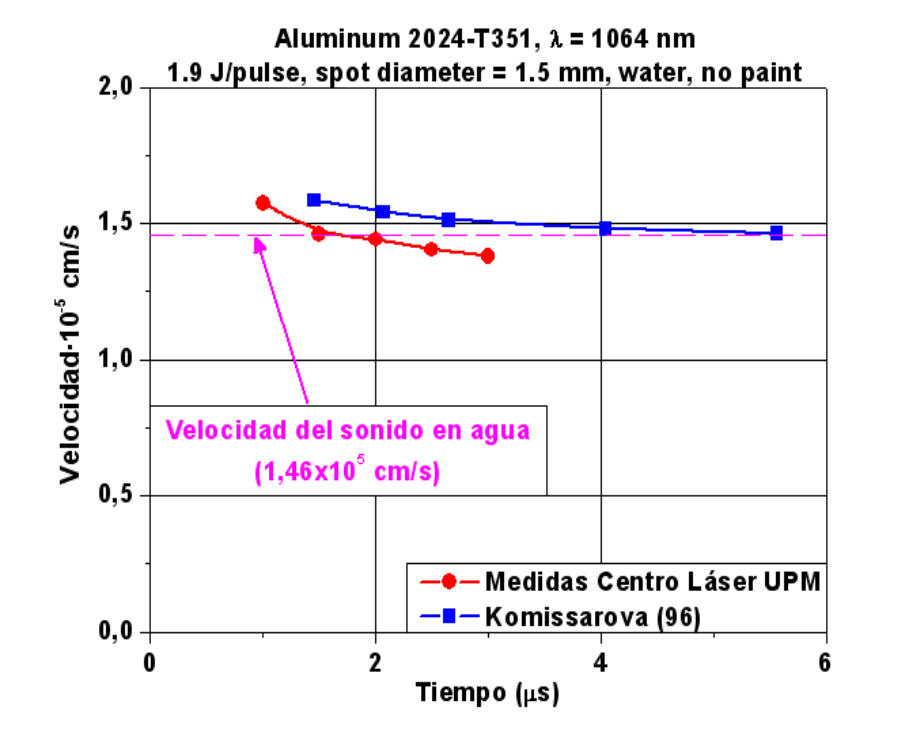

Martí-López, L. et al.: Appl. Optics, 48, 3671-3680 (2009)

Experimental Implementation

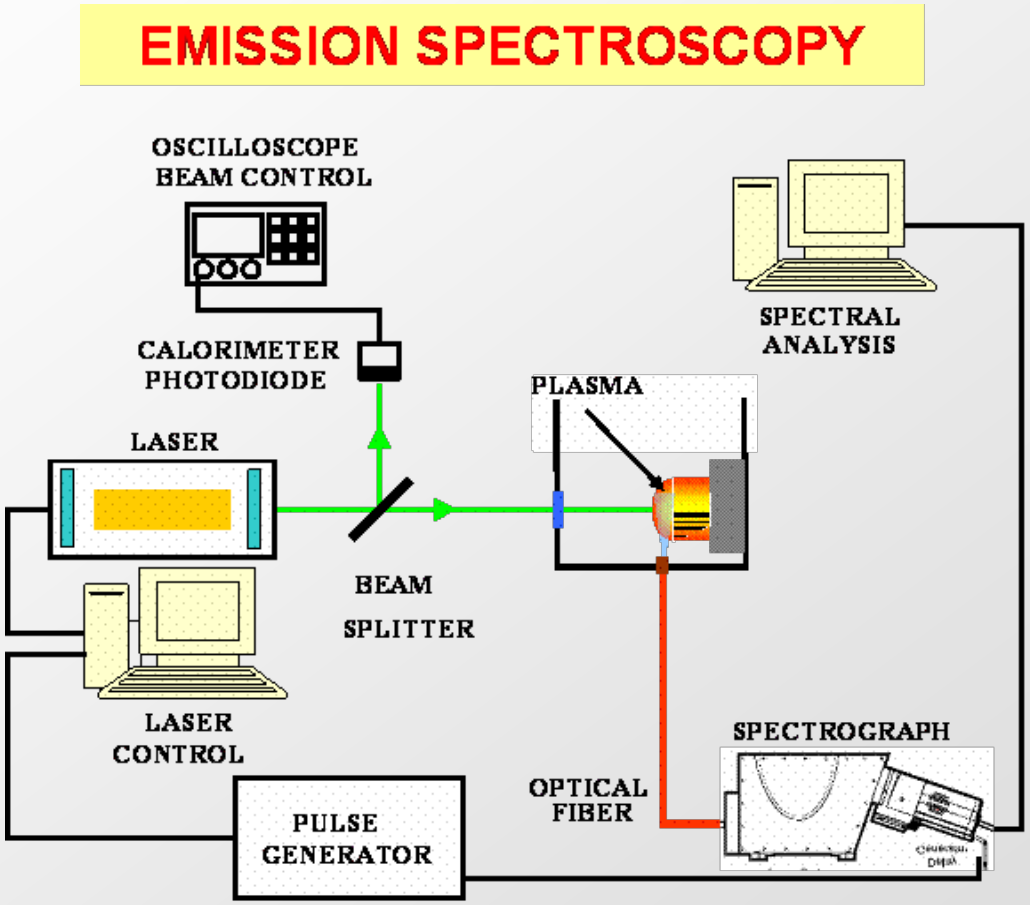

Experimental Implementation

EMISSION SPECTROSCOPY

Stark Broadening → **Electron density n_e**

$$\Delta\lambda_{1/2} = 2w\frac{n_e}{10^{16}}$$

Relative Line Intensity → **Temperature**

$$\ln\left(\frac{\lambda_{mn}I_{mn}}{g_m A_{mn}}\right) = \ln\left(\frac{N(T_{ex})}{U(T_{ex})}\right) - \frac{E_m}{kT_{ex}}$$

Experimental Implementation

EMISSION SPECTROSCOPY

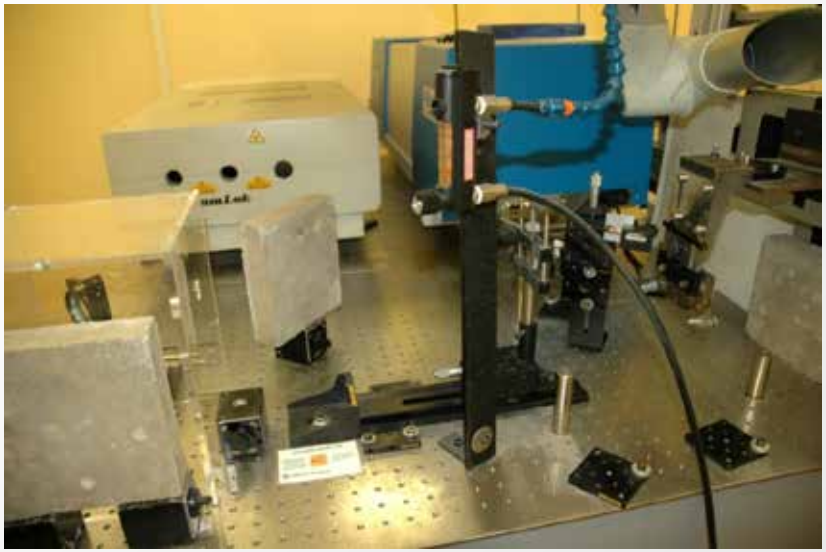

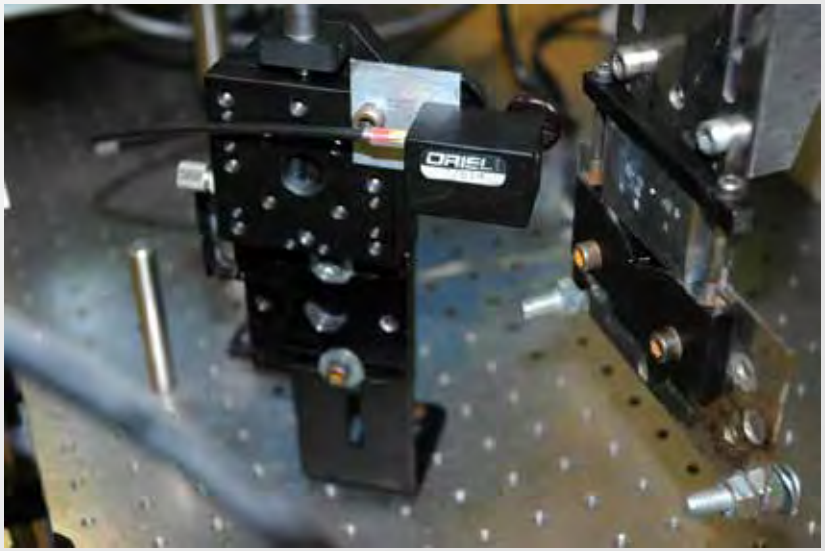

Spectroscopic system calibrated in wavelength with Hg lamp and in intensity with Deuterium lamp

Experimental Implementation

EMISSION SPECTROSCOPY

Electron density determination via Stark effect of Al II line at 2816,2 nm:

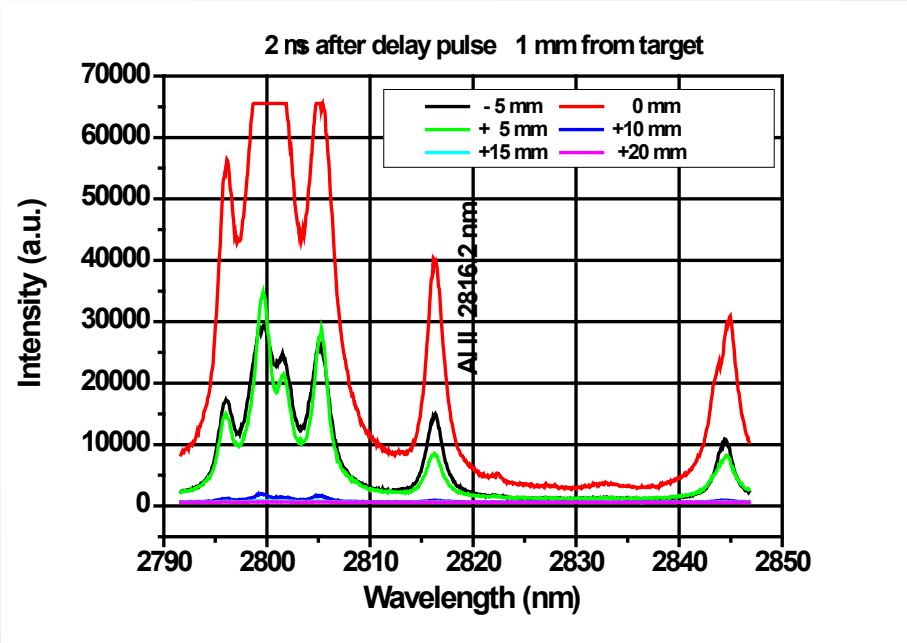

		Delay from laser pulse	
		2 μs	3 μs
Distance from target	1 mm	20.4 10^{16} cm^{-3}	2.4 10^{16} cm^{-3}
	6 mm	17.2 10^{16} cm^{-3}	2.0 10^{16} cm^{-3}

Experimental Implementation

EMISSION SPECTROSCOPY

Electron temperature determination through Boltzmann plot of relative intensities of Mg II lines at 279.5528 nm, 280.2704 nm, 292.8633 nm and 293.6509 nm:

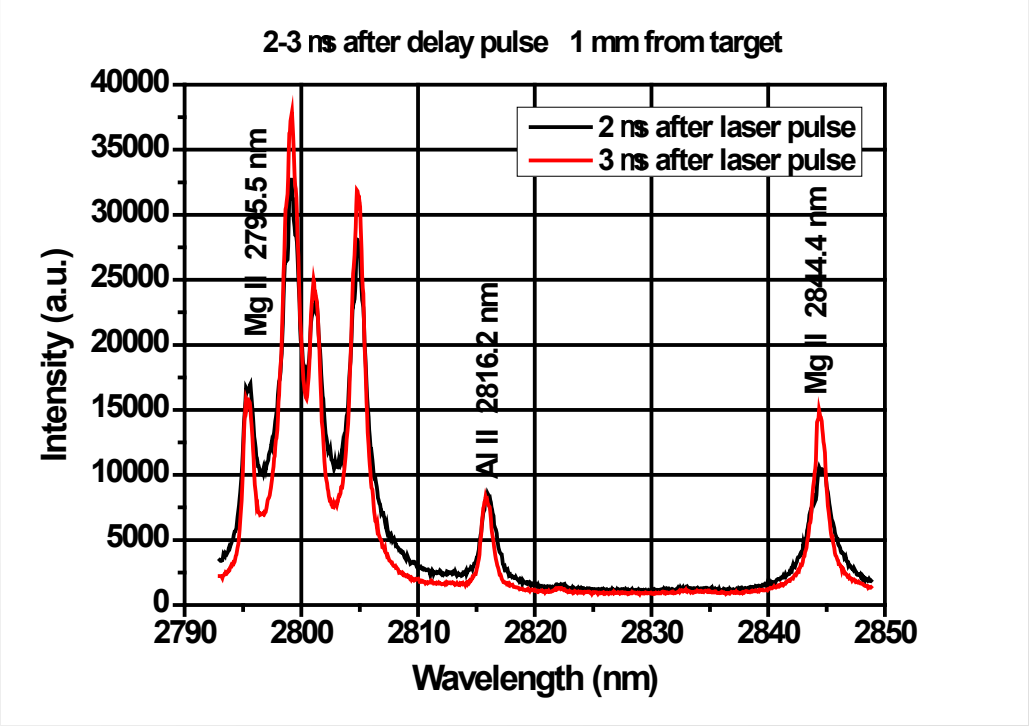

Preliminary electron temperature distributions in the range of 1.0-1.5 eV (i.e. @11 600 - 17 400 K) were found close to the target 2-3 ns after laser shut-down

Experimental Results at CLUPM

Material: Al2024 T3

Pulses: Æ=1,5 mm; t =10 ns; f=10 Hz;
E=1 J/pulse; I=1,41 GW/cm^2

Swept Area : 15x15 mm^2; 2500 pulses/cm^2

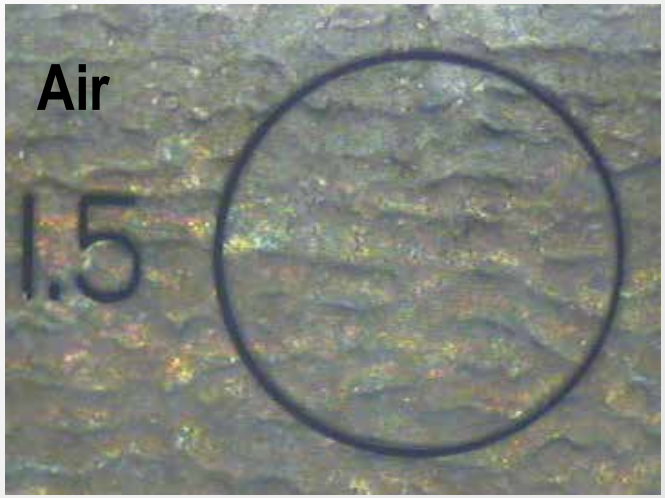

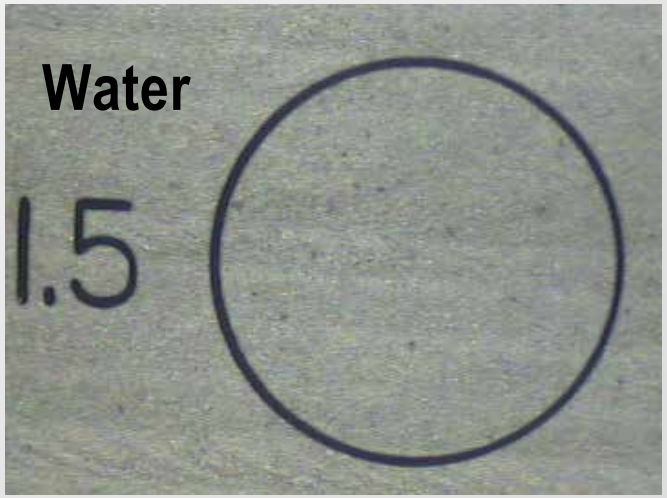

Experimental Results at CLUPM

Experimental Results at CLUPM

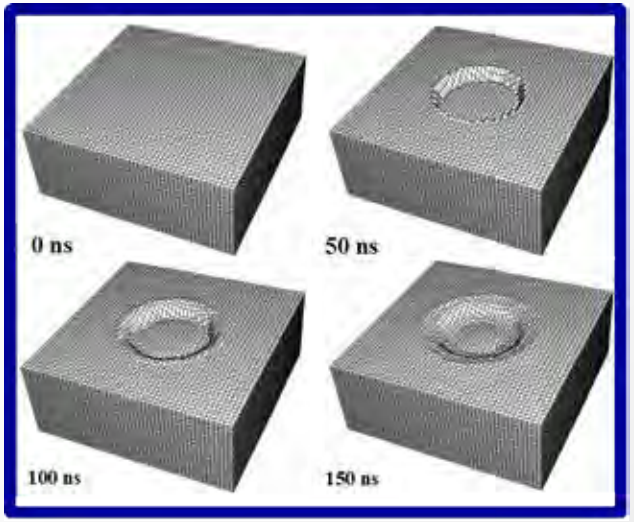

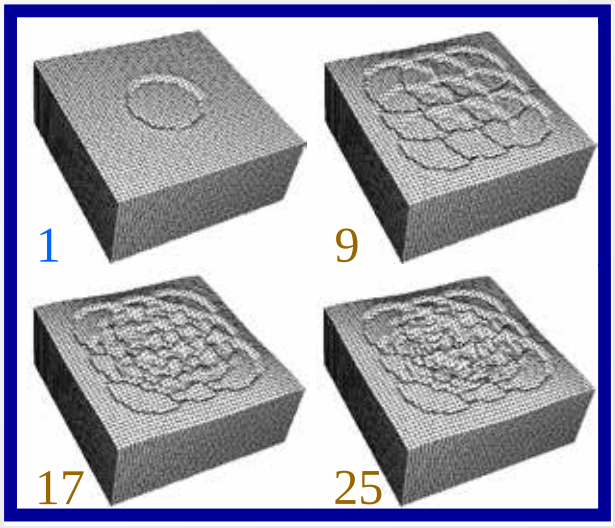

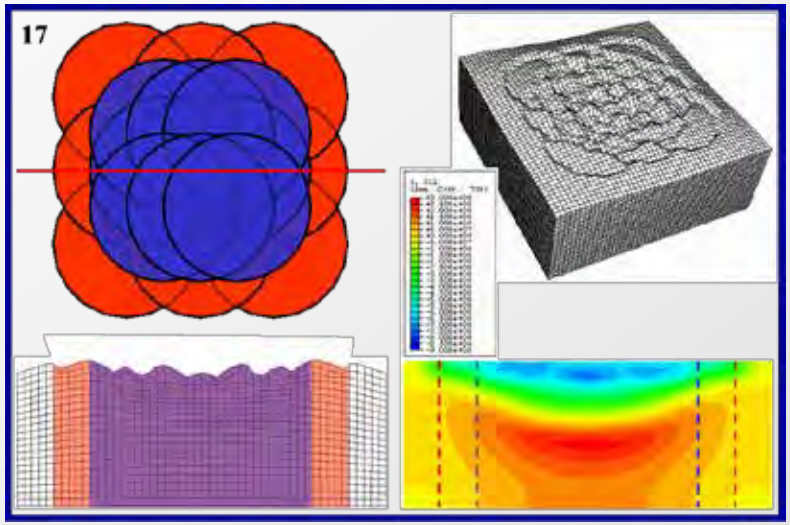

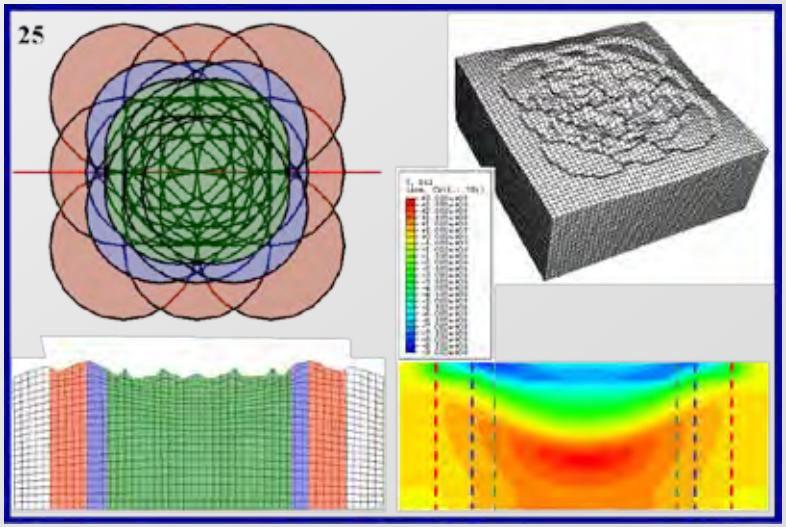

Experimental Results at CLUPM

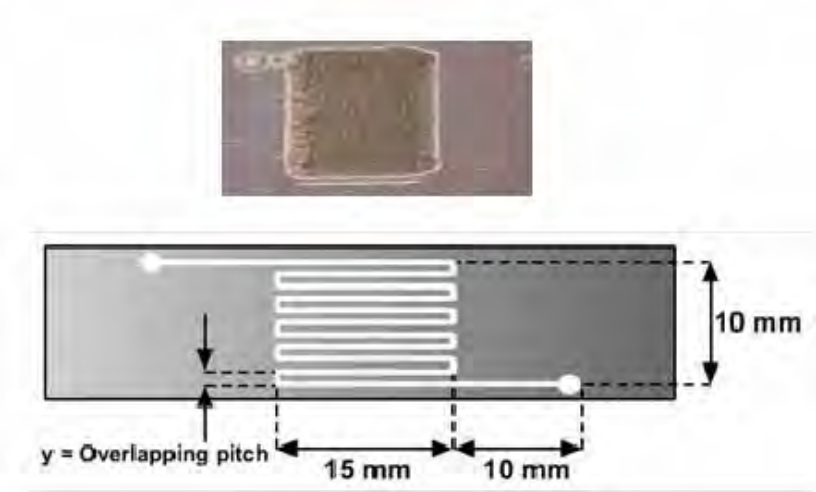

$$\text{Equivalent Overlapping Density} \quad \text{EOD} = \frac{\text{Nº of pulses}}{\text{Total treated surface}} = \frac{\frac{x}{\Delta x}\frac{y}{\Delta y}}{\Delta s} = \frac{\frac{x}{d}\frac{y}{d}}{xy} = \frac{1}{d^2}$$

$$\text{Equivalent Energy Density} \quad \text{EED} = \frac{\text{Nº of pulses} \times \text{Pulse Energy}}{\text{Total treated surface}} = \frac{\frac{x}{\Delta x}\frac{y}{\Delta y}}{\Delta s} E = \frac{\frac{x}{d}\frac{y}{d}}{xy} E = \frac{E}{d^2}$$

$$\text{Equivalent local overlapping factor} \quad \text{ELOF} = \frac{\text{Nº of pulses} \times \text{Pulse Area}}{\text{Total treated surface}} = \frac{\frac{\pi}{4} f^2}{d^2} = \frac{\pi}{4}\left(\frac{f}{d}\right)^2$$

Experimental Results at CLUPM

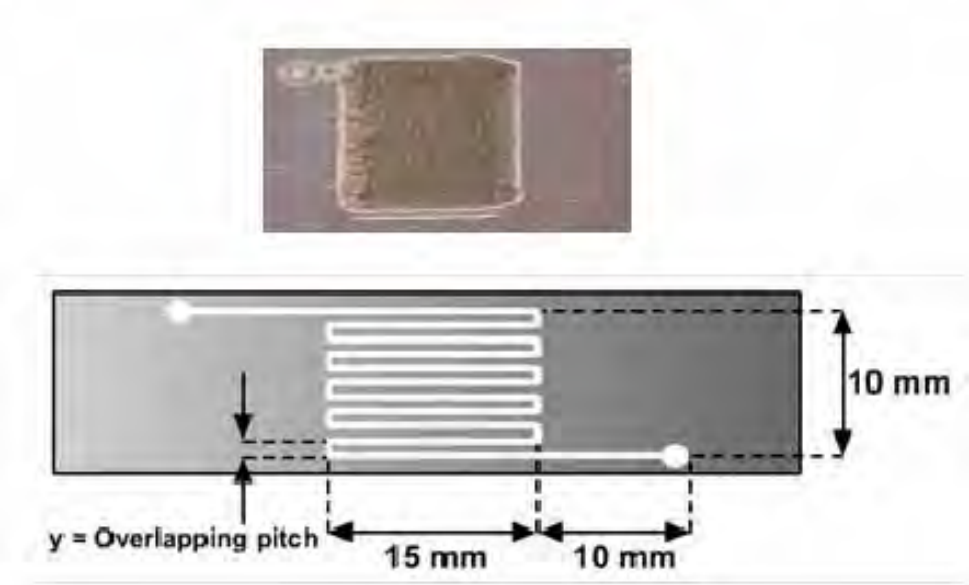

Table I: Relation between overlapping pitch and equivalent number of pulses per unit surface corresponding to the defined sweeping procedure.

Overlapping pitch Y (mm)	Equivalent overlapping density (pulses/cm^2)
0.588	289
0.33	900
0.285	1225
0.2	2500
0.141	5000

Experimental Results at CLUPM

Residual Stresses (According to ASTM E837-08)

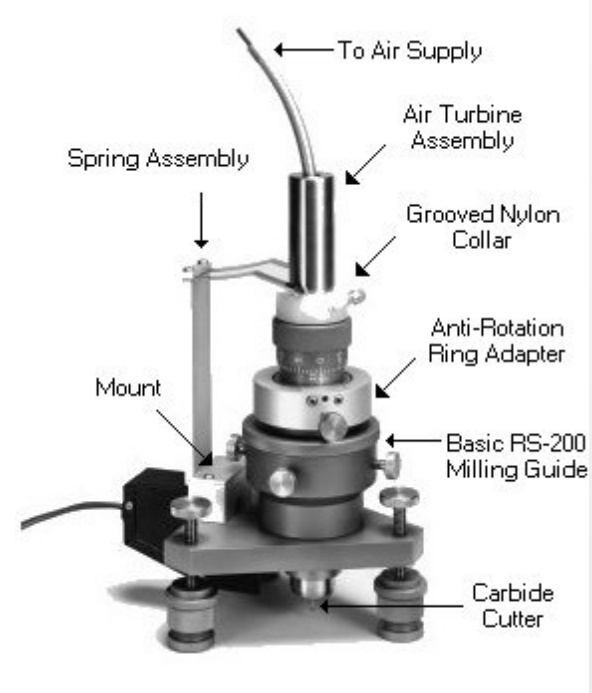

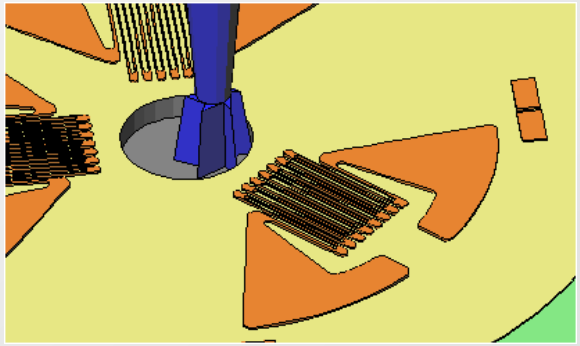

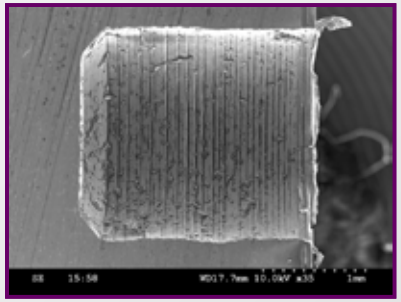

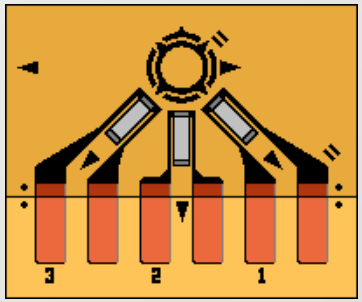

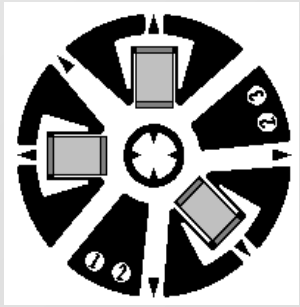

CEA-XX-062UM-120 EA-XX-062RE-120

Experimental Results at CLUPM

Residual Stresses (According to ASTM E837-08)

Al2024-T351

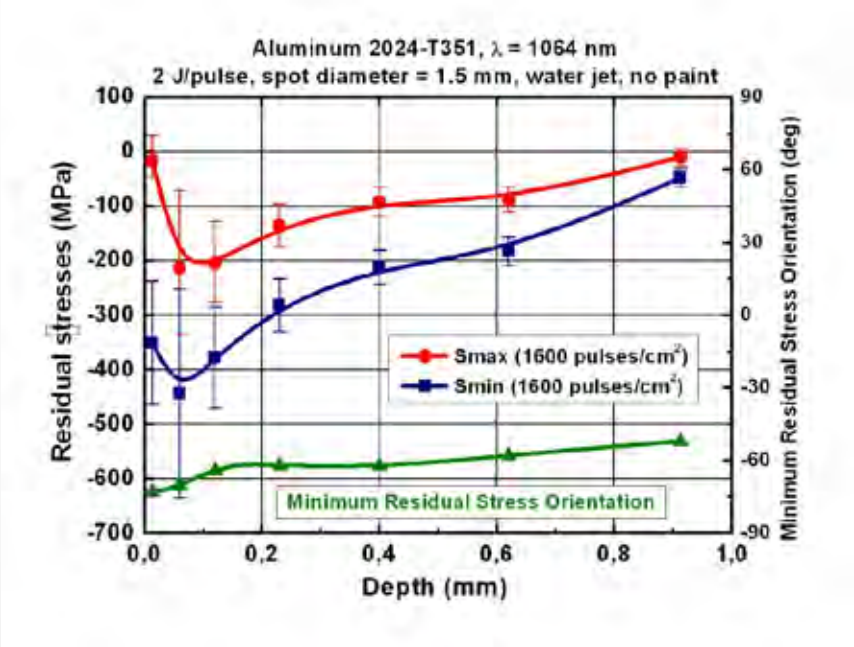

Relatively broad difference between S_{max} and S_{min} in Al2024-T351

Ti6Al4V

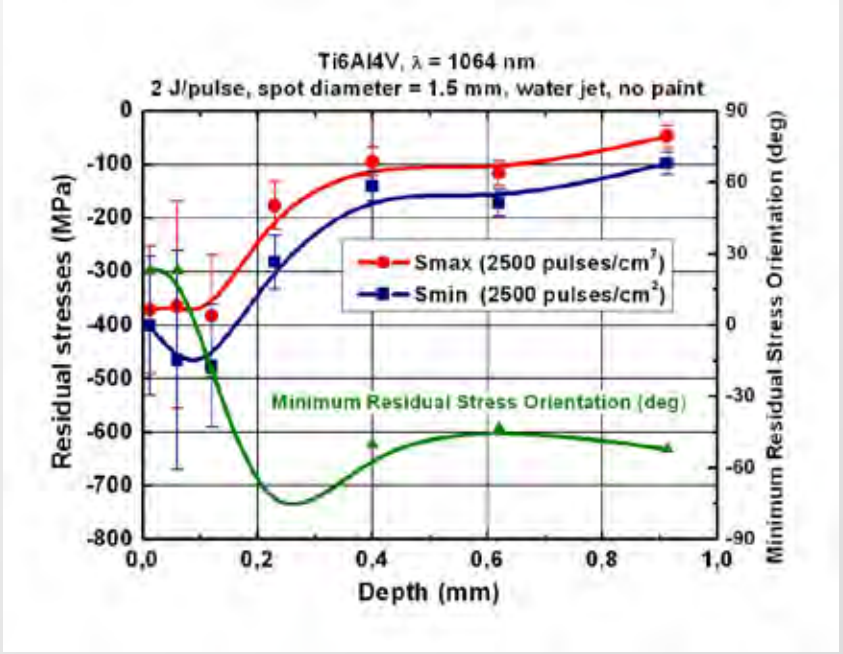

Relatively small difference between S_{max} and S_{min} in Ti6Al4V

Experimental Results at CLUPM

Residual Stresses (According to ASTM E837-08)

Ti6Al4V: Comparison LSP-Shot Peening

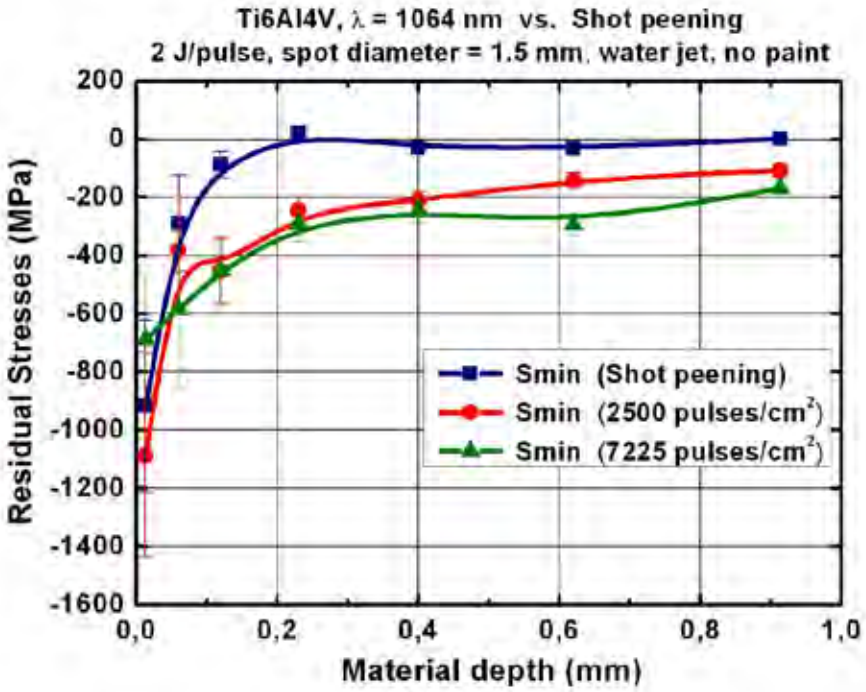

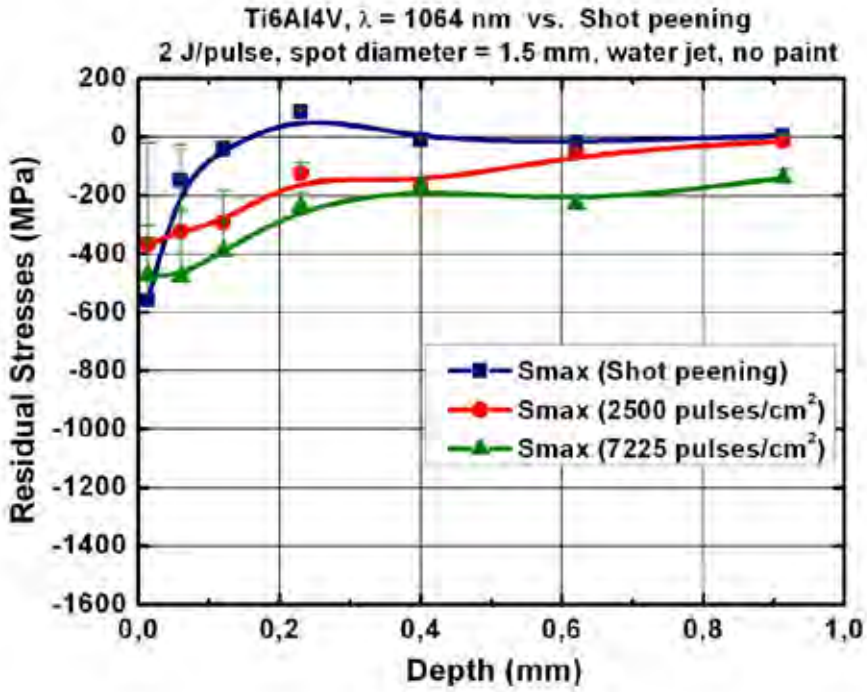

Substantial improvement in Residual Stresses Field in Ti6Al4V vs. to Shot Peening

Decisive improvement in protected depth reached in Ti6Al4V for different irradiation intensities

Experimental Results at CLUPM

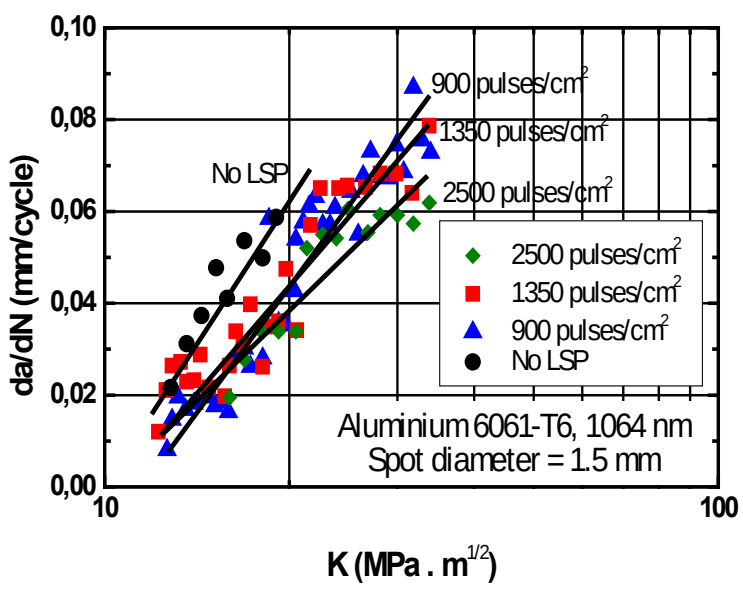

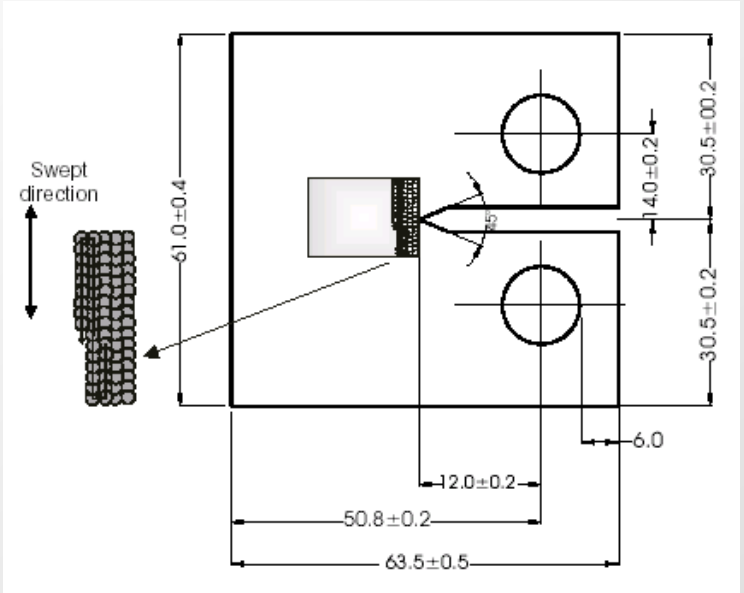

$$\frac{da}{dN} = C.K^{m}$$

Pulse density (cm^{-2})	C (mm/cycle)	M (dimensionless)
0 (No LSP treatment)	$4x10^{-13}$	7.664
900	$8x10^{-13}$	6.818
1350	$2x10^{-11}$	5.733
2500	$3x10^{-10}$	4.723

RUBIO-GONZÁLEZ, C. et al.: Mat. Sci. Eng. A., 386 (2004) 291-295

Experimental Results at CLUPM

Process parameters	
Wavelength (nm)	1064
Frecuency (Hz)	10
Energy (J/pulse)	2.8
Pulse width (ns)	~ 9
Spot diameter (mm)	~ 1.5
Overlapping (pulses/cm^2)	900
	1600
Confining medium	Water jet
Absorbent coating	No

900 pul/cm^2 1600 pul/cm^2

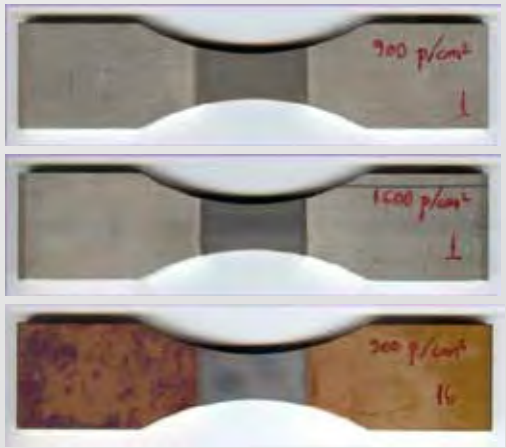

900 pulses/cm^2

1600 pulses/cm^2

900 pulses/cm^2 + Heat treat.: 500 ˚C, 8h

Experimental Results at CLUPM

Residual Stresses:

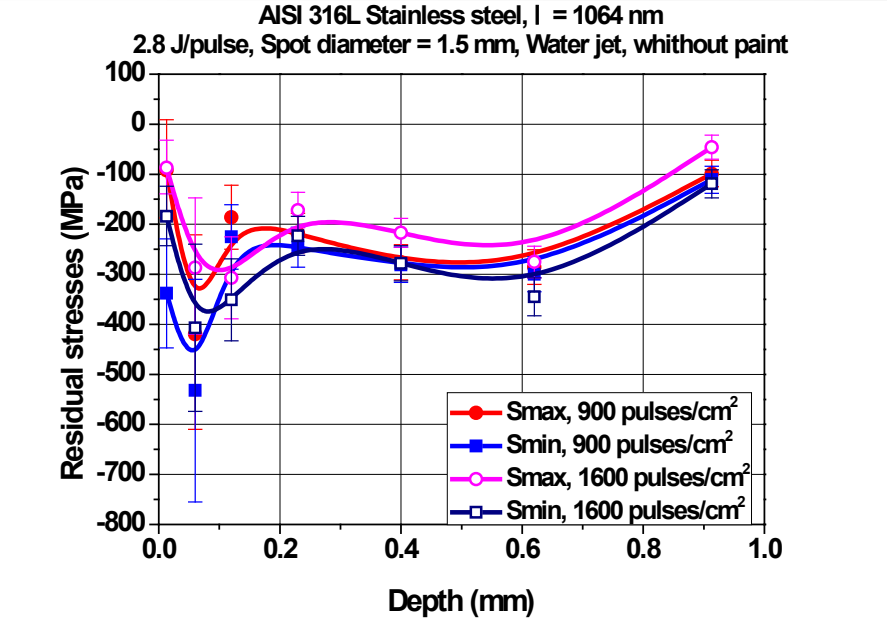

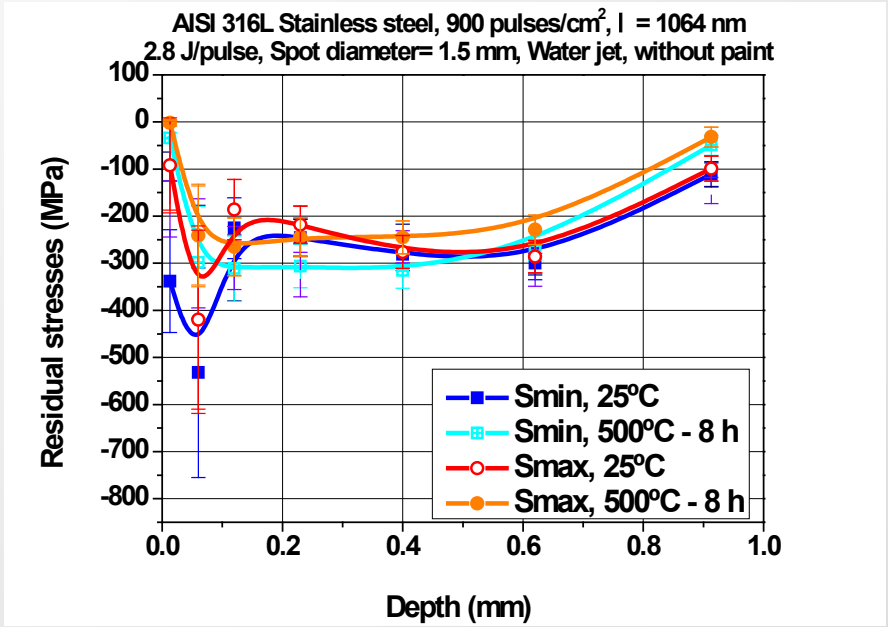

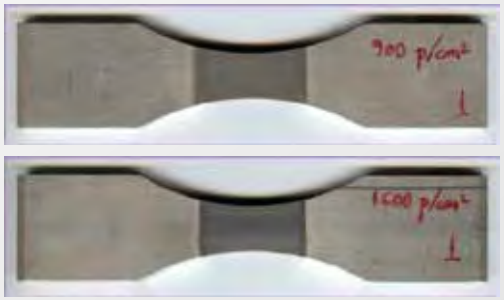

Experimental Results at CLUPM

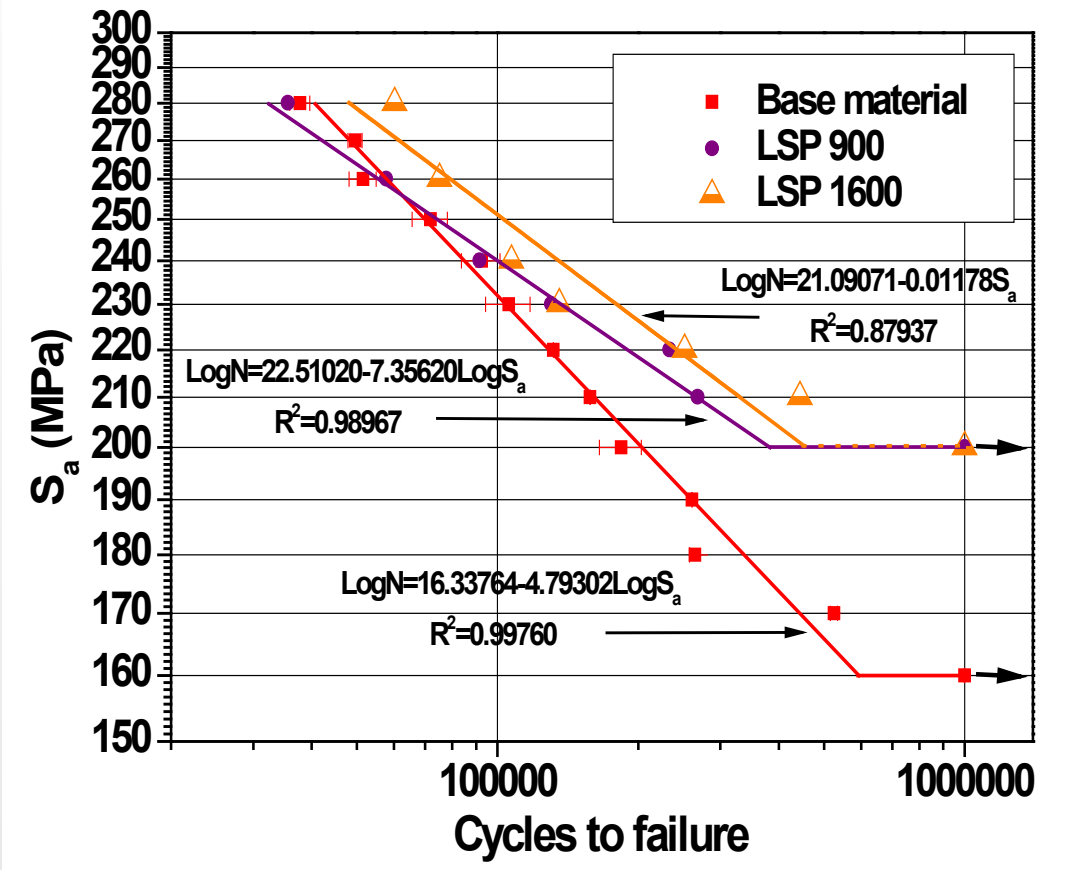

PORRO, J.A. et al.: 3rd ICLP. Japan 10-15 Oct. 2011

Discussion and Outlook

- Short pulse (Q-switched, ns) commercial table top lasers provide a practical solution for the experimental implementation of LSP Processes.
- The need for a practical capability of LSP process control in practical applications has led to the development of comprehensive theoretical / computational models for the predictive assessment of the complex phenomenology involved.
- High intensity laser-plasma interaction has revealed itself as a critical point for a proper process understanding and predictive assessment of LSP processes.
- The developed calculational model (SHOCKLAS) allows a systematic study of LSP processes starting from laser-plasma interaction. The integrated laser-plasma analysis routine, based in realistic material EOSs, provides a unique capability for process parametrization.
- Additionally, the development of the appropriate experimental diagnosis facilities and the connection of numerical simulation to experimental material characterization results enable a fundamental and reliable process understanding capability in view of process industrial implementation.

Discussion and Outlook

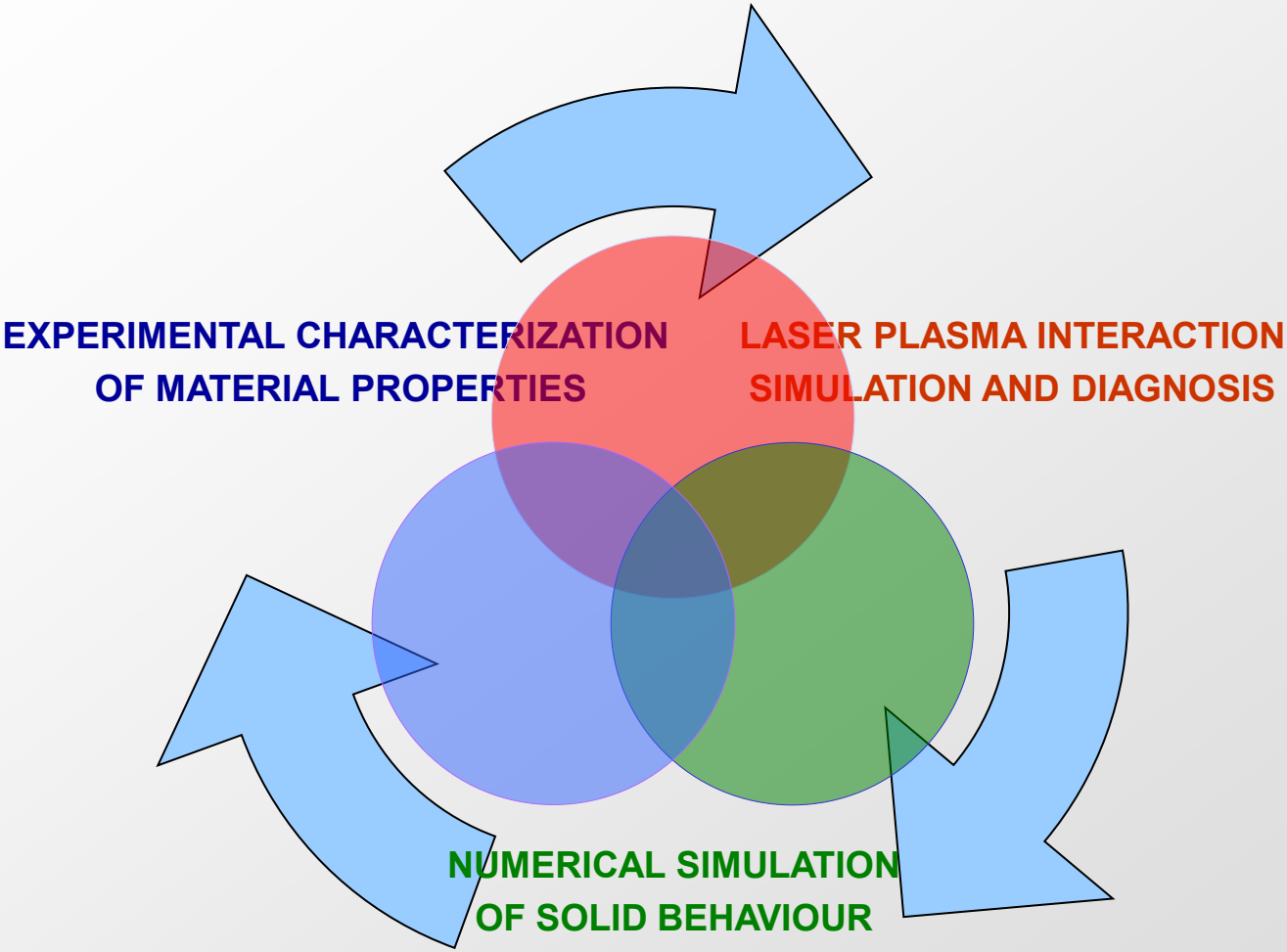

MAIN REFERENCES

1. Ocaña, J.L. et al.: "A Model for the Coupled Predictive Assessment of Plasma Expansion and Material Compression in Laser Shock Processing Applications". In: High-Power Laser Ablation II, Claude R. Phipps, Masayuki Niino, Eds., SPIE Proceedings , Vol. 3885, 252–263 (2000)
2. Ocaña, J.L. et al.: "Predictive assessment and experimental characterization of the influence of irradiation parameters on surface deformation and residual stresses in laser shock processed metallic alloys". In: High-Power Laser Ablation V, Phipps C.R., Ed.. SPIE Vol. 5548, 642-653 (2004)
3. Ocaña, J.L. et al.: Appl. Surf. Sci., 238 (2004) 242-248
4. Ocaña, J.L. et al.: Appl. Surf. Sci., 238 (2004) 501-505
5. Rubio-González, C. et al.: Mat. Sci. Eng. A., 386 (2004) 291-295
6. Ocaña, J.L. et al.: "Laser Shock Processing as a Method for Surface Properties Modification of Metallic Materials". In: Shot Peening and other Mechanical Surface Treatments, V. Shulze, A. Niku-Lari, Eds. I.I.T.T. Paris (2005), 466-471.
7. Sanchez-Santana, U., et al.: Wear, 260 (2006) 847-854
8. Rubio-González, C. et al.: Appl. Surf. Sci., 252 (2006) 6201-6205
9. Morales, M. et al.: "Numerical Simulation of Plasma Dynamics in Laser Shock Processing Experiments". In: Proceedings of LPM2008. 1-6 (2008)
10. Morales, M. et al.: Surf. & Coat. Tech. 202 (2008) 2257–2262
11. Martí-López, L. et al.: Appl. Opt. 48 (2009) 3671-3680
12. Morales, M. et al.: Appl. Surf. Sci. 255 (2009) 5181–5185
13. Ocaña, J.L. et al.: Mat. Sci. Forum, Vols. 638-642 (2010) pp 2446-2451
14. Morales, M. et al.: Mat. Sci. Forum, Vols. 638-642 (2010) pp 2682-2687
15. Morales, M. et al.: J. Optoelectr. and Adv. Mat., 12 (2010) 718-722

Laser Shock Microforming of Thin Metal Sheets with Q-Switched ns Lasers

J.L. Ocaña, J.A. Porro, C. Correa, M. Morales, J.J. García-Ballesteros

Centro Láser UPM. Universidad Politécnica de Madrid

Campus Sur UPM. Edificio La Arboleda.

Ctra. de Valencia, km. 7,300. 28031 Madrid. SPAIN

Tel.: (+34) 913363099. Fax: (+34) 913363000.

email: jlocana@etsii.upm.es

Laser Shock Microforming of Thin Metal Sheets with ns Lasers

OUTLINE:

- Introduction
- Physical Principles. Simulation Model
- Simulation Results
- Experimental Setup. Sample Preparation
- Experimental Results
- Discussion and Outlook

1. INTRODUCTION

- The increasing demands in MEMS fabrication are leading to new requirements in production technology. Especially the packaging and assembly require high accuracy in positioning and high reproducibility in combination with low production costs.
- Conventional assembly technology and mechanical adjustment methods are time consuming and expensive. Each component of the system has to be positioned and fixed. Also adjustment of the parts after joining requires additional mechanical devices that need to be accessible after joining.
- Accurate positioning of smallest components represents an up-to-date key assignment in micro-manufacturing. It has proven to be more time and cost efficient to initially assemble the components with widened tolerances before precisely micro-adjusting them in a second step.
- As mounted micro components are typically difficult to access and highly sensitive to mechanical forces and impacts, contact-free laser adjustment processes offer a great potential for accurate manipulation of micro devices.

1. INTRODUCTION (Cont.)

- Long relaxation-time thermal fields developed in continuous or long-pulse laser forming of metal thin sheets are responsible for the introduction of constraint residual stresses in component assembly processes.
  - Changes in the materials microstructure could cause changes in density and volume and create stresses
  - Chemical reactions of the irradiated surface, e.g. oxidation could take place and lead to stressed surface layers
- The use of ns laser pulses inducing predominantly mechanical deformation stresses provides the capability for a suitable parameter matching in laser bending of MEMS components.
- Theoretical interaction regime description, computational process simulation results and preliminary experimental results and practical issues are presented in this work.

2. PHYSICAL PRINCIPLES

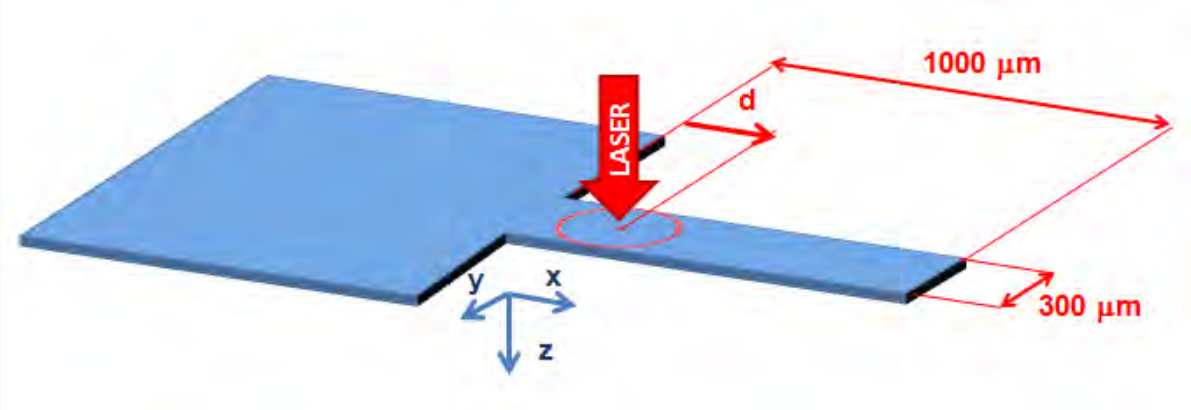

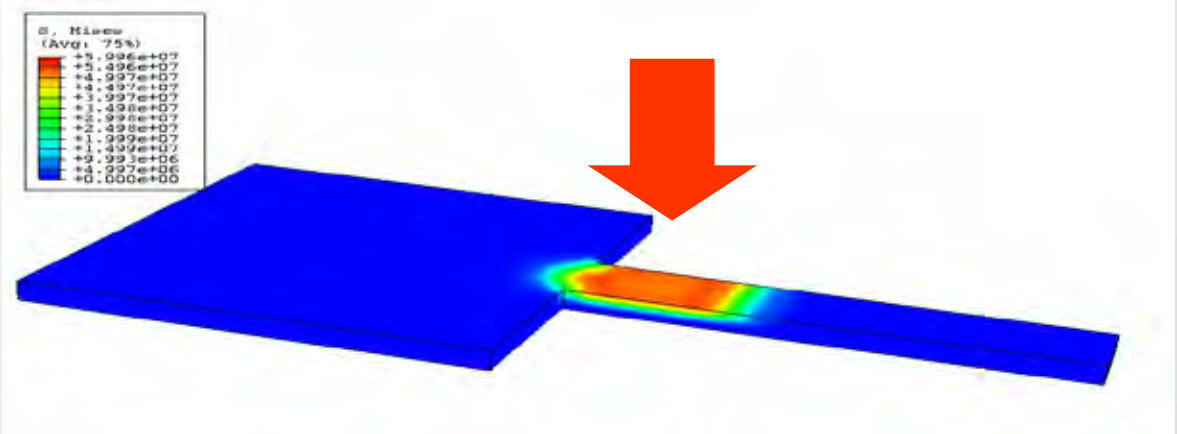

2. PHYSICAL PRINCIPLES

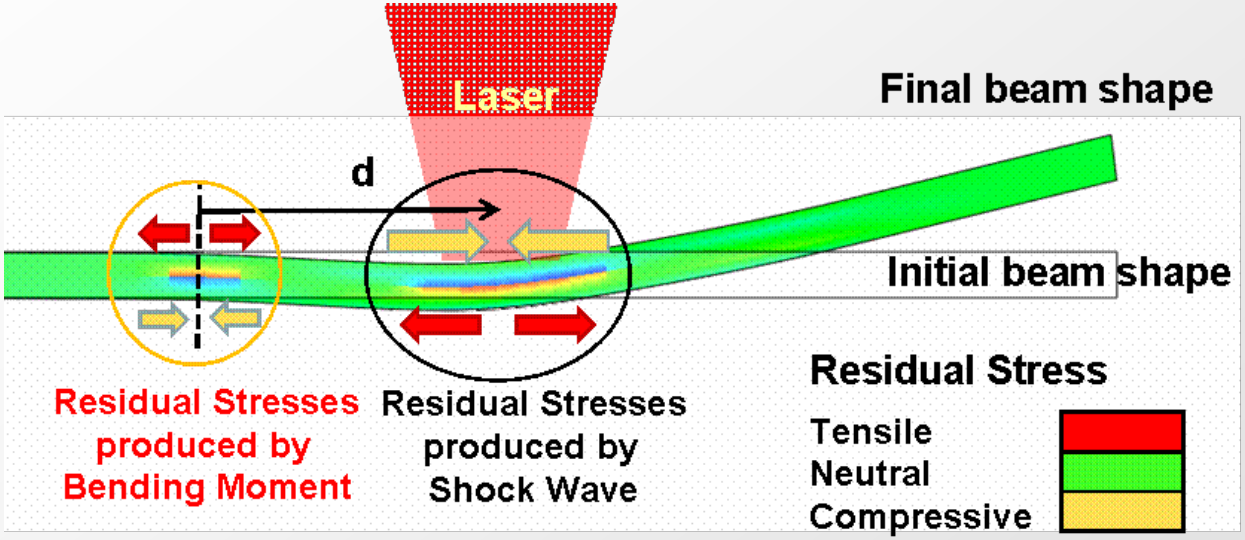

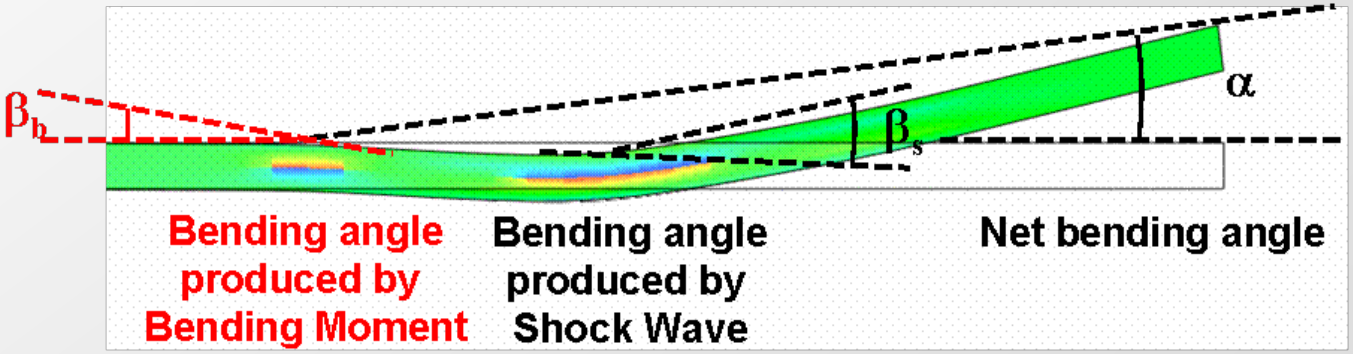

2. NUMERICAL SIMULATION. MODEL DESCRIPTION

PRESSURE PULSE MODEL

LSPSIM

Interface thickness

$$L(t) = \int_0^t [u_1(t) + u_2(t)]\, dt$$

Heating phase

$$I(t) = P(t)\frac{dL(t)}{dt} + \frac{d[E_i(t)L(t)]}{dt}$$

$$P(t) = \frac{2}{3}E_t(t) = \frac{2}{3}\alpha E_i(t)$$

Shock wave relation

$$P = \rho_i D_i u_i$$

Solid/Liquid $D = C + S\,u$

Gas $D = u\left(\frac{\gamma+1}{2}\frac{P}{\rho}\right)^{1/2}$

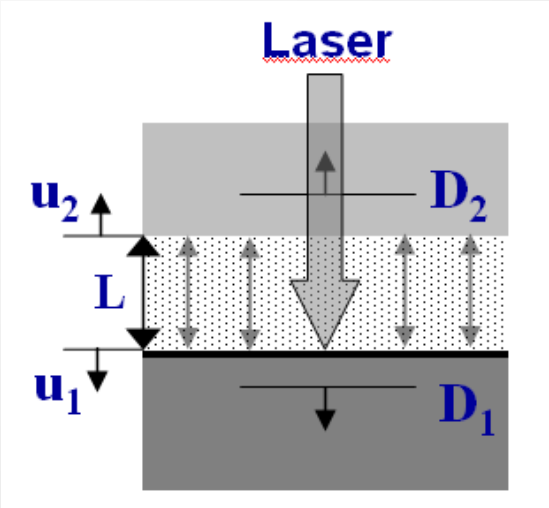

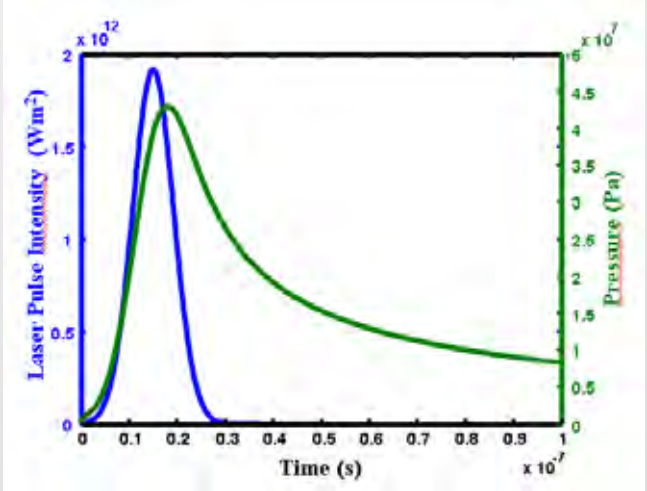

2. NUMERICAL SIMULATION. MODEL DESCRIPTION

FEM MODEL – STRESS-STRAIN ANALYSIS

GEOMETRY AND DIMENSIONS

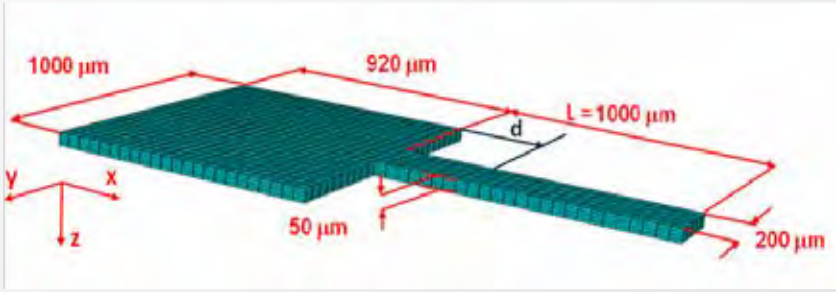

PLASTIC STRAIN

MIN. PRINCIPAL

MAX. PRINCIPAL

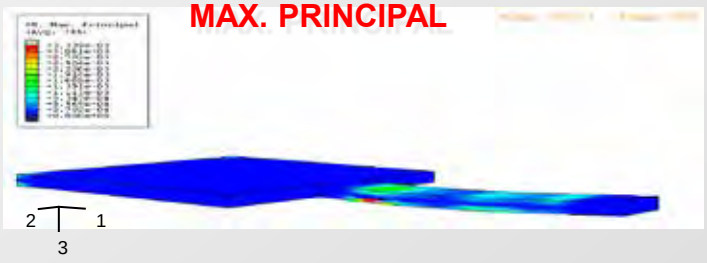

STRESS DISTRIBUTION

S11

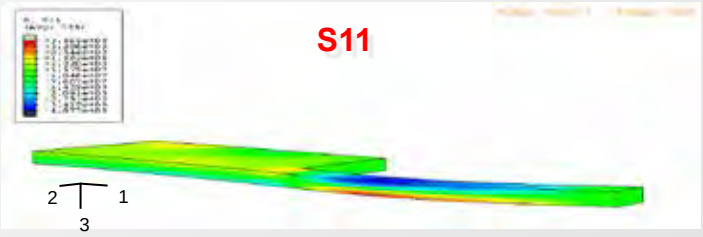

S22

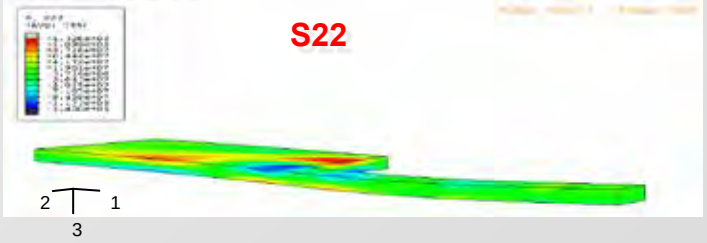

2. NUMERICAL SIMULATION. MODEL DESCRIPTION

MATERIAL PROPERTIES (AISI 304)

Target	AISI 304
Young's Modulus: E [GPa]	193
Poisson's Coeffcient: n	0.25
Densisty: r [kg/m3]	7896
Melting Temperature: Tm [K]	1811
Test Temperature: T0 [K]	300
Inelastic Heat Fraction: X	0.9
Johnson-Cook parameters	
A [MPa]	350
B [MPa]	275
C	0.022
n	0.36
m	1
T_r [K]	300
$\dot{\varepsilon}_0$ [s^{-1}]	1

LSPSIM PARAMETERS

Nd:YAG Laser [nm]	1064
Energy per pulse [mJ]	33 - 150
Pulse length [ns]	9.4
Spot Radius [mm]	175
Confining medium	Air
Interaction parameter a	0.2

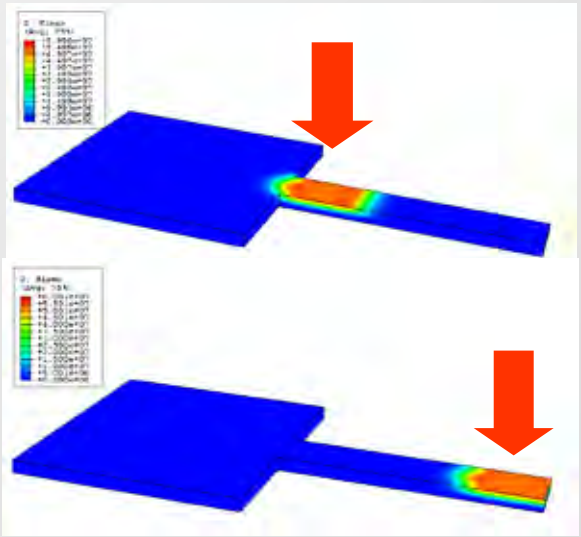

3. NUMERICAL SIMULATION RESULTS

SHOCKLAS EXPLICIT – VON MISES EVOLUTION

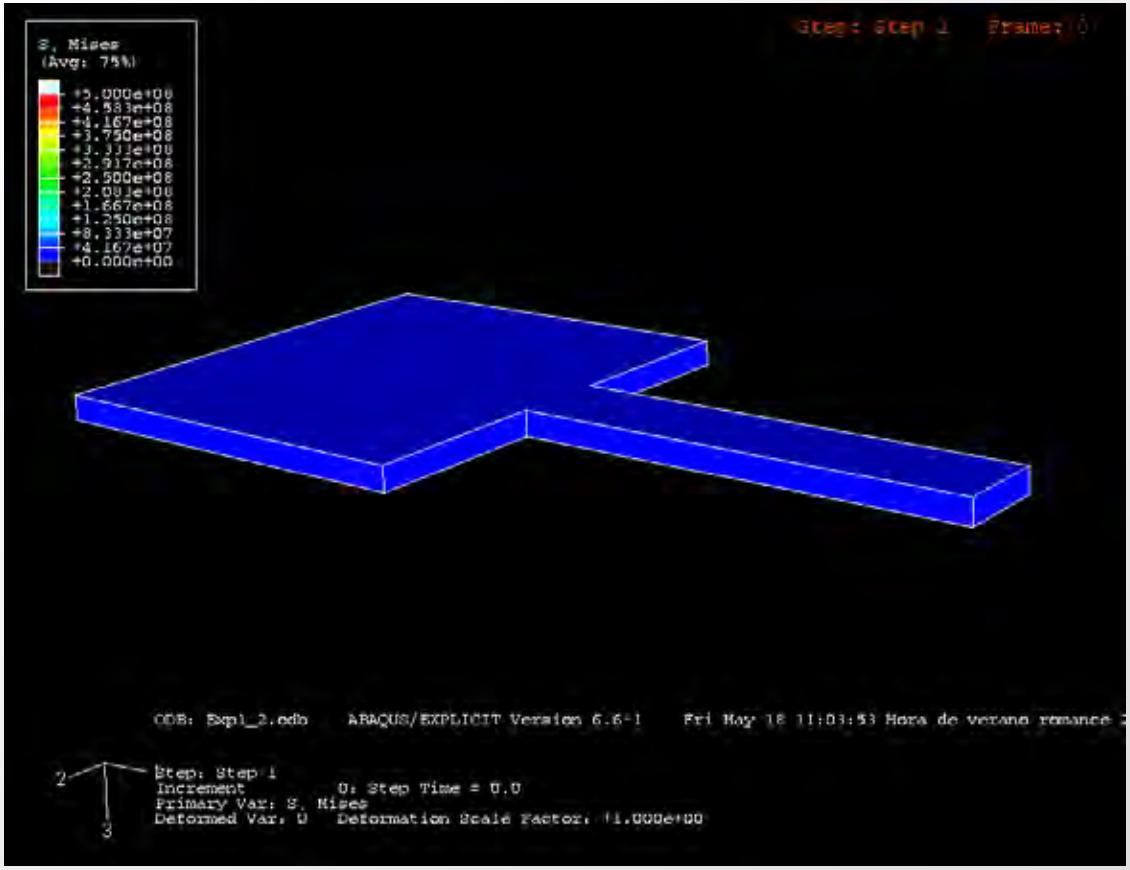

3. NUMERICAL SIMULATION RESULTS

SHOCKLAS EXPLICIT – STRESS (S11) EVOLUTION

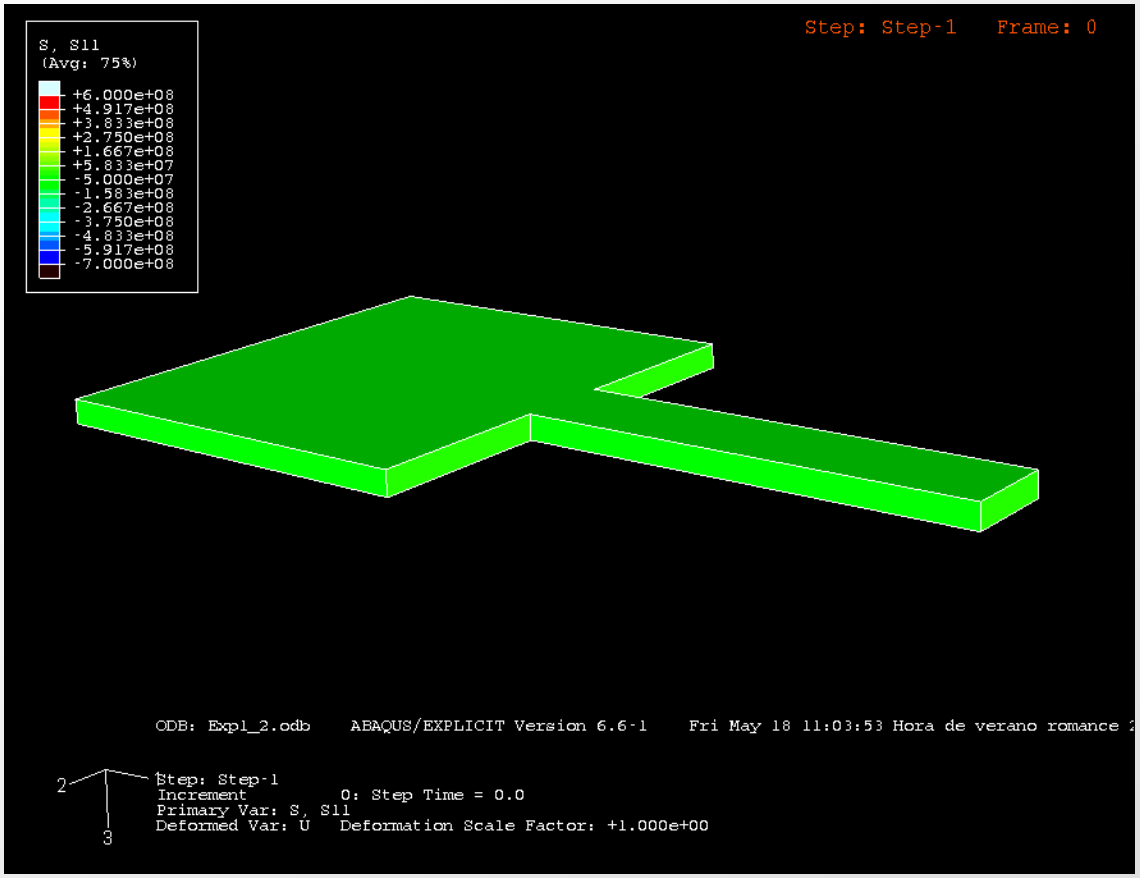

3. NUMERICAL SIMULATION RESULTS

SHOCKLAS STANDARD – STRESS (S11) EQUILIBRATION

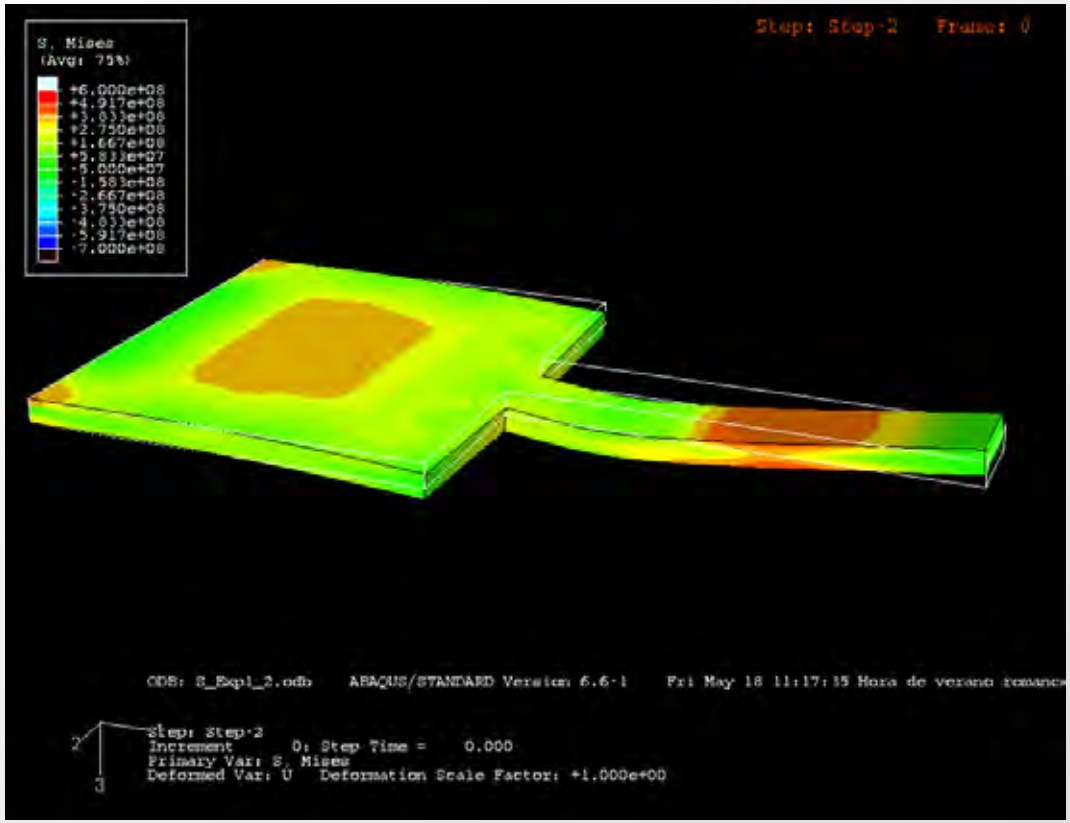

3. NUMERICAL SIMULATION RESULTS

Pulse Energy Parametrization

Nd:YAG Laser [nm]	1064
Energy per pulse [mJ]	variable
Pulse length [ns]	9.4
Spot Radius [mm]	175

Material Model	SS304
Confining medium	Air
Interaction parameter a	0.2
Spot center distance [mm]	150

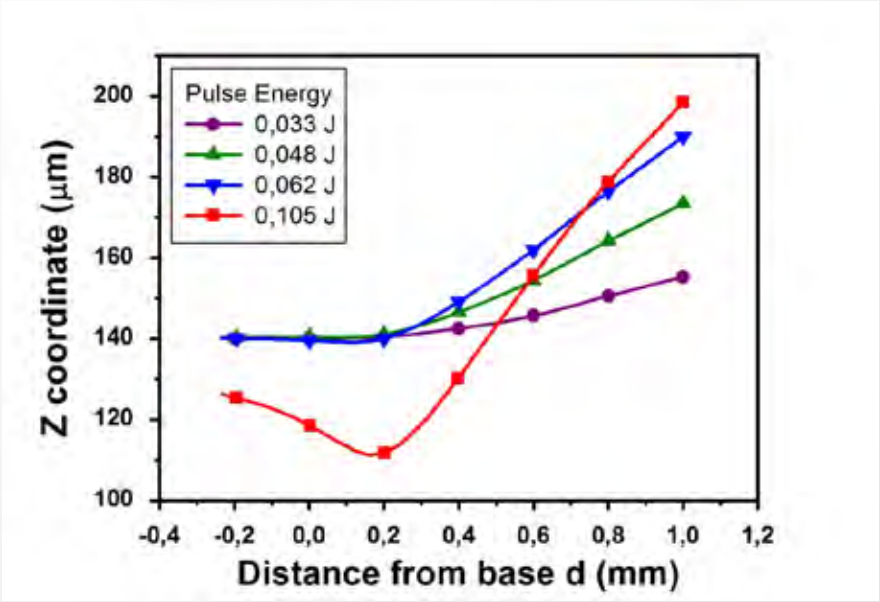

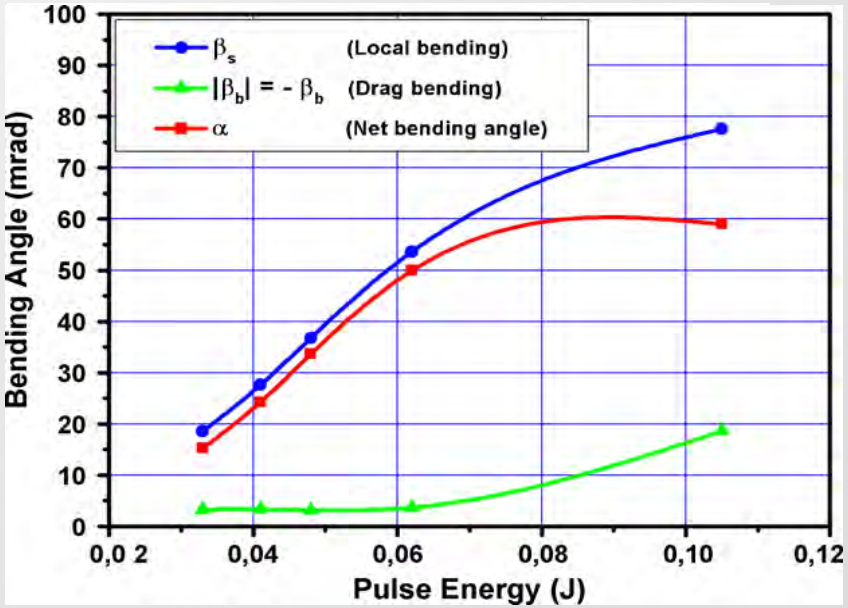

3. NUMERICAL SIMULATION RESULTS

Spot Center Distance Parametrization

Nd:YAG Laser [nm]	1064
Energy per pulse [mJ]	33
Pulse length [ns]	9.4
Spot Radius [mm]	175

Material Model	SS304
Confining medium	Air
Interaction parameter a	0.2
Spot center distance [mm]	variable

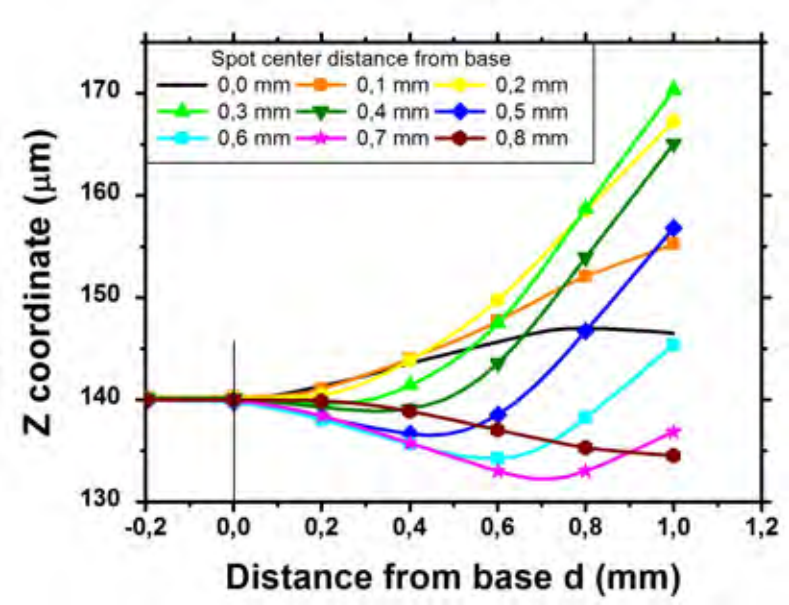

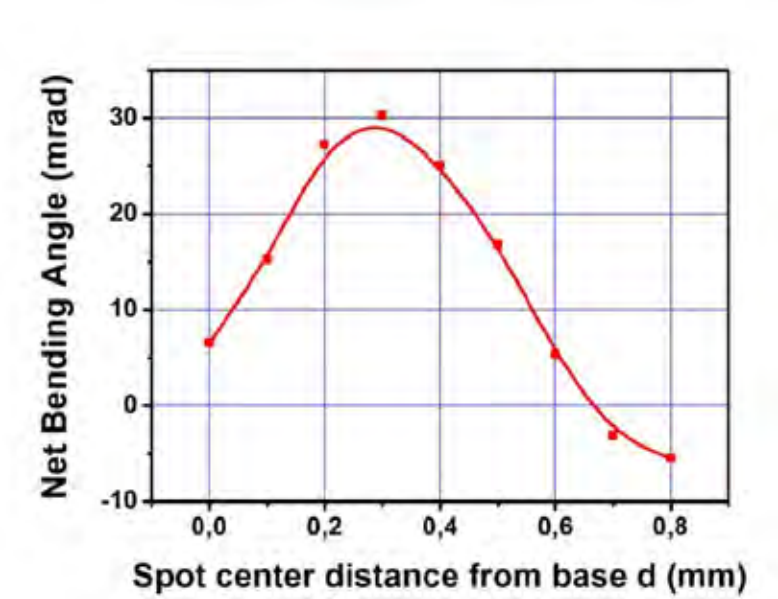

4. EXPERIMENTAL SETUP. SAMPLE PREPARATION

ML-100 LASER WORKSTATION

Laser media	Excimer (KrF)	DPSS 3ω
Wavelength (nm)	248	355
Pulse duration (ns)	3–7 ns	<12 ns (at 50 kHz)
Beam shape/mode	Rectangular (3.5 × 6 mm)	TEM_{00} ($M^2 < 1.3$)
Operating frequency	0–300 Hz	15–300 kHz
Average power (W)	0.3–5 (at 300 Hz)	5 W (at 50 kHz)

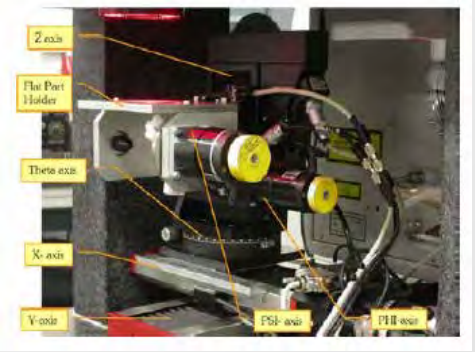

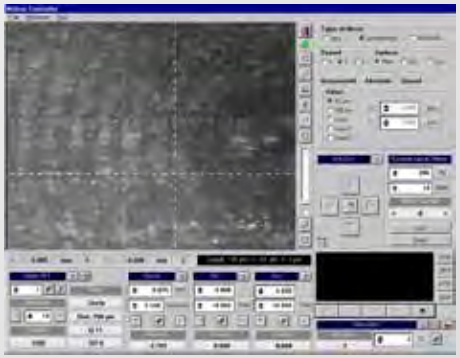

- Dual Excimer/DPSS Laser processing
- Multiaxis (6) System
- Work volume: 120*100*50 mm
- XY accuracy: 1 mm
- Global positioning accuracy: 40 mm
- CCD direct vision (x 500)

AISI 304
1000 x 200 x 50 mm

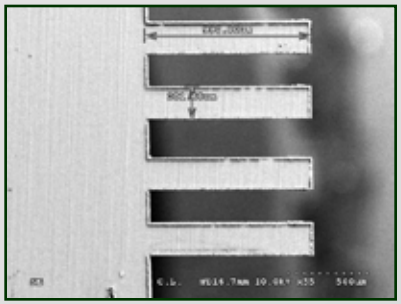

4. EXPERIMENTAL SETUP. SAMPLE PREPARATION

SEM IMAGES OF LASER CUT SHEET

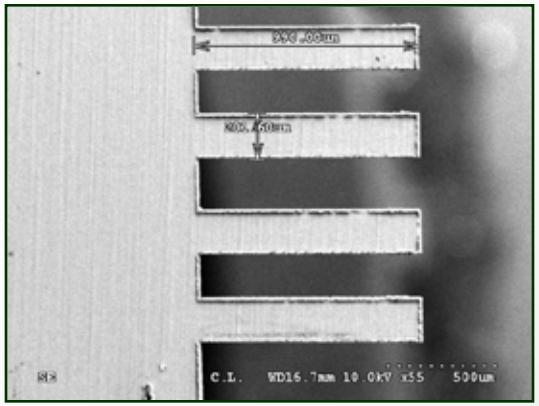

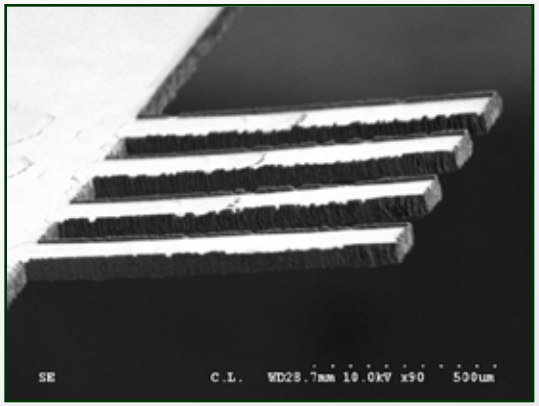

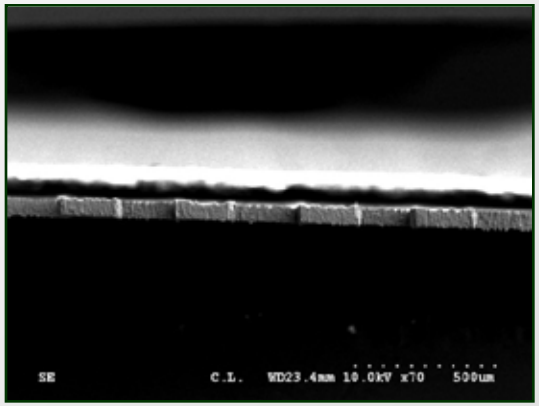

CONFOCAL IMAGES OF LASER CUT SHEET

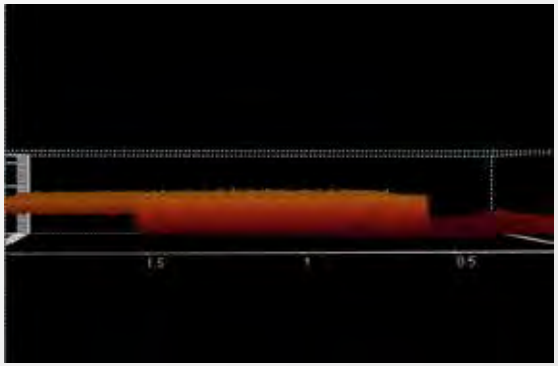

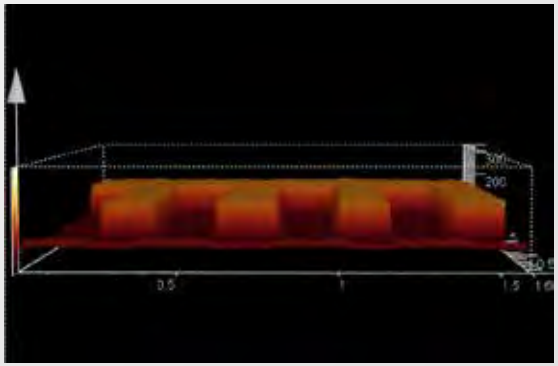

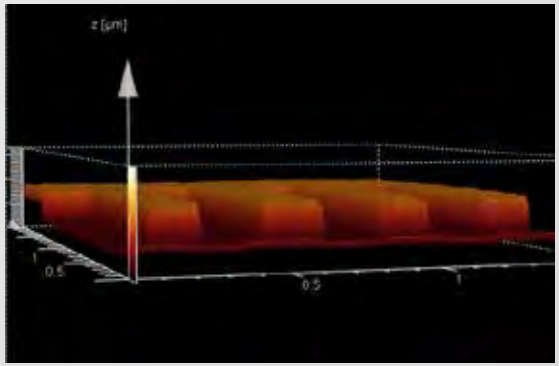

4. EXPERIMENTAL SETUP. SAMPLE PREPARATION

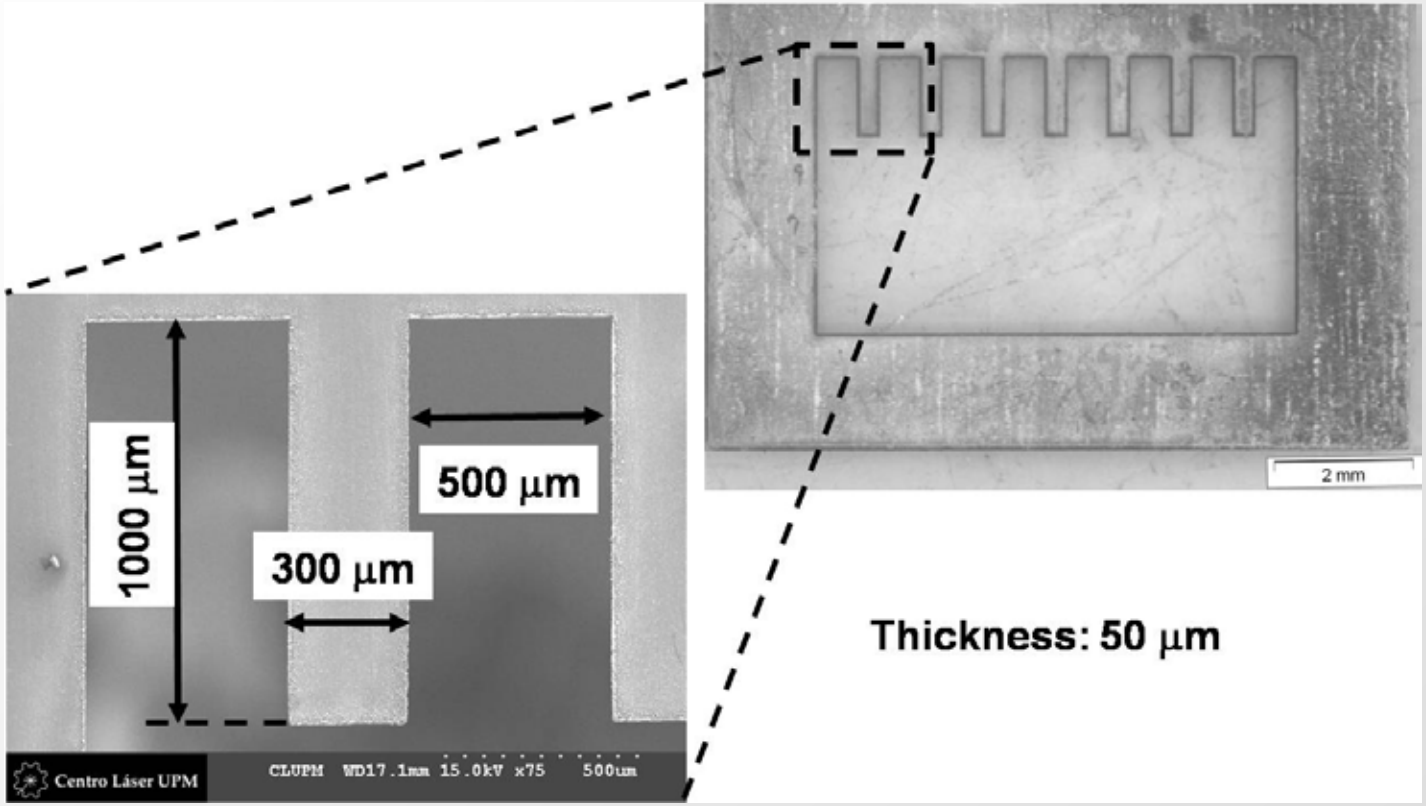

4. EXPERIMENTAL SETUP. SAMPLE IRRADIATION

Nd:YAG Laser Wavelength [nm]	1064
Energy per pulse [J]	1.651
Laser Pulse length FWHM [ns]	9
Laser Beam radius [mm]	14
Confining layer	Air
Thin sheet material	AISI 304
Thin sheet thickness [mm]	50

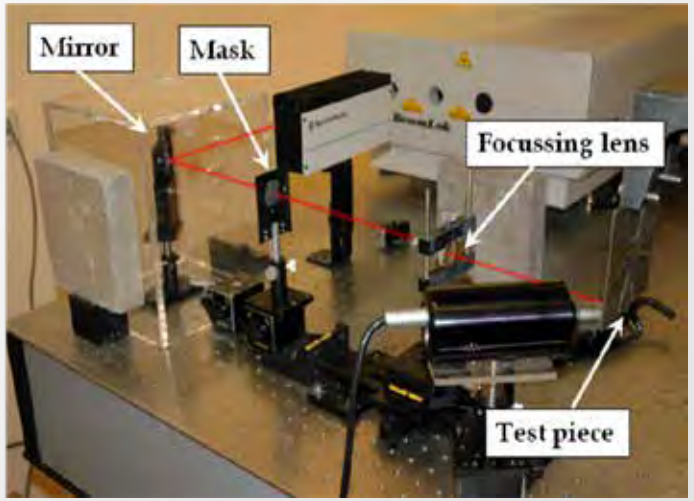

5. EXPERIMENTAL RESULTS. INFLUENCE OF SPOT CENTER DISTANCE

SEM IMAGES

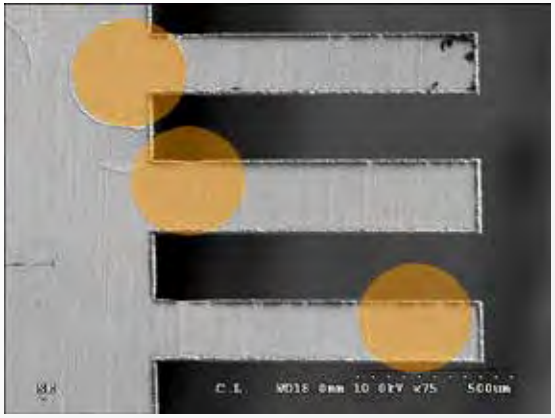

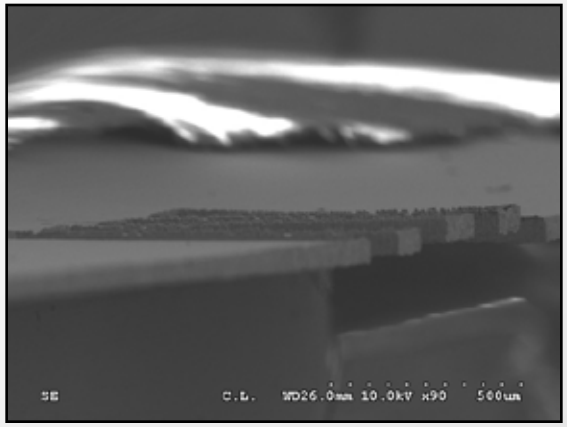

CONFOCAL MICROSCOPY

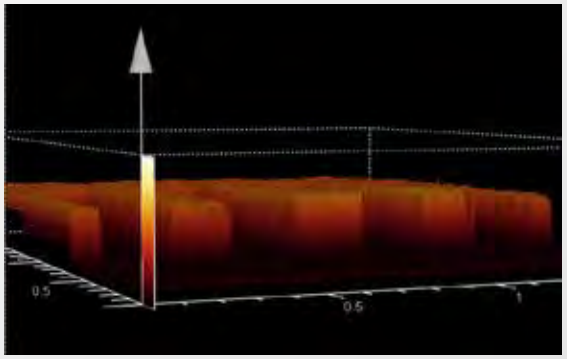

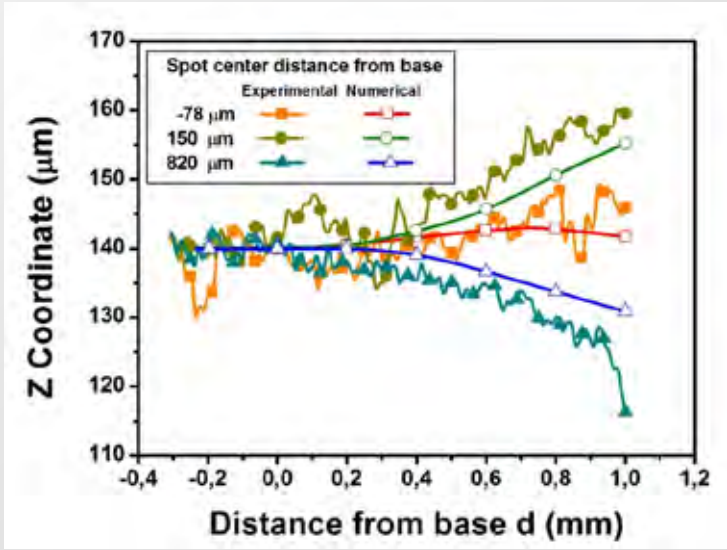

5. EXPERIMENTAL RESULTS. INFLUENCE OF NUMBER OF PULSES

SEM IMAGES

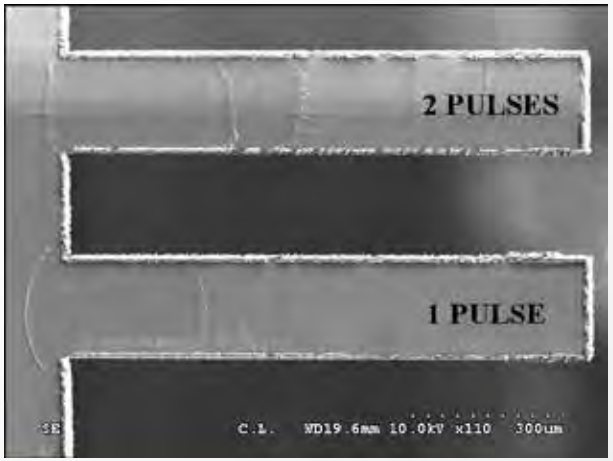

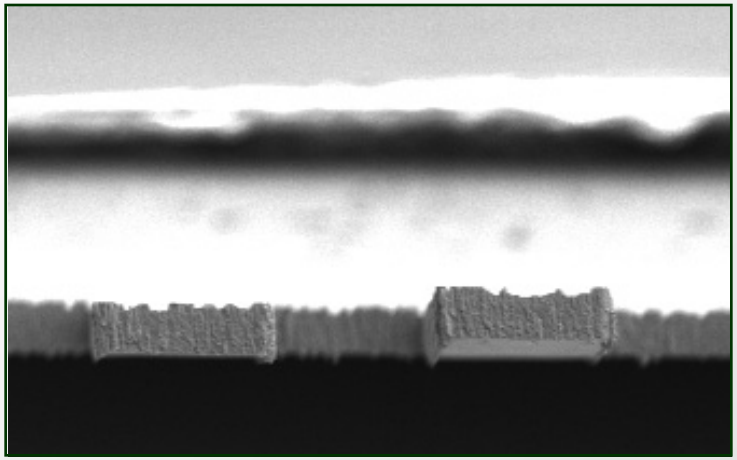

CONFOCAL MICROSCOPY

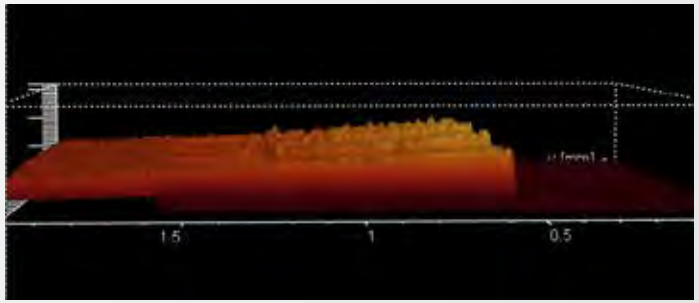

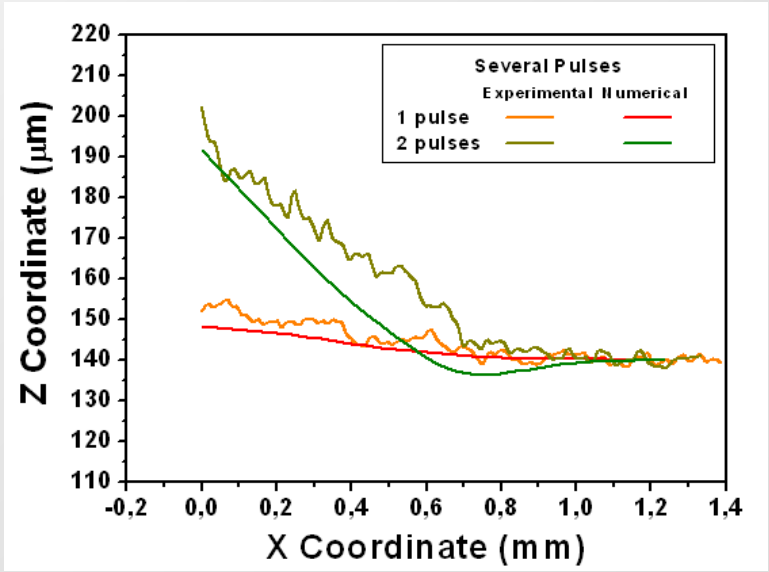

5. EXPERIMENTAL RESULTS. INFLUENCE OF NUMBER OF PULSES

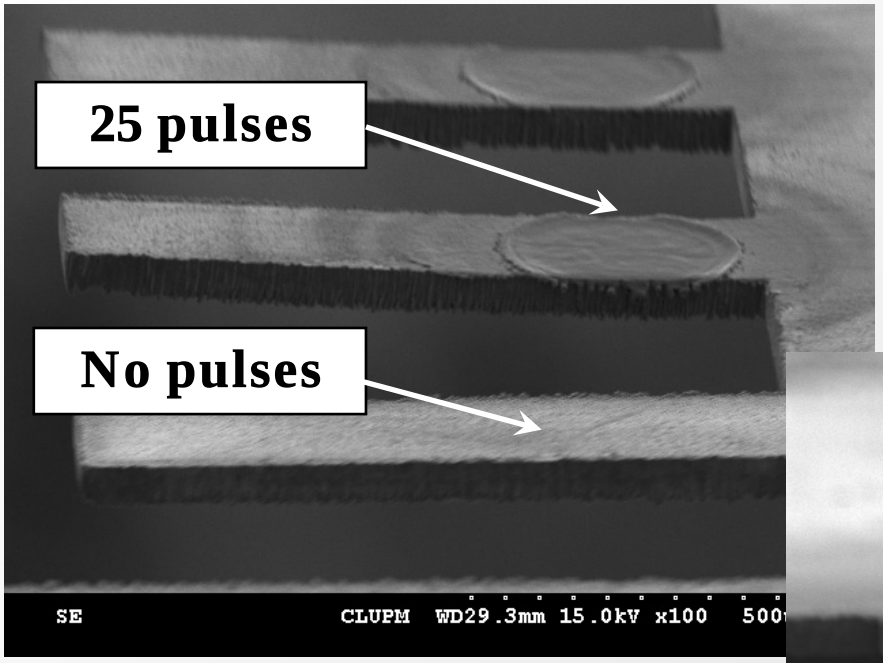

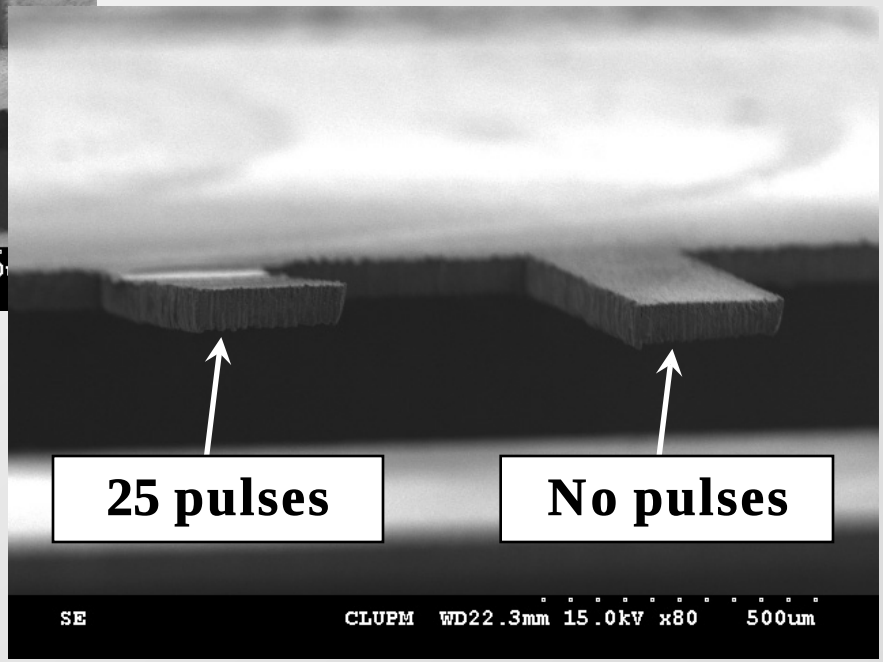

5. EXPERIMENTAL RESULTS. INFLUENCE OF NUMBER OF PULSES

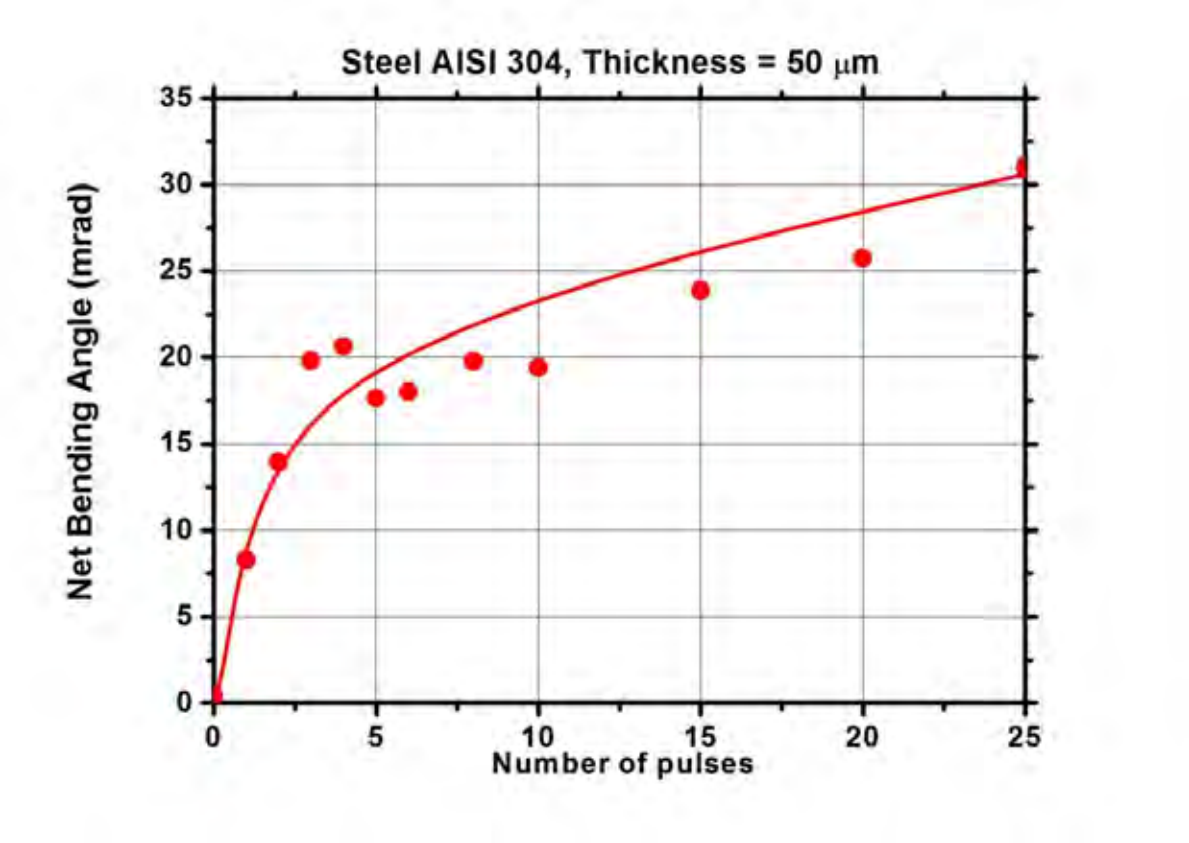

5. EXPERIMENTAL RESULTS. LAST RESULTS

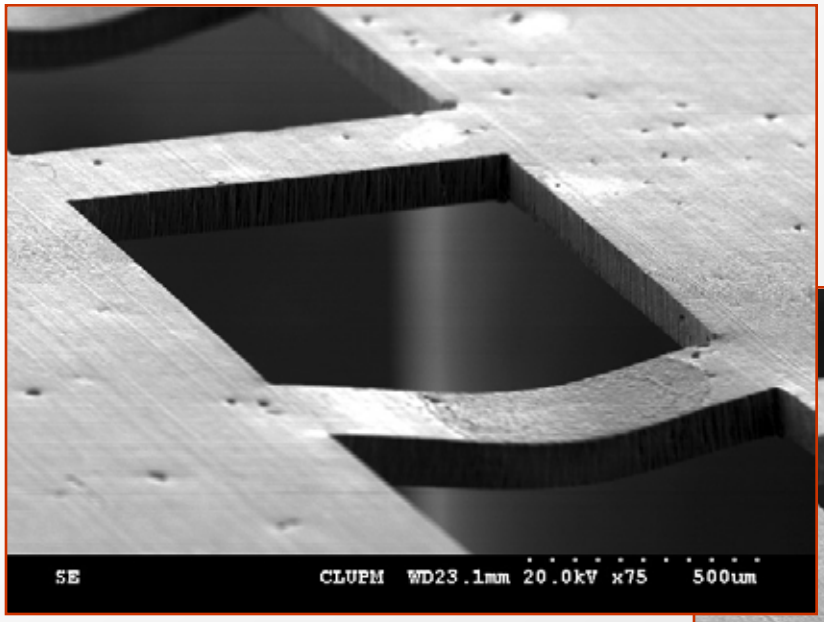

4 pulses

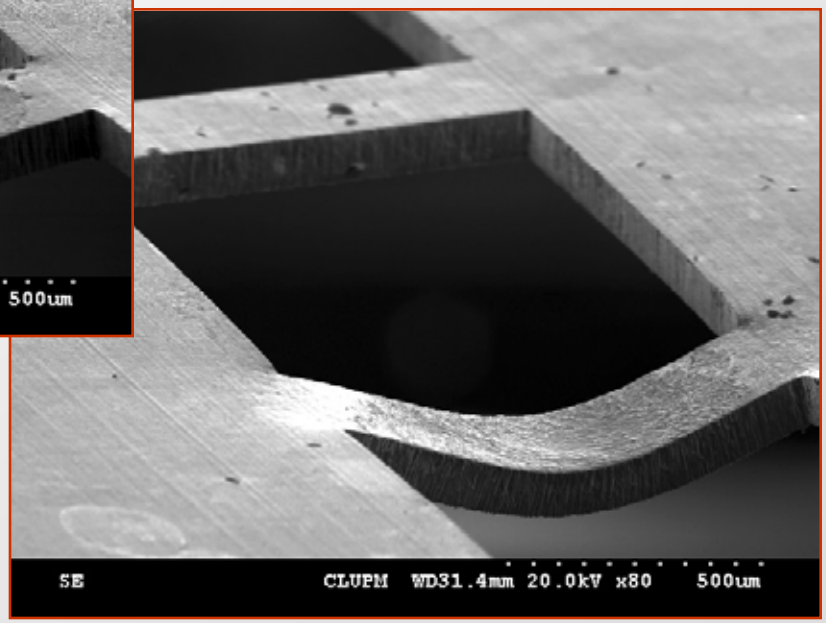

1 pulse

5. EXPERIMENTAL RESULTS. LAST RESULTS

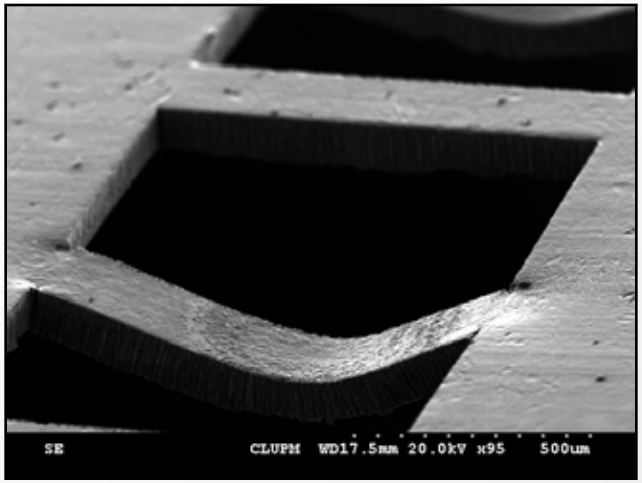

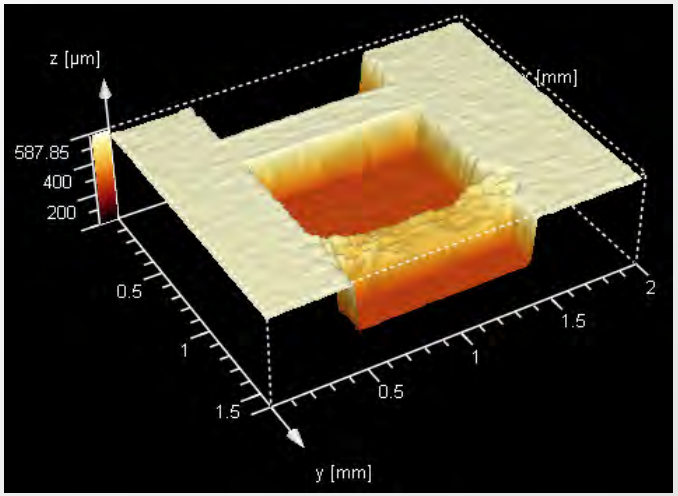

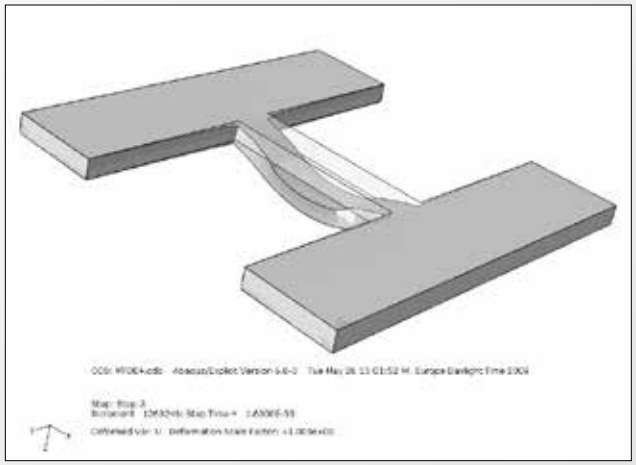

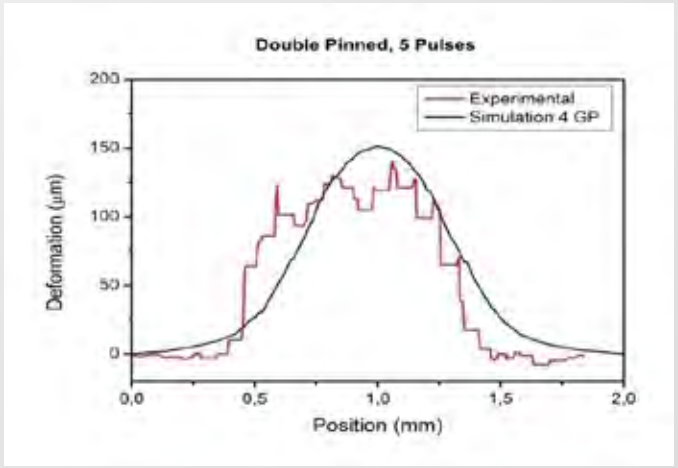

5. EXPERIMENTAL RESULTS. LAST RESULTS

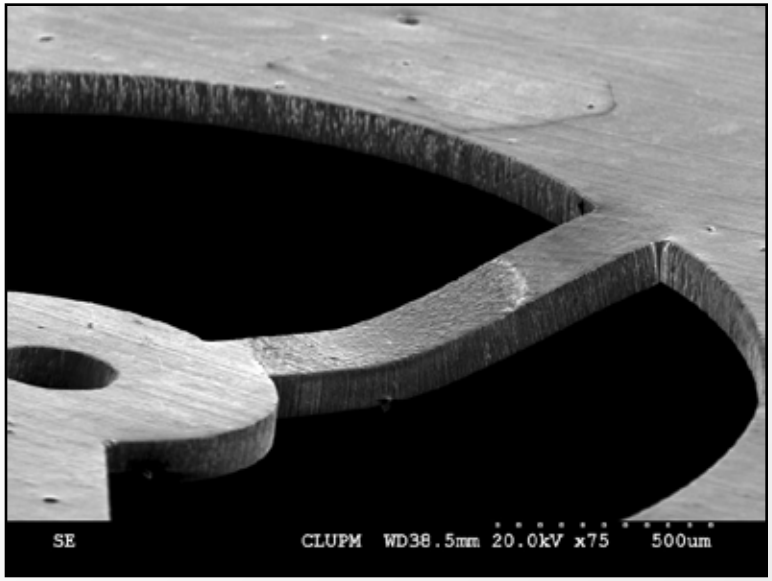

5 pulses

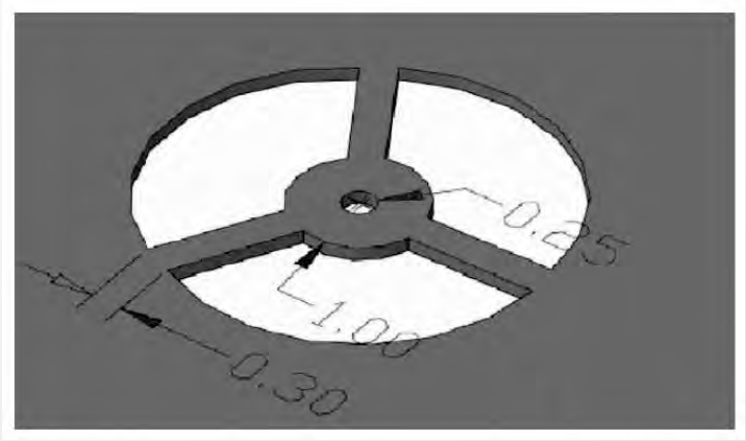

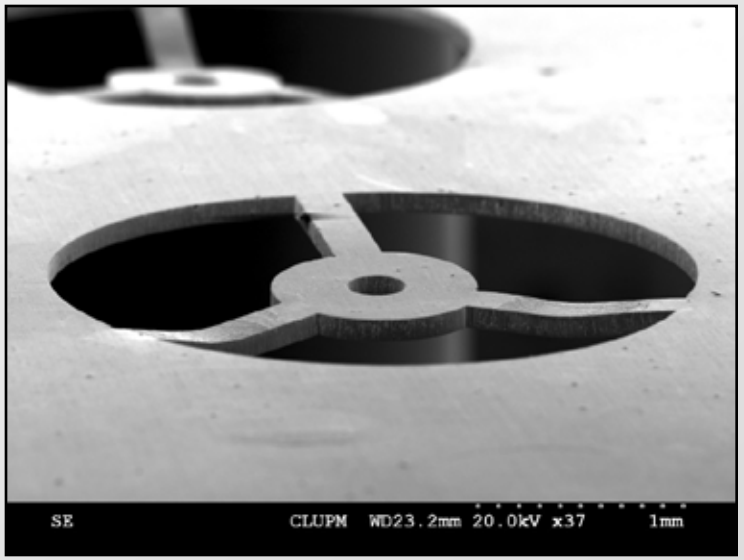

5 pulses in two arms

6. DISCUSSION AND OUTLOOK

- The suitability laser micro-bending of thin metal strips by means of ns pulsed lasers with average power in the range of several Watt has been experimentally demonstrated.
- Numerical simulation of the process has shown as critical parameters:
  - Pulse energy
  - Spot center distance relative to pinned end
- Simulations of single-end pinned targets show the presence of two bending components.
  - Overall angular displacement from beam clamping
  - Local bending at beam incidence position
- According to the authors' experience, the use of ns laser pulses is expected to provide a really suitable parameter matching for the laser bending of an important range of MEMS sheet components
- On the basis of the developed experience, the laser microforming and adjustment stresses release of arbitrary geometry components can be envisaged


Thank you for
your attention !

The LSP Team at CLUPM

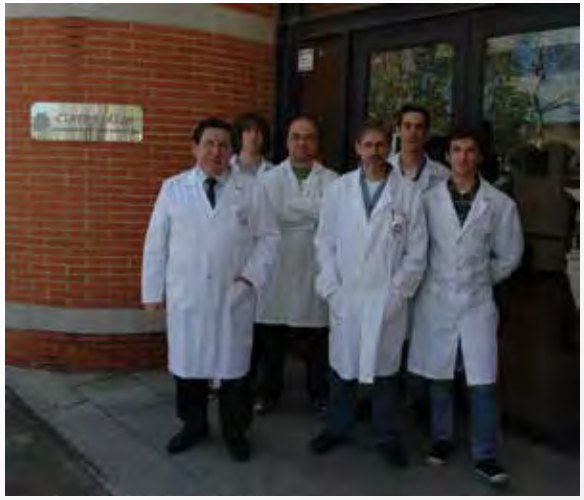

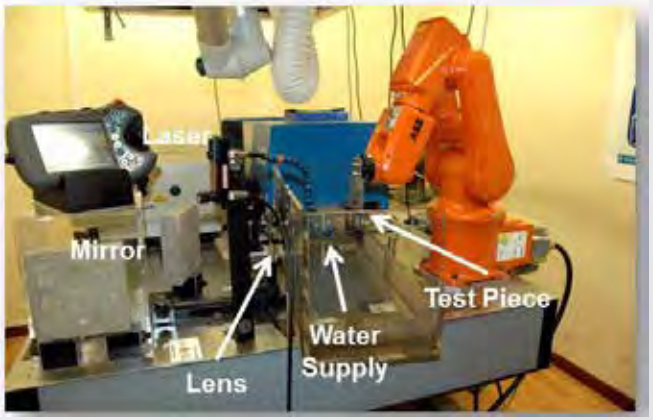

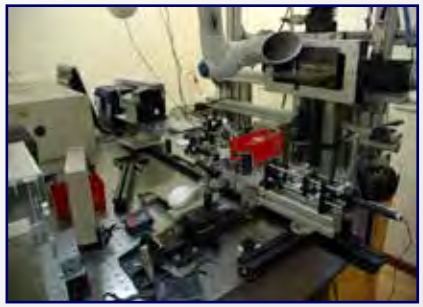

Work partly supported by MICINN/MINECO (Spain; Projects MAT2008-02704/MAT and MAT2012-37782) and EADS-CASA (Spain)

The UPM Laser Centre (CLUPM)